



LIFE Environment and Resource Efficiency
LESSWATT PROJECT
Project n. LIFE16 ENV/IT/000486
Duration: October 2017 - November 2021

Innovative wireless tool for reducing energy consumption and GHGs emission of water resource recovery facilities



GUIDE BOOK



Project financed by the European Commission
within the LIFE Programme Call 2016

> PROJECT



LIFE Environment and Resource Efficiency
LESSWATT PROJECT
Project n. LIFE16 ENV/IT/000486
Duration: October 2017 - November 2021

> PARTNERS



University of Florence (UNIFI)
Department of Civil and Environmental Engineering (DICEA)
Via di Santa Marta, 3 - 50139 Firenze, Italy
www.dicea.unifi.it



CUOIODEPUR S.p.A.
Via Arginale Ovest, 81
56020 San Romano - San Miniato (PI), Italy
www.cuoiodepur.it



Ghent University (UGENT)
Dept. of Mathematical Modelling, Statistics and Bioinformatics
(BIOMATH) Coupure Links 653 - B-9000 Gent, Belgium
www.biomath.ugent.be



UTILITATIS
pro acqua energia ambiente
Via Ovidio 20 - 00193 Roma, Italy
www.utilitatis.org



WEST SYSTEMS S.r.l.
Via Donato Giannotti, 24
50124 Firenze, Italy
www.westsystems.com

Table of contents

1.	Introduction	3
2.	Drone structure	3
2.1	Frame	4
2.2	Inflatable floats	5
2.3	Conveying hood	6
2.4	Control and sampling systems	7
2.4.1	Control Box	8
2.4.1.1	Positioning and navigation system	10
2.4.1.2	Software for remote control	19
2.4.2	Sampling Box	20
2.4.2.1	Instrumentation technical characteristics	23
2.4.2.2	Instrumentation calibration	29
3.	Drone assembly	32
3.1	Frame	32
3.2	Conveying hood	35
3.3	Assembly of the frame and conveying hood	37
3.4	Assembly of the inflatable floats	38
3.5	Assembly of the collection tube	39
3.6	Propellers assembly	40
3.7	Control box and sampling box assembly	44
3.8	Probes	45
3.9	Propellers alignment	46
4.	Starting procedure and use of the drone	47
4.1	Preliminary operation	47
4.2	GPS connection	51
4.3	Configuration and start of the automatic mission	52
4.4	Manual mission	56
5.	WS-SCADA software	57
5.1	Starting a sampling session	60
5.2	Measurement phases	62



5.3	Output files.....	63
6.	Prolonged stationary test.....	66
7.	End of Sampling	66
8.	Technical drawings.....	67
9.	Types of measurements	69
10.	Introduction to the protocol for energy/GHGs minimization	71
11.	Case studies	71
11.1	Case study 1: Cuoiodepur WRRF.....	71
11.2	Case study 2: San Colombano WRRF	75
11.3	Case study 3: Eindhoven WRRF	88
11.4	Case study 4: Tilburg WRRF	95
12.	LESSWATT protocol	96



1. Introduction

The LESSDRONE instrument was designed and built to carry out independently measurements on the concentration of gases inside the air that comes out of the oxidation tanks (off-gas). The instrument mainly consists of three parts: the frame and the support structure, the part dedicated to automatic positioning and the actual instrument part dedicated to the measurement and analysis of the off-gas characteristics.

The LESSDRONE evaluates the oxygen transfer efficiency in standard conditions and in process water (α SOTE) by the off-gas method, which is based on a mass balance in the gaseous phase between the oxygen content of the reference gas (atmospheric air) and the off-gas (from the oxidation tank surface), and measures the GHG concentrations (CO_2 , CH_4 , N_2O). The LESSDRONE is also able to measure the off-gas flow rate and therefore it is possible to calculate the GHG direct emissions in terms of mass ($\text{kgCO}_{2,\text{eq}}/\text{d}$). From the plant data, the electricity consumption for aeration is obtained and GHG indirect emissions are estimated by using the specific electricity production factor ($\text{kgCO}_{2,\text{eq}}/\text{kWh}$).

In parallel with the measurements the LESSWATT protocol for minimization of energy expenditure and GHGs emissions in WRRFs was developed. The proposed protocol is built on top of the existing protocols for modeling and optimization of WRRFs and it extends them with the target of Carbon Footprint (CF) reduction using innovative advanced modeling paradigms and high frequency data collected by LESSDRONE.

2. Drone structure

The drone is composed of a steel support frame, removable and foldable, to which 6 independent inflatable cylinders are anchored, one for each arm of the frame. At the center of the frame there is a hood that has the function of conveying the gases, which come out of the liquid surface, inside the collection pipe.

On the upper part of the frame there is a housing for the two boxes which respectively contain the analysis instrumentation and the control devices.



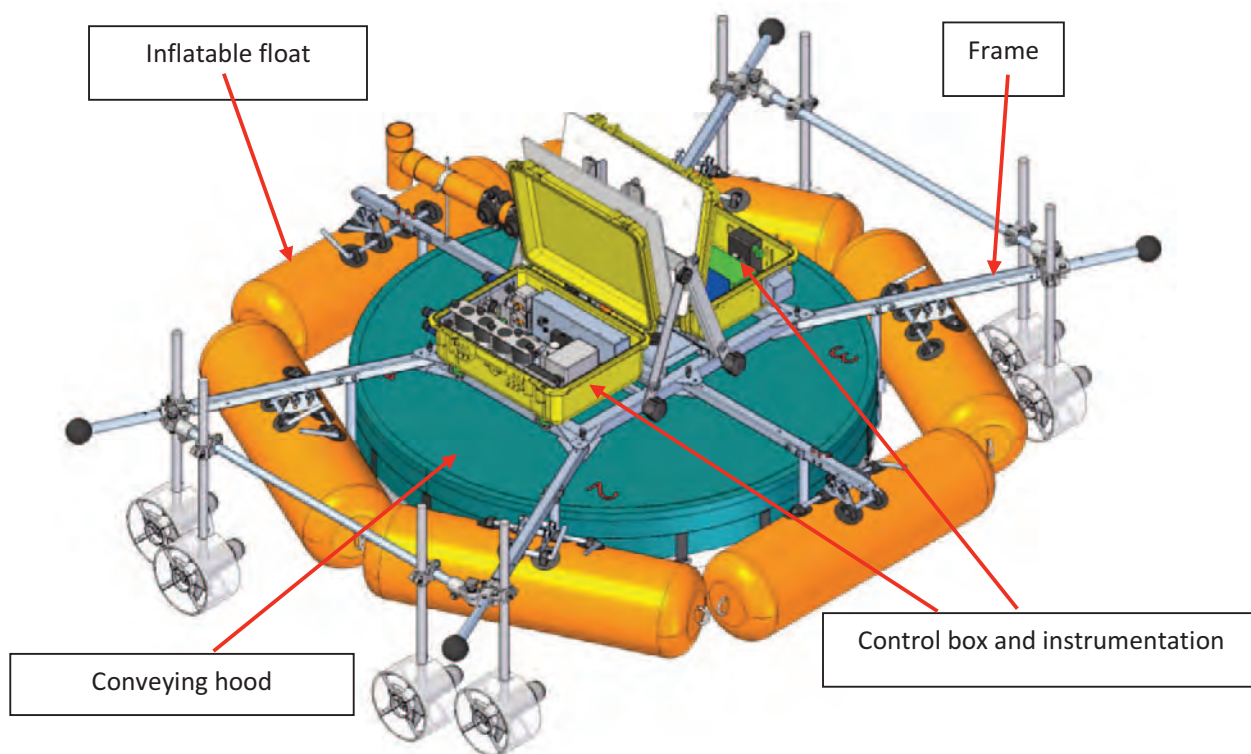


Figure 1: 3D elaboration view of the drone

2.1 Frame

The drone frame has been designed to provide robust support for the instrumentation and for the flotation and propulsion system. To improve the transportability of the instrument, the frame has been designed to be dismantled and closed in order to occupy as little space as possible during the transport phase.

The frame consists of a central part, made of square section stainless steel tubes, on which 6 arms are hinged with the function of supporting and anchoring the respective inflatable floats.

Four of the six arms described, have the function of supporting the thrusters and for this they have an appendix that extends their length in an adjustable way.

A vertical tube is anchored on all the arms and serves as a support for the frame of the conveyor hood.

Another 2 arms are hinged to the adjustable ones to give greater resistance to the structure and to support the further thrusters.

The upper part of the frame holds the two housings of the boxes and, in the central part, also the system to stretch the conveyor hood.



Above the central part of the frame, the triangular aluminum castle is hooked to lift the drone.

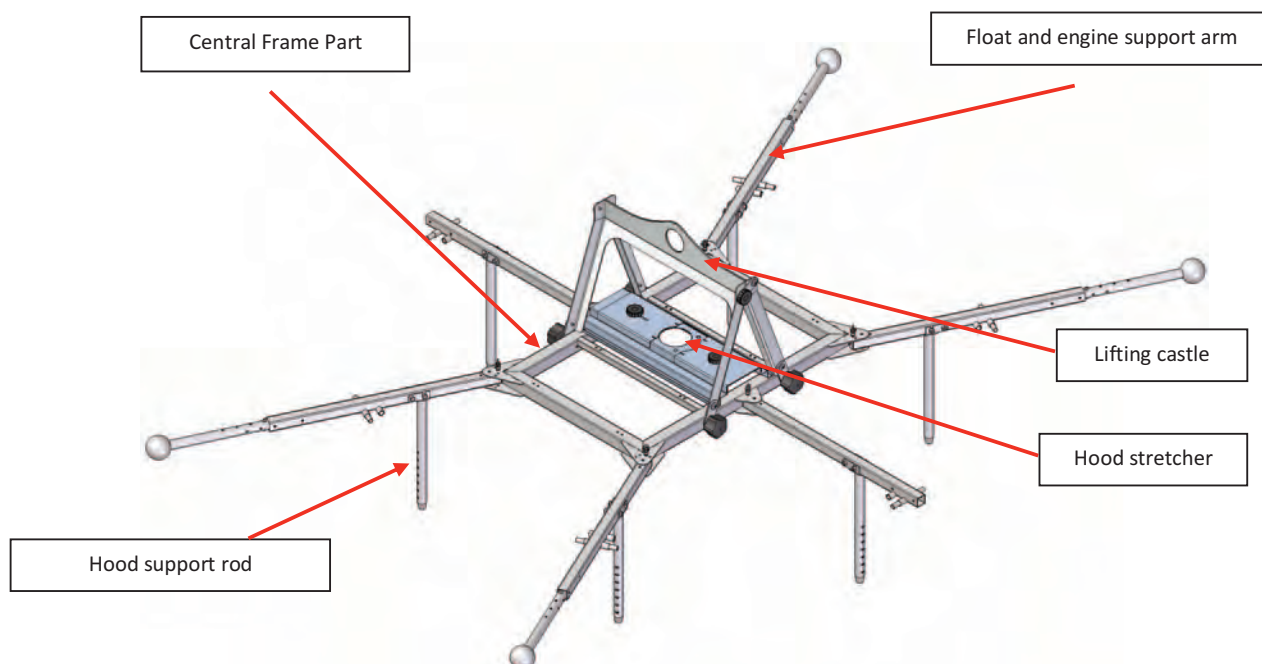
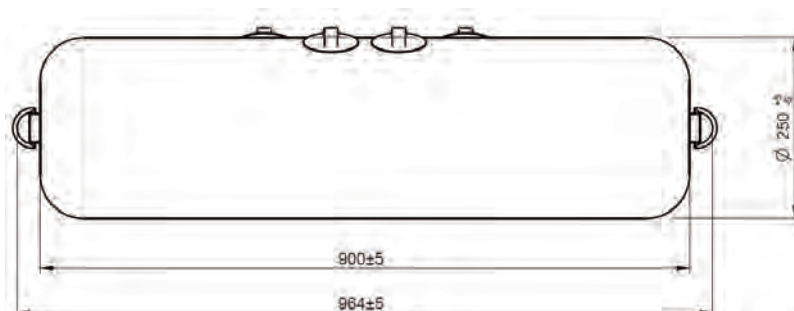


Figure 2: 3D elaboration view of the drone frame

2.2 Inflatable floats

To give the floating part greater reliability, 6 cylindrical inflatable structures have been made with thick rubberised fabric.

The structures are anchored to the arms of the frame through two linchpins that fit into the respective holes on the rubber grommets glued on the inflatable.



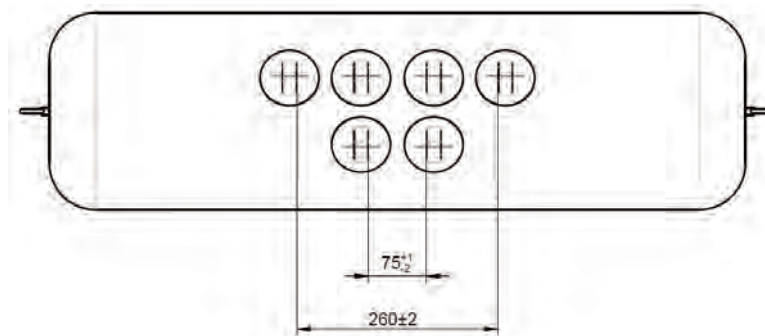


Figure 3: Floats view and dimensions

The floats are equipped with a Bravo type valve for inflation. The recommended inflation pressure is approximately 0.24 bar.

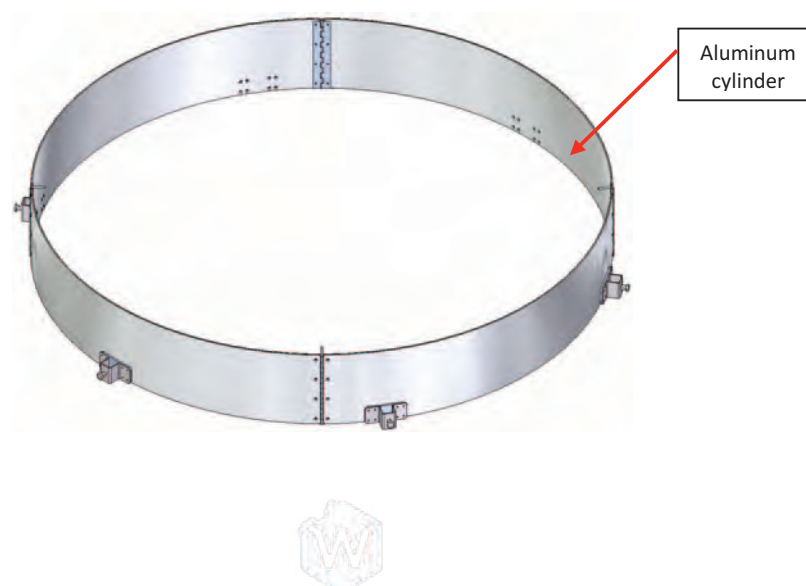
2.3 Conveying hood

The conveyor hood is positioned in the center of the frame, anchored to the vertical rods.

The hood consists of an anodized aluminum cylinder 2 mm thick and 200 mm high, divided into 4 sections to be easily disassembled with reduced dimensions for transport. Six omega supports are installed on the cylinder allowing the hood to be anchored to the frame vertical rods.

The cylinder is covered on the upper part by a suitably shaped rubberized fabric to cover the upper half of the cylinder.

At the center of the tarp there is a flanged hole that allows to connect the air coming out of the hood with a collection pipe on which the outlet speed is then measured and the sample is taken for analysis.



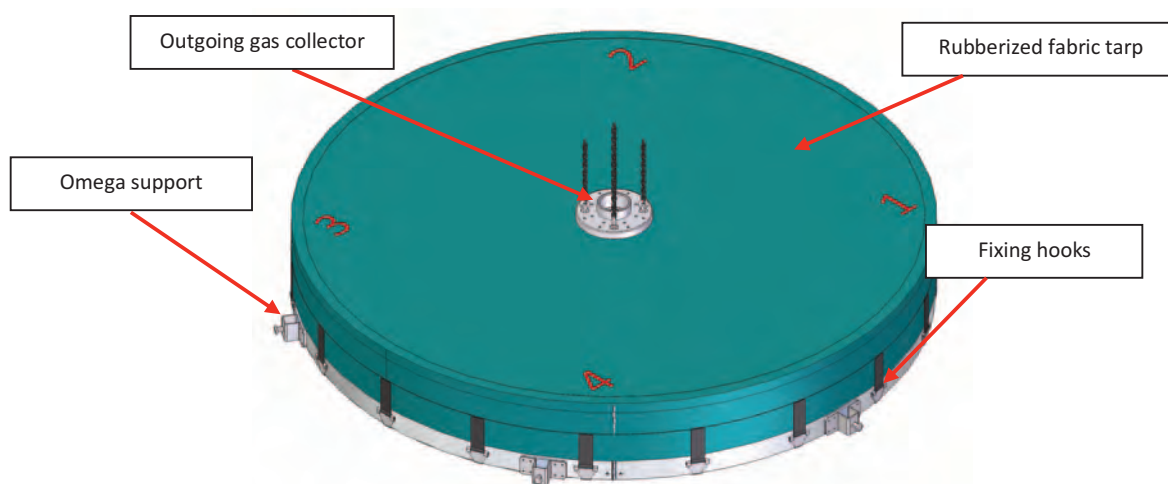


Figure 4: Conveying hood views

On the edge of the cover tarp have been installed a series of hooks, which have the function of fixing the tarp to the aluminum cylinder.

2.4 Control and sampling systems

The control and analysis system consist of two distinct boxes: one dedicated to the control and the positioning of the drone (Control Box) and the other dedicated to the instrumentation and analysis (Sampling Box). The two boxes are connected to each other through a specific multipolar cable that allows data communication on the RS-485 BUS and the transport of the power supply (12-14 Vdc).

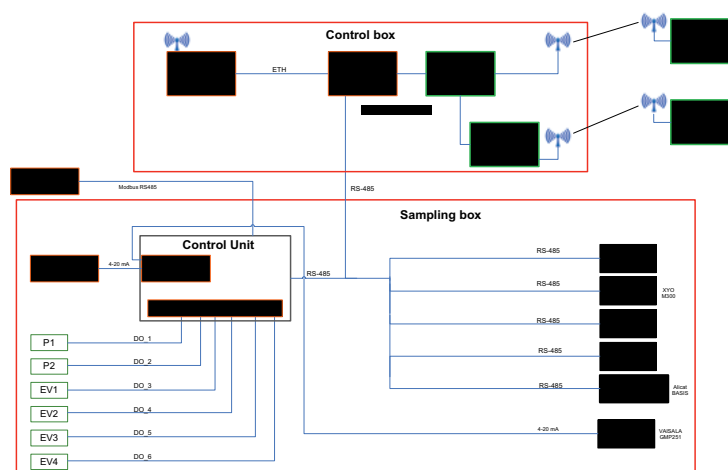


Figure 5: Control Box – Sampling Box connection diagram



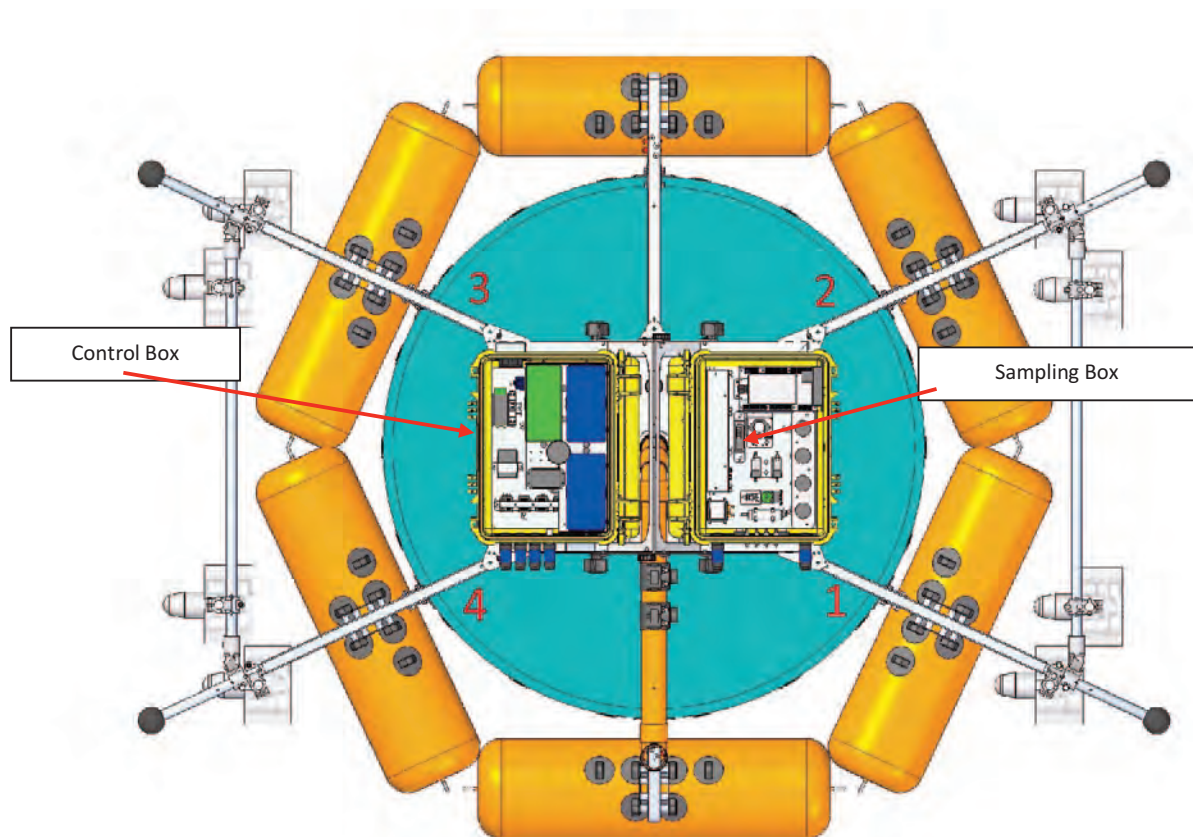


Figure 6: Control Box and Sampling Box disposition on the frame support

2.4.1 Control Box

Inside the control box there are the devices dedicated to the propulsion and navigation system, the PC, the 4G router for remote connection and the batteries (four battery packs dedicated to the propulsion system and one battery for the control system and the sampling and analysis unit).

The PC inside the Control Box mainly has a dual function, managing the sampling and data acquisition phases through the WS-SCADA software and managing the mission planning and parameter display part through the open source Mission Planner software.



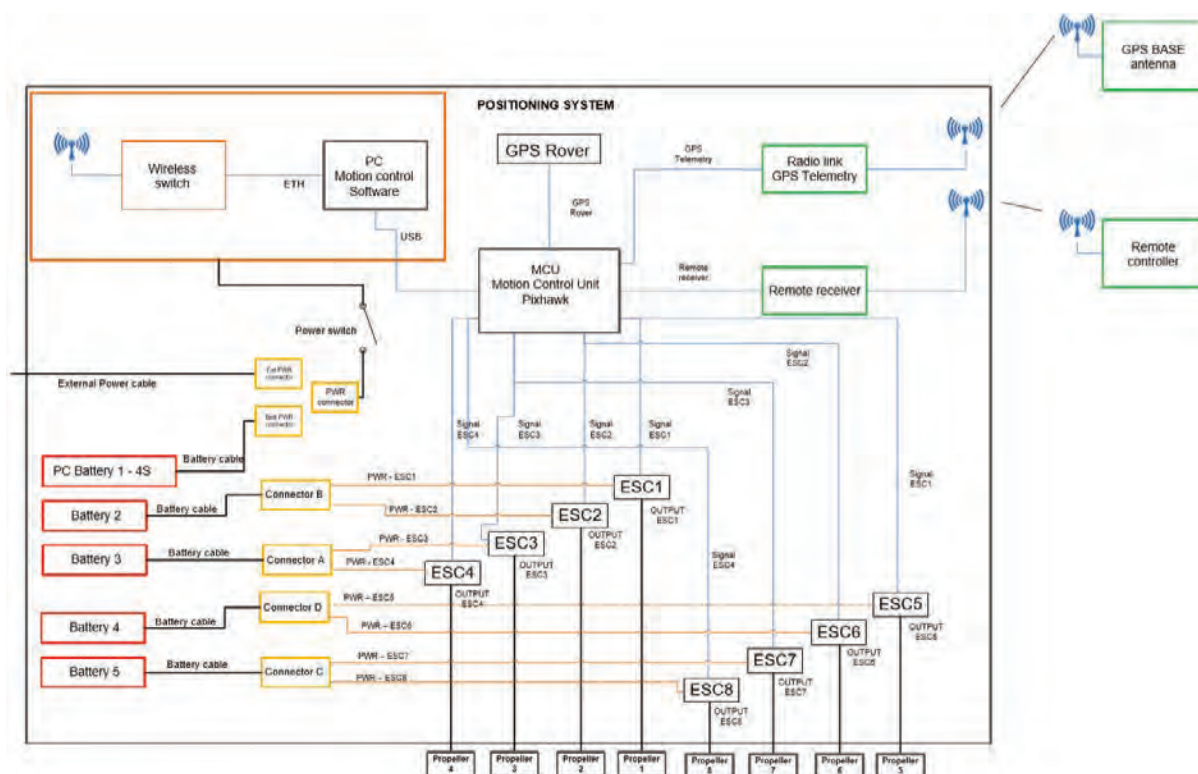


Figure 7: Connection diagram of the devices inside the Control Box

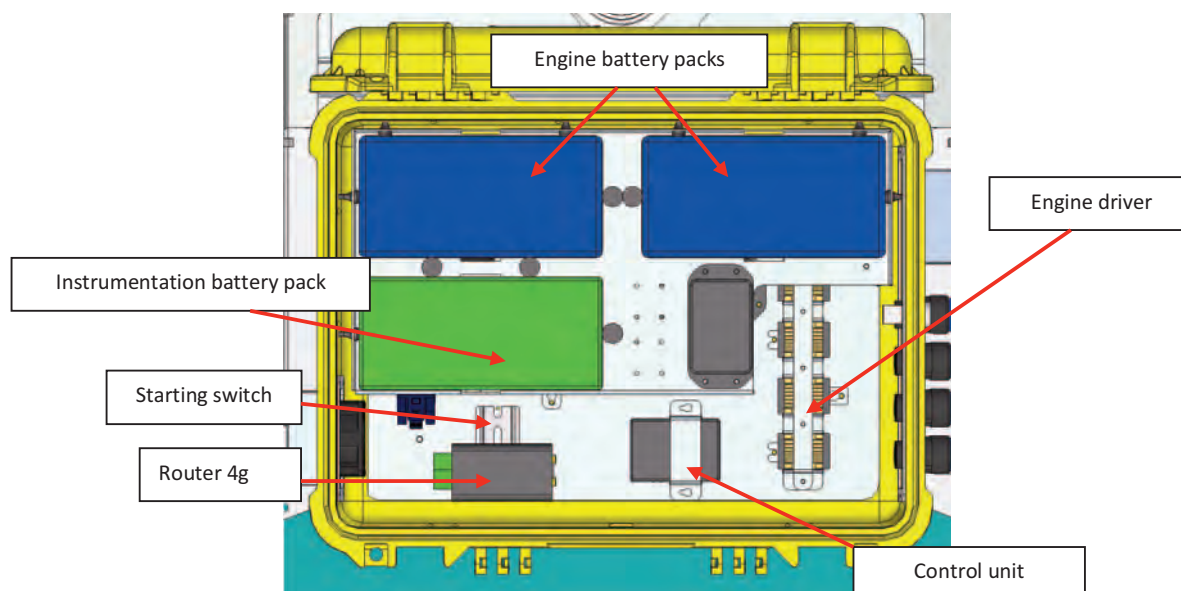


Figure 8: Internal view of the Control Box

2.4.1.1 Positioning and navigation system

The navigation and positioning system consist of the MCU (Motion Control Unit) composed by the "pixhawk" device to which both the communication systems (remote control, GPS) and the propeller piloting devices (ESC - Electronic Speed controller) are connected.

MCU (Motion Control Unit)

The control unit consists of a controller (Pixhawk), which is very popular in the world of drone developers and which has the characteristic of having an open source development environment and a community of developer users

"Pixhawk" is an independent open-hardware project that aims to provide the standard for readily available, high-quality, low-cost autopilot hardware projects for academic communities, hobbies and developers.



Figure 9: Pixhawk 3 Unit Control

The technical characteristics of the control unit are shown below

Pixhawk Pro Characteristics	
Mechanical	
Weight	83g
Size	72 x 50 x 23 mm
Spacing	20mm
Operating T°	-20°C to 60°C
Hardware	
Processors	IO processor STM32F1



	FMU processor STM32F4
Sensors	LIS3MDL
	MPU9250
	ICM 20602
	MS5611
Indicator	RGB LED
Electrical	
Supply Voltage	4.7V / 5.3V
Power Supply	Power Module, USB
	Independant servo Rail
Average current consumption	200mA
Logic level voltage	3.3V
Ports	
PWM	x14
CAN	x2
I2C	x2
RSSI INPUT / SBUS OUTPUT	x1
SERIAL	x6
SBUS / PPM INPUT	x1
POWER REDUNDANT	x2
DEBUG PORTS	x2

ESC (Electronic Speed Controller)

The ESC drivers have the function of regulating the rotation speed of the propellers and, therefore, the power, by adjusting the current supplied towards the propellers themselves.





Figure 10: Driver ESC for brushed motors

Technical characteristics

Motor Driver (ESC)	
Material	Aluminium alloy + plastic
Dimentiom	42 * 28 * 17mm
Weight	54g
Constant current	35A
Peak current	160A
Supply voltage	Li-Po batteries or 5,3 S NiMH batteries
BEC Output	1A / 5V

ROUTER 4G

Inside the Control Box there is a router "Teltonika RUT955 H7V3C0". This highly secure and reliable industrial device is an LTE router with WiFi equipped with Ethernet interfaces, digital and analogic I / O, RS232, RS485, GNSS (GPS), microSD and USB. It allows both data connection via a 4G SIM card present inside and a wireless connection, whose signals are amplified thanks to the presence of three external antennas, two for Wi-Fi and one for mobile connection.

The Teltonika router in the Lessdrone also performs the function of serial converter (rs485 / rs232) - ethernet, receiving the signals coming from the Sampling Box and transmitting them to the PC, and the function of network switch, through the four ethernet ports present.





Figure 11: Teltonika Router RUT955 H7V3C0

Hardware	
Mobile	4G (LTE) – Cat 4 DL up to 150 Mbps, UL up to 50 Mbps; DC-HSPA+; UMTS; TD-SCDMA; EDGE; GPRS
CPU	Atheros Wasp, MIPS 74Kc, 550 MHz
Memory	16 MB Flash, 128 MB DDR2 RAM
Ethernet	4 x 10/100 Ethernet ports: 1 x WAN (configurable as LAN), 3 x LAN ports
Power supply	9 – 30 VDC, 4 pin DC connector
PoE (passive)	Passive PoE over spare pairs. Possibility to power up through LAN port, not compatible with IEEE802.3af and 802.3at standards
Inputs	3 x Inputs (Digital, Digital galvanically isolated, Analog) + 1 Digital Input on power connector
Outputs	2 x Outputs (30 V, 250 mA digital open collector output / 24 V, 4 A SPST relay output) + 1 Digital O.C. Output on power connector
Connectors	1 x 4 pin DC, 4 x Ethernet, 2 x Mobile SMA, 2 x WiFi RP-SMA, 1 x GPS SMA, 1 x RS232, 1 x 6 pin RS485, 1 x 10 pin I/O, USB 2.0
Memory Card	microSD, Hinge Type slot
SIM	2 x external SIM holders
Status LEDs	1 x bi-color connection status, 5 x connection strength, 4 x LAN status, 1 x Power
Operating temperature	-40 °C to 75 °C
Housing	Aluminium housing, plastic panels
Dimensions	100 mm x 110 mm x 50 mm
Weight	287 g
Software	
Operating system	RutOS (OpenWrt based Linux OS)
SIM switch	2 SIM cards, auto-switch cases: weak signal, data limit, SMS limit, roaming, no network, network denied, data connection fail
Multiple PDN	Possibility to use different PDNs for multiple network access and services
Network protocols	TCP, UDP, IPv4, IPv6, ICMP, NTP, DHCP, DNS, HTTP, HTTPS, SSL v3, TLS, ARP, PPPoE, UPNP, SSH, Telnet, SNMP, VRRP, PPP, SMPP, MQTT, Wake On Lan (WOL)
Networking features	NAT, Static/Dynamic routing, Firewall, OpenVPN, IPsec, H.323 and SIP-alg protocol NAT helpers, allowing proper routing of VoIP packets
Unique networking features	VLAN, Load balancing, Mobile quota control, WEB Filter, Load Balancing, Network Backup, Auto Failover
Connection monitoring	Ping Reboot, Periodic Reboot, Wget Reboot, LCP and ICMP for link inspection
Authentication	Pre-shared key, digital certificates, X.509 certificates
Keep settings	Update FW without losing current configuration
Monitoring & Management	WEB UI, SSH, SMS, SNMP, JSON-RPC, FOTA, RMS
Supported languages	Busybox shell, Lua, C, C++
Development tools	SDK package with build environment provided

Figure 12: Teltonika Router RUT955 Data Sheet



GPS

The Pixhawk control unit is connected directly with the GPS Rover installed inside the Control Box and it is also connected with the GPS Base through a radio connection.

In this version of the drone the system with dual GPS and differential correction was adopted as it was assembled in the first version drone.

The first GPS (Rover) is directly connected to the control unit (Pixhawk) and it allows the direct detection of the position of the drone, as well as the orientation. To improve radio signal reception, the GPS (Rover) is connected to an antenna placed externally at the top of the Control Box.

The second GPS (Base) is positioned in a fixed point at a distance from the drone and communicates with the control unit via a radio link.

The communication between the control system and the two GPS (Rover + Base) allows to perform a real-time relative position correction (RTK) which can lead, in conditions of optimal satellite visibility, to have centimeter accuracy on the detected position of the Rover.

The use of the drone's on-board GPS (Rover) alone allows to identify the position with a maximum precision of about 5 meters.



Figure 13: Rover GPS e related antenna (above) e Base GPS (below)

The technical characteristics of the two GPS systems and the Rover antenna are shown below:



Sirius RTK GNSS Rover (M8P)	
Mechanical	
Size	diameter 61mm
Weight	43g
Operating T°	-20°C to 60°C
Electrical	
Supply Voltage	5V
Average Current Consumption	33mA
Hardware	
Chip	M8P-2
Sensor	LIS3MDL
Antenna	Active
Data	
Input Protocol	RTCM3 UBX NMEA
Output Protocol	RTCM3 UBX NMEA
Logs	UART
GNSS	
Signal	Beidou GPS Glonass Galileo
Tracking Channels	72
Update Rate	14Hz / 5Hz
Positioning	
Accuracy	0.025 m + 1 ppm CEP
Convergence Time	<60s



TW3740 / TW3742 Multi-Constellation Antenna

Specifications Vcc = 3V, over full bandwidth, T=25°C

Antenna

Architecture	Dual, Quadrature Feeds
2 dB Bandwidth	47 MHz
Antenna Gain (with 100mm ground plane)	4.25 dBic
Axial Ratio (over full bandwidth)	<2 dB typ., 3 dB max.

Electrical

Filtered LNA Frequency Bandwidth	1559 to 1606 MHz
Polarization	RHCP
LNA Gain	TW3740: 40 dB min., TW3742: 38dB min
Gain flatness	+/- 2 dB, 1559 to 1606 MHz
Out-of-Band Rejection	<1500 MHz >32 dB (TW3740) >50dB (TW3742)
	>1640 MHz >35 dB >70 dB
VSWR (at LNA output)	<1.5:1 typ. 1.8:1 max
Noise Figure	TW3740: 1 dB typ. TW3742: 3dB typ.
Supply Voltage Range (over coaxial cable)	2.5 to 16 VDC nominal (12VDC recommended max.)
Supply Current	19 mA typ.
ESD Circuit Protection	15 KV air discharge

Mechanicals & Environmental

Mechanical Size	66.5 mm dia. x 21 mm H
Operating Temp. Range	-40 to +85 °C
Storage Temperature Range	+45 to +85 °C
Enclosure	Radome: EXL9330, Base: Zamak White Metal
Weight	150 g
Attachment Method	Permanent 3/4" (19mm) through hole mount
Environmental	IP67, RoHS, REACH, and RED compliant
Shock	Vertical axis: 50 G, other axes: 30 G
Vibration	3 axis, sweep = 15 min, 10 to 200 Hz sweep: 3 G
Salt Spray	MIL-STD-810F Section 509.4

SIRIUS RTK GNSS Base (M8P)

Mechanical	
Size	107 x 107 x 84mm
Weight	390g
Operating T°	-20°C to 60°C
Electrical	
Supply Voltage	5V
Average Current Consumption	33mA
Hardware	
Chip	M8P-2
Sensor	None
Antenna	Active



Data	
Input Protocol	RTCM3 UBX NMEA
Output Protocol	RTCM3 UBX NMEA
Logs	USB UART
GNSS	
Signal	Beidou GPS Glonass Galileo
Tracking Channels	72
Update Rate	14Hz / 5Hz
Positioning	
Accuracy	0.025 m + 1 ppm CEP
Convergence Time	<60s

Batteries

The control system is powered by a 20 Ah LiPo 4S capacity battery pack and a rated voltage of 14.8 Vdc which allow the control system and the sampling system to be autonomous for about 10 hours.

The propellers are powered by four 44 Ah LiPo 3S battery packs each with a rated voltage of 11.1 Vdc. The propellers autonomy mainly depends on the conditions of use of the drone and can vary from 1 hour to 4 hours approximately.

The characteristics of the batteries described are shown below:

Instrumentation Battery	
Minimum Capacity:	20000mAh
Configuration:	4S1P / 14.8V / 4Cell
Constant Discharge:	10C
Peak Discharge (10sec):	20C
Pack Weight:	1770g
Pack Size:	202 x 93 x 46mm
Charge Plug:	JST-XH
Discharge Plug:	XT90



Propeller Battery	
Minimum Capacity:	44000mAh
Configuration:	3S2P / 11.1V / 3Cell
Constant Discharge:	10C
Peak Discharge (10sec):	20C
Pack Weight:	2655g
Pack Size:	202 x 93 x 75mm
Charge Plug:	JST-XH
Discharge Plug:	XT90

Propellers

The drone is driven by eight double blade propeller motors, powered at 12 Vdc, each of which capable of delivering a thrust of about 8.2 kgf

These motors are presented in a free propeller configuration, for this reason supports have been designed and built to be installed on the propeller that allow the protection of them from any external impacts and to channel the flow of fluid inside.

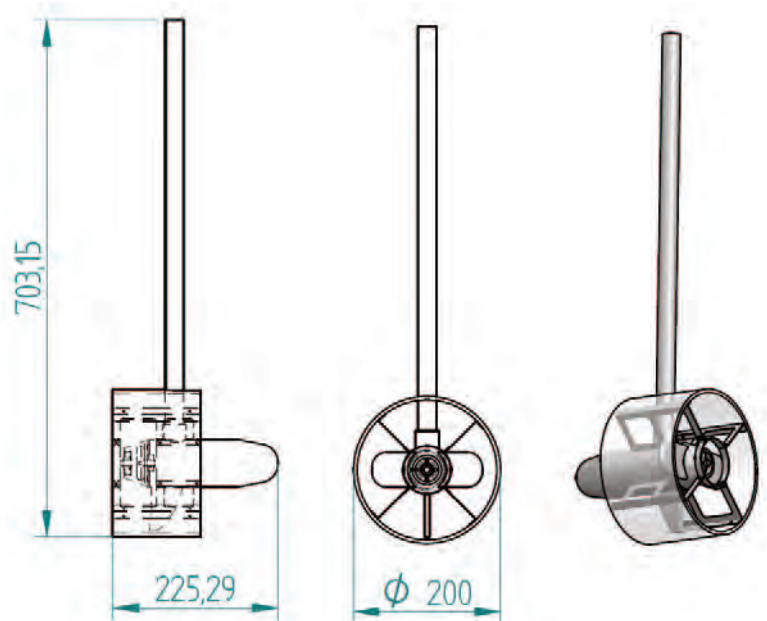


Figure 14: View of the propeller complete with support and protection cage



2.4.1.2 Software for remote control

In the PC, inside the Control Box, two software for remote control are installed, allowing the management of the drone and the ongoing tests via an internet connection.

Anydesk

Anydesk is a software for connecting to a computer remotely. To connect to the Lessdrone PC using the Anydesk software, it is necessary to download it to your personal computer and have an internet connection.

Once downloaded, open the software and connect, via the "Remote Desktop", by entering the ID credentials "312193165" and the password "Lesswatt2018". Once connected, you will have access to the PC and, therefore, to all the functions of the drone.

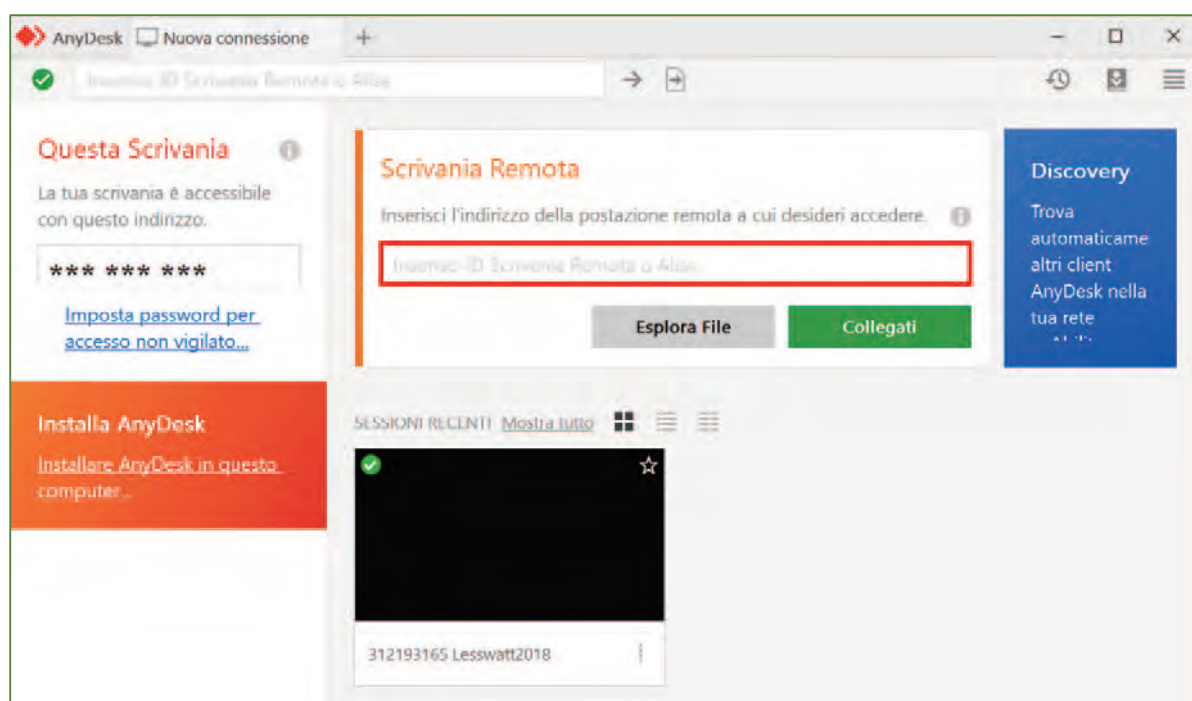


Figure 15: Anydesk screenshot

TeamViewer

TeamViewer is a software for connecting to a computer remotely and represents an alternative in case of malfunction of the Anydesk software. To connect, download the software and install it on your PC. To access the computer of the Lessdrone, enter, through the "Controlla computer remoto" function, the ID credentials "1266165323" and the password "Lesswatt2018". Once connected, you will have access to the PC and, therefore, to all the functions of the drone.



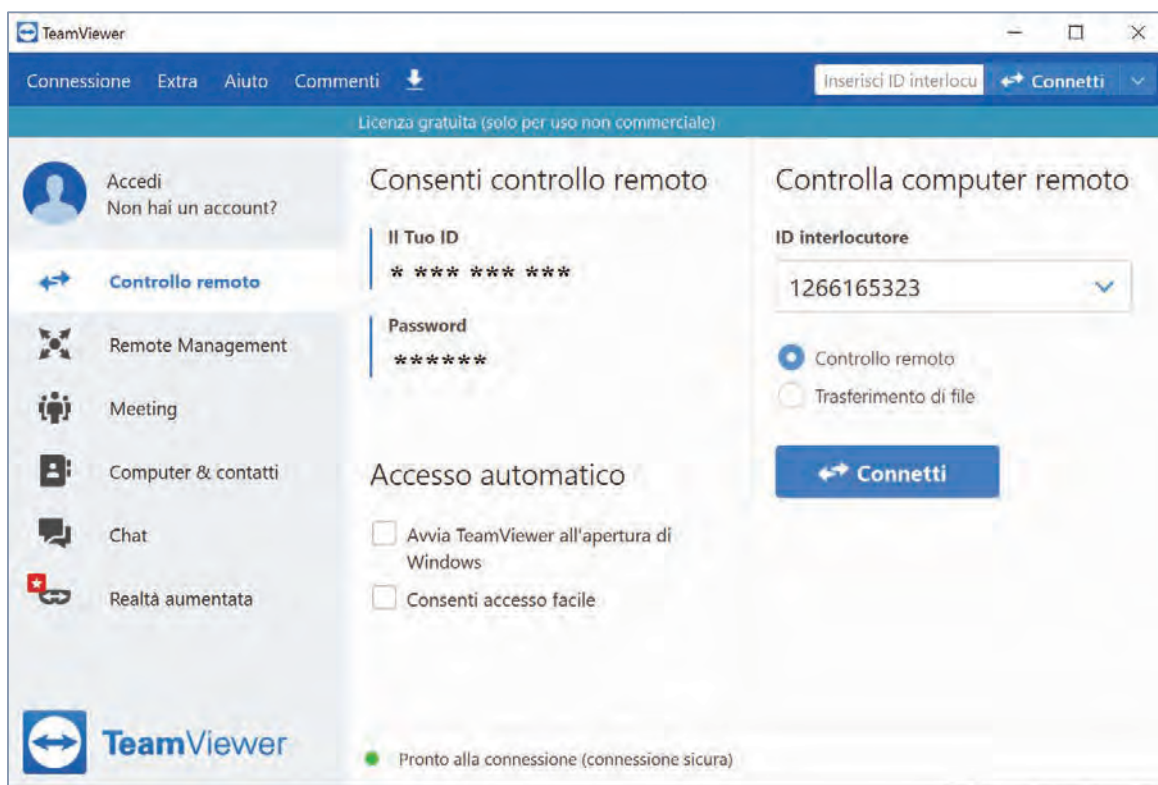


Figure 16: TeamViewer screenshot

2.4.2 Sampling Box

The instrumentation needed to carry out analyzes on the off-gas sample is housed inside the Sampling Box.

The air velocity and dissolved oxygen probes are also connected to the box.

The first is inserted inside the collection tube and measures the speed of the air passing through the tube itself, the second is hung from the drone frame and measures the concentration of dissolved oxygen in the liquid.

Sampling circuit

The sampling circuit is contained within the Sampling Box and is controlled by the local control unit (LCU) which manages the digital and analog I/O system and communicates with the WS-SCADA software installed on the PC.



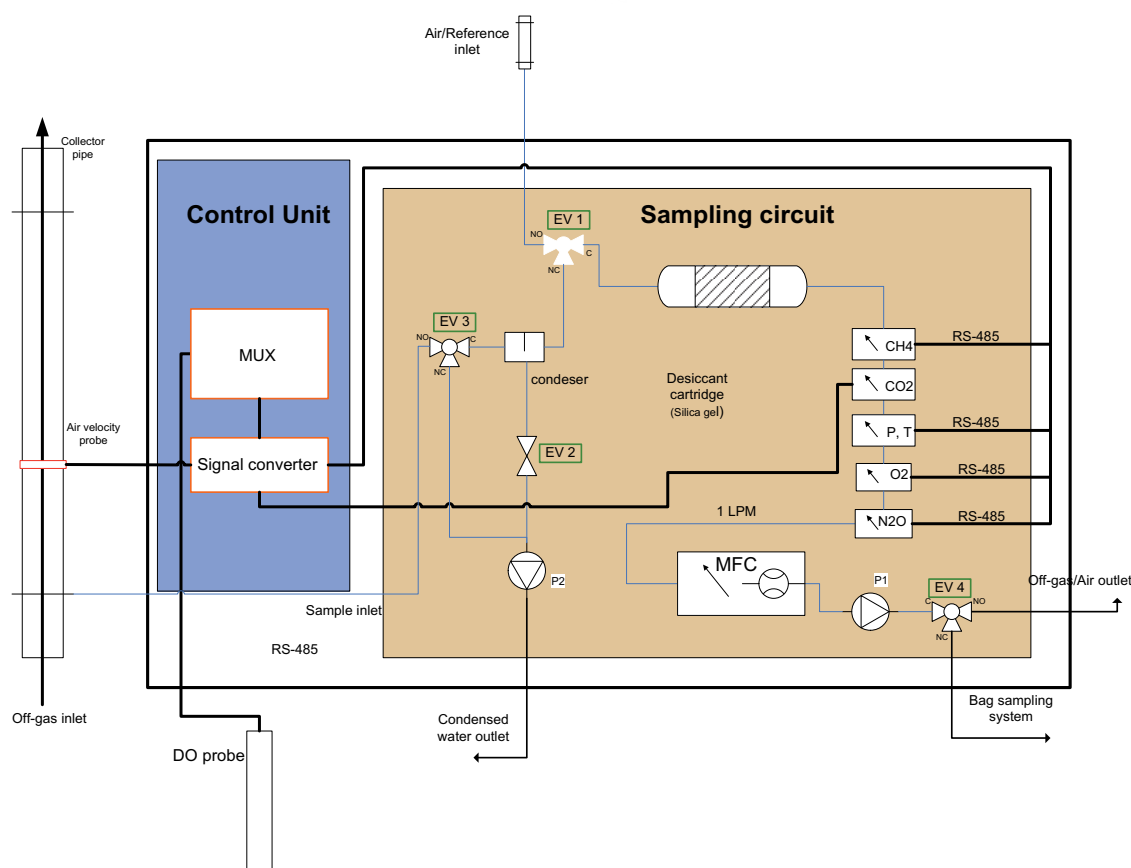


Figure 17: Sampling Box and sampling circuit

The sampling circuit takes the sample from the collection tube through a clamp saddle that connects with a suction tube with an external diameter of 4 mm. The tube connects to the Sampling Box through one of the bulkhead fittings on the interface flange.

The sample passes through a condensate collection system consisting of a section of steel pipe on which there are 3 fittings to form a T (sample inlet, sample outlet and condensate drain). Subsequently, the sample passes through the silica gel section consisting of four cartridges placed in parallel to form a total volume of approximately 700 cc of silica gel, which has the function of removing the residual moisture from the sample.

After the silica gel cartridges, the sample enters the analysis part where the analyzers of CO₂, CH₄, N₂O, O₂ are installed in series on the line and also provides the accessory measurements of humidity, temperature and pressure.

The sampling flow is regulated by a mass flow controller (MFC), controlled through the data bus by the control unit, which acts on the circuit upstream of the sampling pump.

The sample is then pushed by the pump outside the Sampling Box.



To complete the sampling circuit there are:

- The system for emptying the condensate collection section, consisting of two solenoid valves and a peristaltic pump. This is automatically activated by the control software when necessary.
- A 3-way inlet solenoid valve that allows you to choose whether to aspirate the sample from the collection tube or from a second inlet dedicated to the reference test to be performed in the air.
- A solenoid valve at the pump outlet which allows the sample to be diverted to a second outlet where it is possible to connect a sampling bag to be kept on board the drone.

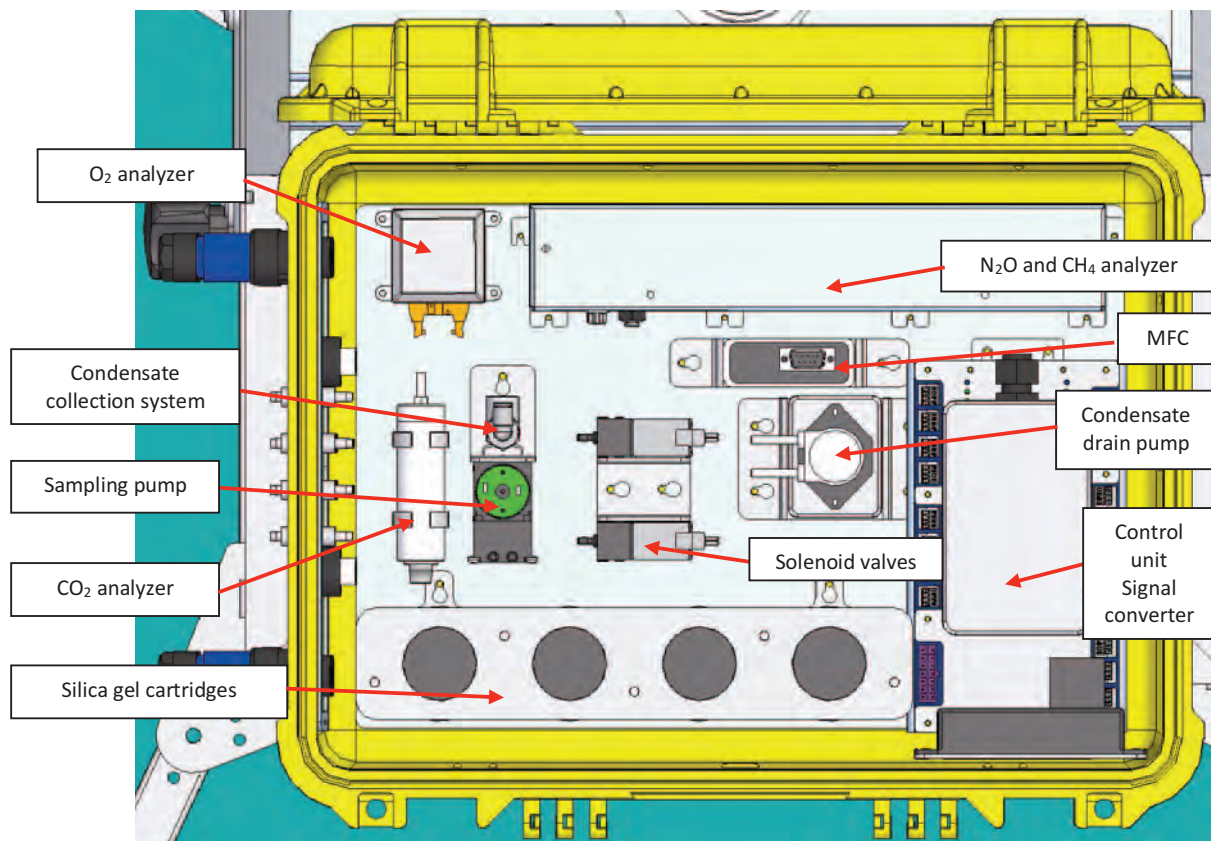


Figure 18: Sampling Box view and sampling circuit



2.4.2.1 Instrumentation technical characteristics

CO₂ analyzer

The carbon dioxide sensor chosen works with the principle of Near-Infrared absorption (NIR), is presented in a remarkably compact format for the measurement ranges of interest (0 – 20%).

The technical characteristics of the selected sensor are shown below (Vaisala GMP251):



Vaisala - GMP251 Carbon Dioxide Probe	
Measurement range	0 ... 20 %CO ₂
Accuracy at 25 °C (77 °F) and 1013 hPa	
At 5 %CO ₂	±0.1 %CO ₂
0 ... 8 %CO ₂	±0.2 %CO ₂
8 ... 20 %CO ₂	±0.4 %CO ₂
Operating temperature of CO ₂ measurement	-40 ... +60 °C (-40 ... +140 °F)
Storage temperature	-40 ... +70 °C (-40 ... +158 °F)
Weight, probe	45 g
Materials	
Probe housing	PET plastic
Filter	PTFE membrane, PET plastic grid



Connector	Nickel plated brass, M12 / 5 pin
IP rating, probe body IP65	probe body IP65
Connector	M12 5-pin male
Dimensions	
Probe diameter	25 mm
Probe length	96 mm

O₂ probe

The sensor used (first series of XYO sensors) adopts optical fluorescence technology for detecting oxygen concentration.



PERFORMANCE CHARACTERISTICS

(T_A=20 °C, P_A=1013 mbar. Following extreme temperature fluctuations, re-calibration may be required.)

Characteristics		Min.	Typ.	Max.	Unit
Oxygen measuring range	ppO ₂ partial pressure	0		300	mbar
	O ₂ concentration (XYO...P)	0		25	%O ₂
ppO ₂ partial pressure	Accuracy			2	%FS
	Resolution			0.1	mbar
O ₂ concentration (XYO...P)	Accuracy	Determined by ppO ₂ and pressure accuracy			
	Resolution			0.01	%
Pressure sensor (XYO...P)	Measuring range	500		1200	mbar
	Accuracy			±5	
	Resolution			1	
Temperature	Measuring range	-30		60	°C
	Accuracy	Indication only			
	Resolution			0.1	°C
Response time (10 to 90 %)			<30		s
Lifetime		5			years



N₂O analyzer

The sensor for N₂O works with the principle of Near-Infrared absorption (NIR) and has a fair sensitivity to CO₂. During the laboratory tests it was possible to characterize the response of the sensor to CO₂, in this way it will be possible to obtain the real concentration of N₂O calculated on the basis of the CO₂ concentration detected by the CO₂ sensor.



Detection Method	Dual channel Non-Dispersive InfraRed (NDIR)
Dimensions	depending on the sensor model (type of gas and range, see §5.1)
Source drive freq.	1 to 2Hz
Data refresh rate	5 to 10 seconds
Response time (t ₉₀)	15 to 40s @20°C ambient and @1l/min
Warm up time	<30s @20°C operational <30 minutes @20°C (full spec)
Operating conditions	Temperature 0°C to 50°C linear compensated
	Humidity 0-95% RH (non-condensing) not compensated
	Pressure 800-1150hPa not compensated
Pressure dependency	+1.5% reading per kPa deviation from normal pressure of 100kPa
Storage temperature	-40°C to 85°C
Analog Output	4-20mA, 0-5V
Analog Input	2 available for third-party devices
Digital I/O	4OUT: Open collector, ground referred, protected 4 IN: 0-5 V protected up to 24Vdc

Gas	Measurement Range *	Accuracy**	Zero Res. (ppm)	Full Scale Res.	Zero Repeatability (ppm)	Full Scale Repeatability (ppm)	Model
N ₂ O	0-2000ppm	±1% FS	1	1% FS	±10	±20	NG2-F-1



CH₄ analyzer

The methane sensor works with the principle of Near-Infrared absorption (NIR), below are the technical characteristics.



Detection Method	Dual channel Non-Dispersive InfraRed (NDIR)
Dimensions	depending on the sensor model (type of gas and range, see §5.1)
Source drive freq.	1 to 2Hz
Data refresh rate	5 to 10 seconds
Response time (t ₉₀)	15 to 40s @20°C ambient and @1l/min
Warm up time	<30s @20°C operational <30 minutes @20°C (full spec)
Operating conditions	Temperature 0°C to 50°C linear compensated
	Humidity 0-95% RH (non-condensing) not compensated
	Pressure 800-1150hPa not compensated
Pressure dependency	+1.5% reading per kPa deviation from normal pressure of 100kPa
Storage temperature	-40°C to 85°C
Analog Output	4-20mA, 0-5V
Analog Input	2 available for third-party devices
Digital I/O	4OUT: Open collector, ground referred, protected 4 IN: 0-5 V protected up to 24Vdc



Gas	Measurement Range *	Accuracy**	Zero Res. (ppm)	Full Scale Res.	Zero Repeatability (ppm)	Full Scale Repeatability (ppm)	Model
	0-2000ppm	±4% FS	5	4% FS	±15	±100	NG2-C-1

Air velocity sensor

The air speed is measured in the collection duct, placed above the collection tarp, through the use of a hot wire anemometer which will be inserted approximately in the middle of the duct and positioned in the center of the section. The anemometer is connected with a cable to the instrumentation box which contains its electronic board which transmits the analog signal to the data acquisition system.

The technical characteristics of the selected sensor are shown below (TSI 8465).



Anemometro - TSI 8465	
Accuracy	±2.0% of reading, ±0.5% of full scale
Field Selectable Range	25 ft/min up to 10,000 ft/min
Repeatability	< ±1% of reading
Response to Flow	0.2 seconds
Input Power	11 to 30VDC or 18 to 38 VAC, 350mA max
Output	Impedance Voltage mode: < 1 ohm, 20mA max source current
	Resistance Current mode: 500 ohms maximum load
	Signal Field selectable 0 to 5V, 0 to 10V, 2 to 10V, 0 to 20mA, 4 to 20mA



Dissolved oxygen sensor

For the measurement of oxygen dissolved in water, the RDO Pro-X sensor is used, based on oxygen fluorescence for measurement in water.

The probe is suitable for working in the operating conditions of wastewater treatment plants and requires no maintenance other than replacing the membrane when it runs out.



The technical characteristics are shown below:

Specifications	
Measurement System Performance	Range: 0 to 20 ppm, 0 to 200 % saturation Resolution: Below 10 ppm; 0.01 ppm, 0.1 % sat Above 10 ppm; 0.1 ppm, 0.1 % sat Accuracy: ±0.1 ppm up to 8 ppm, ±0.2 ppm from 8 to 20 ppm Step Response Time: 90 % in 30 seconds (at 25 °C) 95 % in 37 seconds
Operational Environment	Temperature Range: 0 °C to 50 °C (32 °F to 122 °F) Maximum Pressure: 300 psig @ 50 °C Maximum Flow Rate: No flow required
Power Requirements [†]	Voltage Range: 8 to 36 VDC
IP Rating	Environmental: IP-67 with cap off, IP-68 with cap installed
Construction	Sensor Head Material: Delrin & Polystyrene Weight: 0.93 lbs (without cable) Dimensions: 8 inches long (203.2 mm), 1.85 inch diameter (47 mm) Mounting Requirements: 1.25 inch NPT (internal thread on back of sensor for adapting to immersion hardware and floats)
Units Of Measure	Measurement Units: Dynamic Luminescence Quenching Temperature Units: °C, °F

Figure 19: Technical characteristics of DO sensor

Acquisition system

The acquisition card collects data from all peripherals and sensors and sends them via an RS-485 data bus to the PC residing on board the drone where the WS-SCADA software is running.



The interface card has been developed by West Systems to allow the connection of the acquisition system with sensors and automation devices. The card allows you to implement the automations through the digital outputs and control the devices connected via the serial port (RS-232 o RS-485)

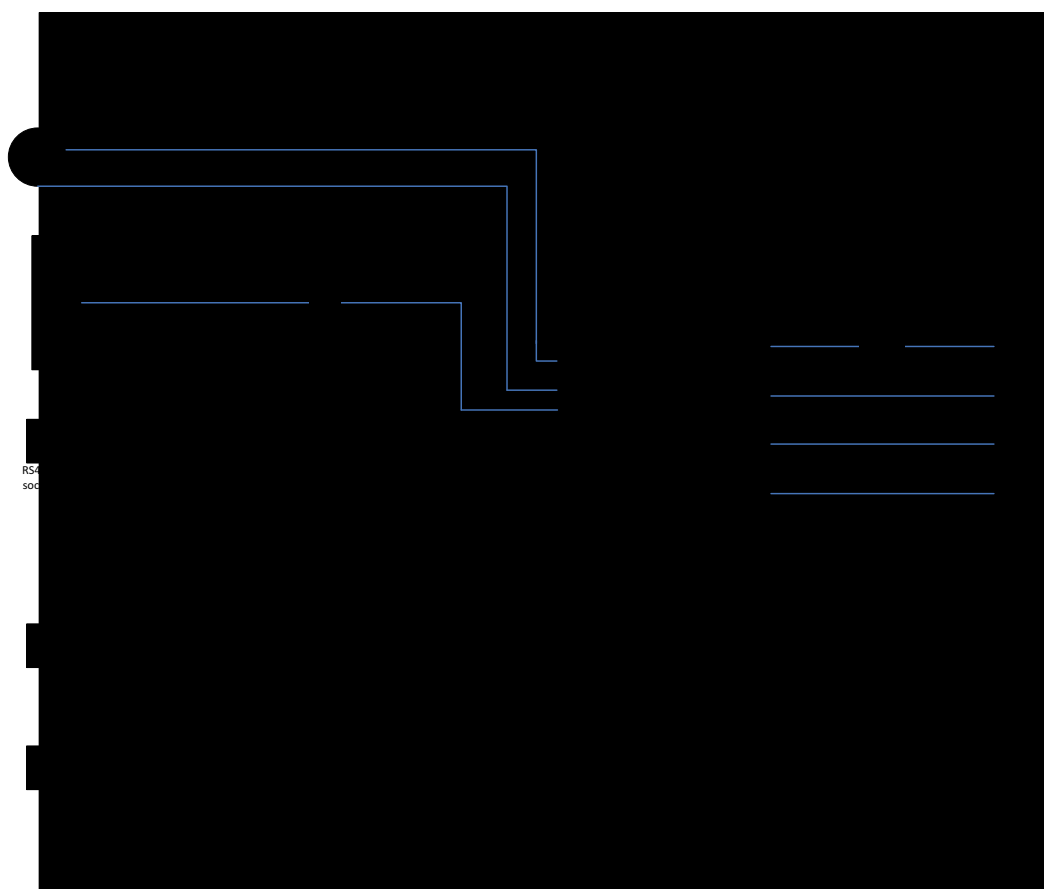


Figure 20: Electrical connection diagram of the electronic interface card.

The board is connected, via the RS-485 bus, to the PC and consequently to the WS-SCADA software which acquires the data from the sensors, saving them within a database and also manages the timings relating to the measurement operations.

Through the SCADA software configuration interface, it is possible to configure the measurement parameters and the relative timings.

2.4.2.2 Instrumentation calibration

Reliability and the possibility of operating in aggressive environments, such as the oxidation tanks of the treatment plants, were fundamental criteria for the choice of instrumentation inside the Lessdrone Sampling Box. For this reason, the selected probes do not require regular calibration.



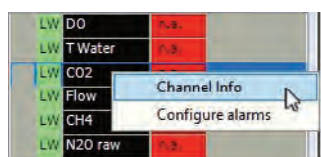
Despite this, before carrying out the field tests, it is recommended to carry out a check of the values measured by the instrumentation through the introduction of gas with a known concentration.

If there is a difference between the measurement and the expected value, it is possible to correct the measured value by using the "ChannelGainOffset" software present in the Lessdrone PC (C:\West\Scada\source). This software does not perform a real calibration of the instrumentation but allows you to change, according to the set criteria, the value returned by the probe and displayed in the WS-SCADA acquisition and control software.

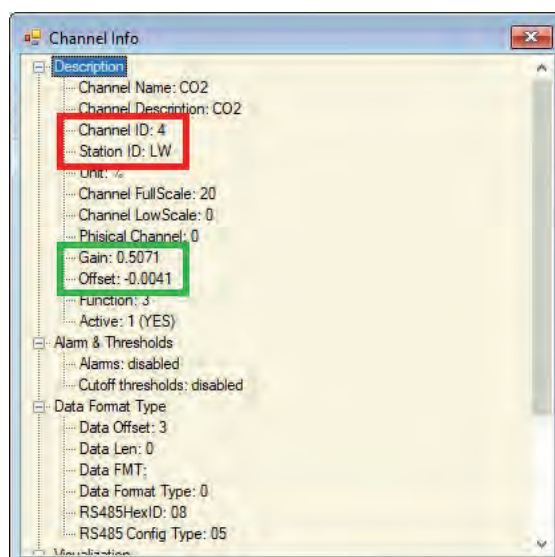
To carry out the calibration it is necessary to know at least 2 concentration values of the quantity of interest. Usually reference is made to the "zero concentration" value and to a "known concentration" value. In any case, having a greater number of concentration values available, the calibration accuracy will be better.

Build a graph, also using a spreadsheet, whose points will have the known concentration values as ordinate and the corresponding measured values as abscissa. Perform a linear regression of the points obtained and display the equation of the obtained straight line which will be in the form " $y = a x + b$ ". The value of a will corresponds to the *gain* and the term b to the *offset*. These values must be set to calibrate the sensor at known concentrations.

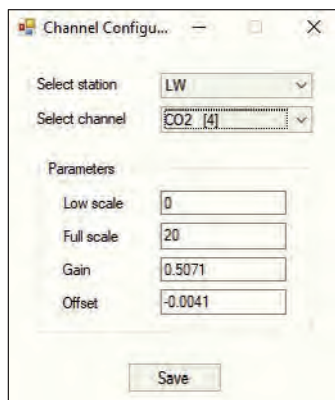
At this point it is necessary to obtain the information relating to the channel of the quantity of interest on WS-SCADA. Open WS-SCADA, right click on the quantity of interest (e.g. CO₂) and select "Channel Info"



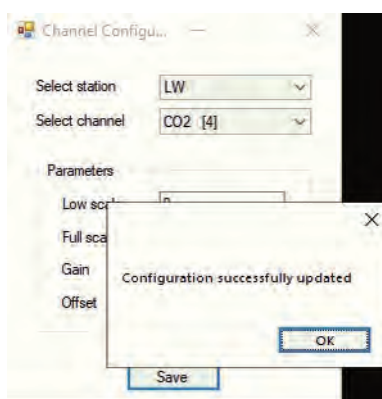
The window will display all the information relating to the selected channel. In particular, it is possible to view the Gain and the Offset currently set and the ID of the selected station and channel.



Once the "Channel ID" and "Station ID" information has been obtained, **close WS-SCADA** and open the "ChannelGainOffset" software. Use the relative drop-down menus to set the information just obtained.



The information relating to the selected channel will automatically be loaded. Set the new Gain and Offset values previously calculated and click the "Save" button. A new window will inform you of the outcome of the operation.



Press the "OK" button and close the software. Now you can re-open WS-SCADA and check the new values set through the "Channel Info" function.



3. Drone assembly

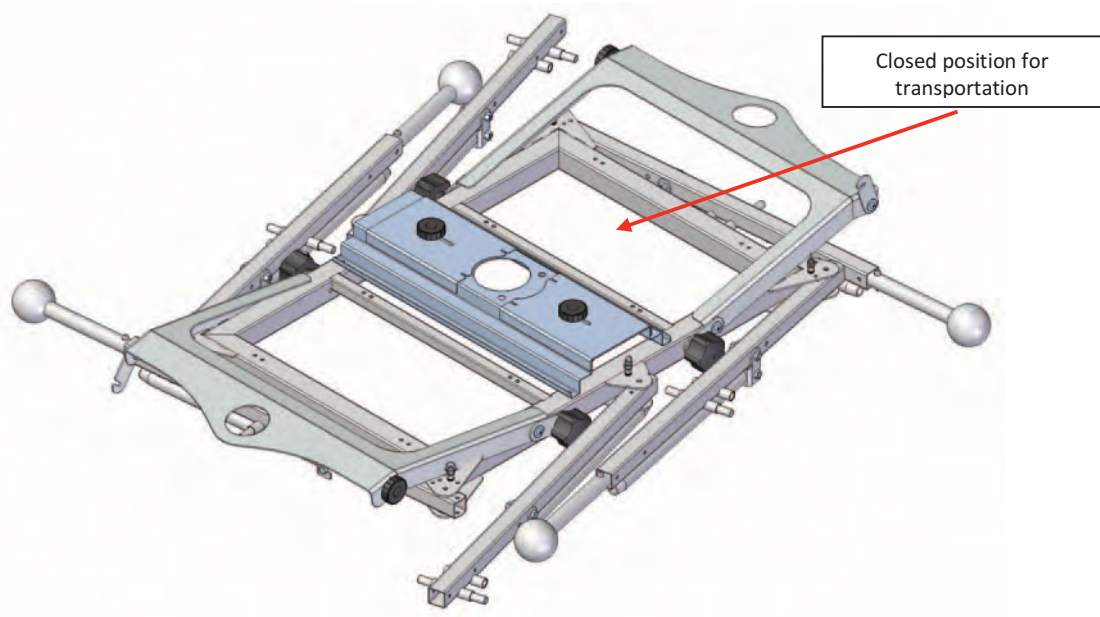
The Lessdrone instrument has been designed to be dismantled, making it easily transportable. Below is the correct assembly procedure to be carried out before being able to proceed with use in the oxidation tank.

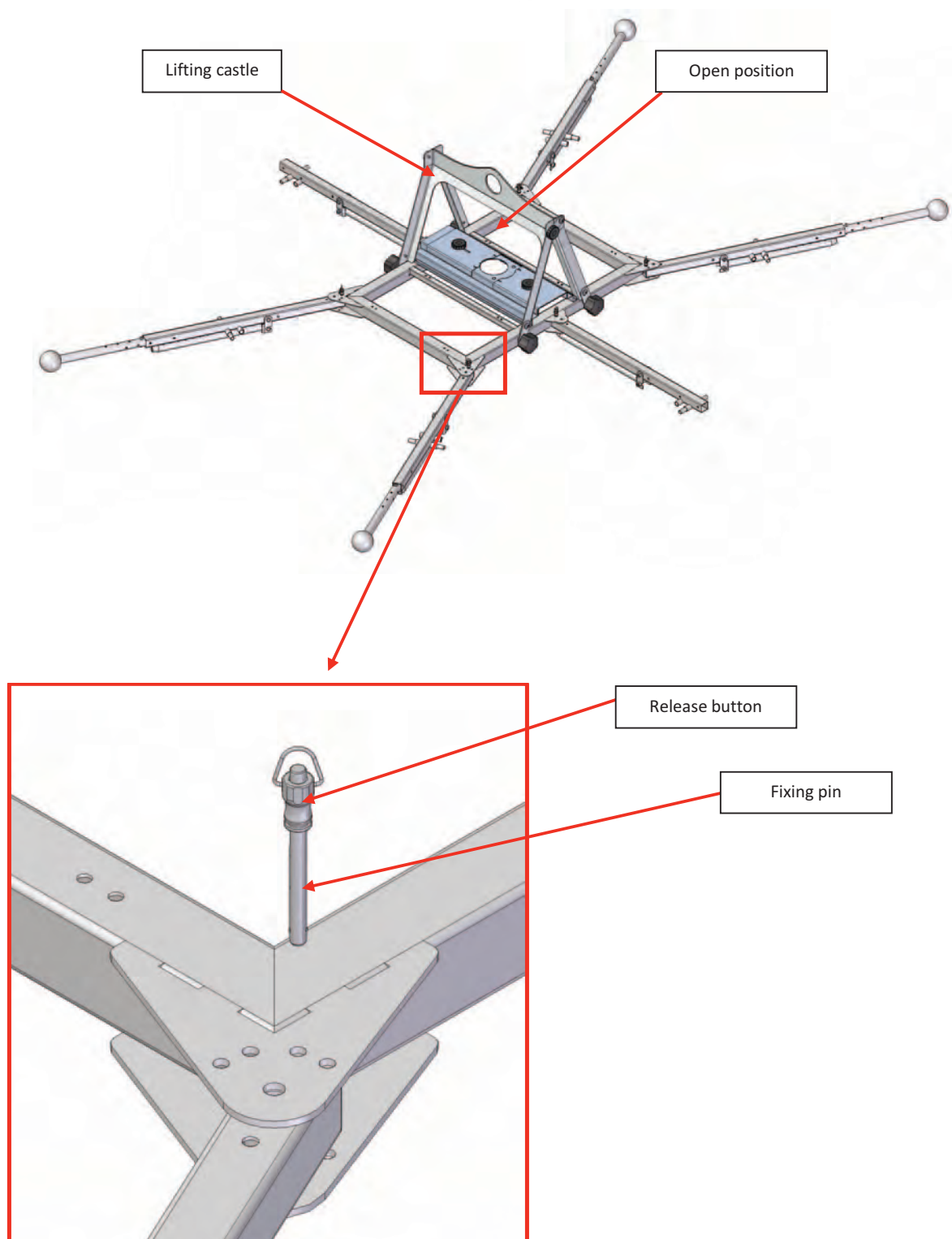
3.1 Frame

First take the closed frame in transport mode and extend the arms to the position shown in the figure.

To do this it is necessary to remove the fixing pins present in the point of anchorage of the arms to the frame. By removing the pins, it is possible to rotate the arms to the desired position and then lock them in position by reinserting the pin.

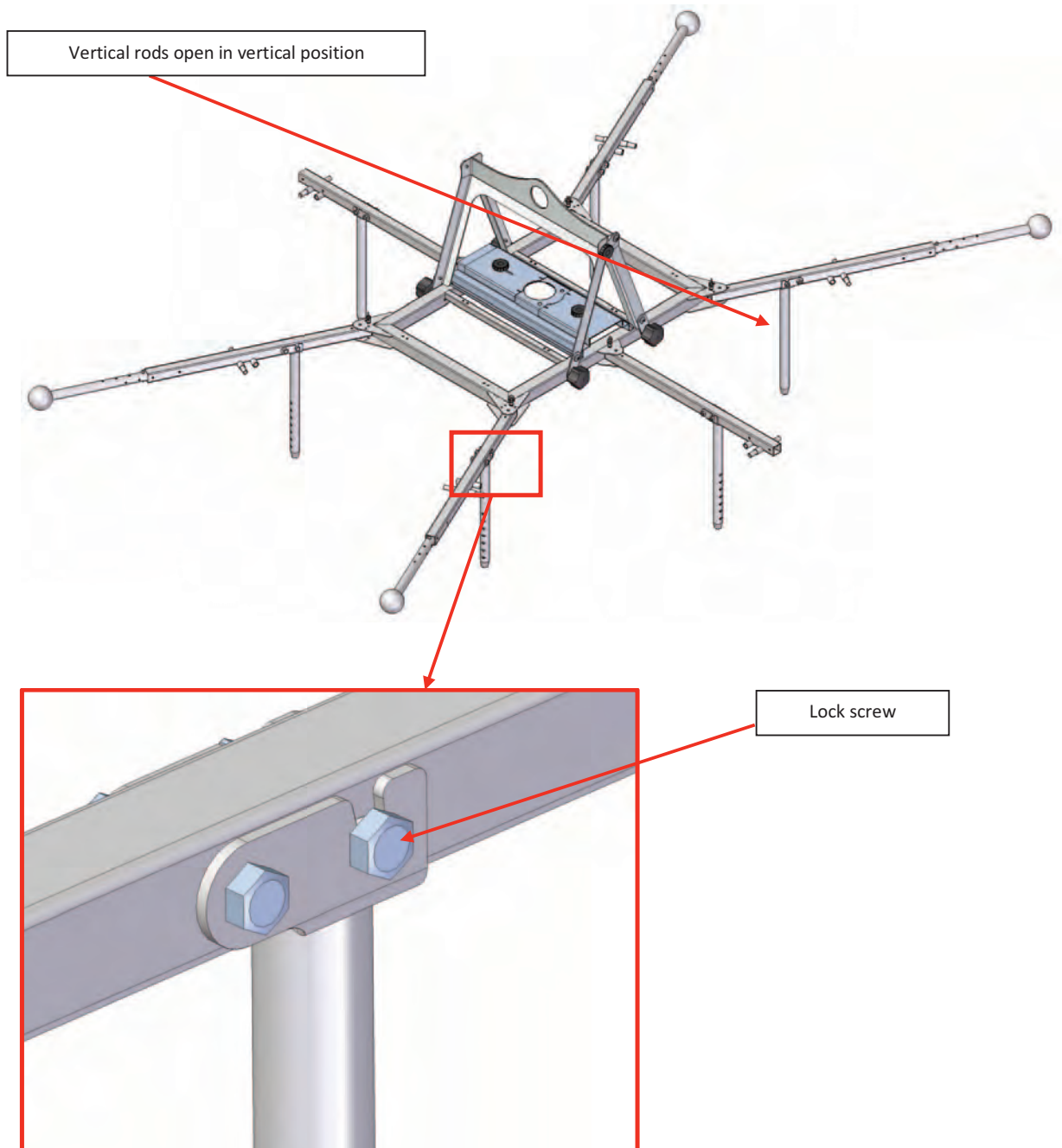
The fixing pins have a spring lock which can be removed using the button on the head. These pins are anchored to the frame through a steel cable.





Once the arms of the frame have been opened, it is necessary to extend the vertical rods supporting the hood. The vertical rods are anchored to the arms with a hexagonal screw that allows them to rotate to move from the horizontal to the vertical position.

Once in vertical position it is necessary to tighten the second screw to block the movement of the rod and keep it in vertical position.

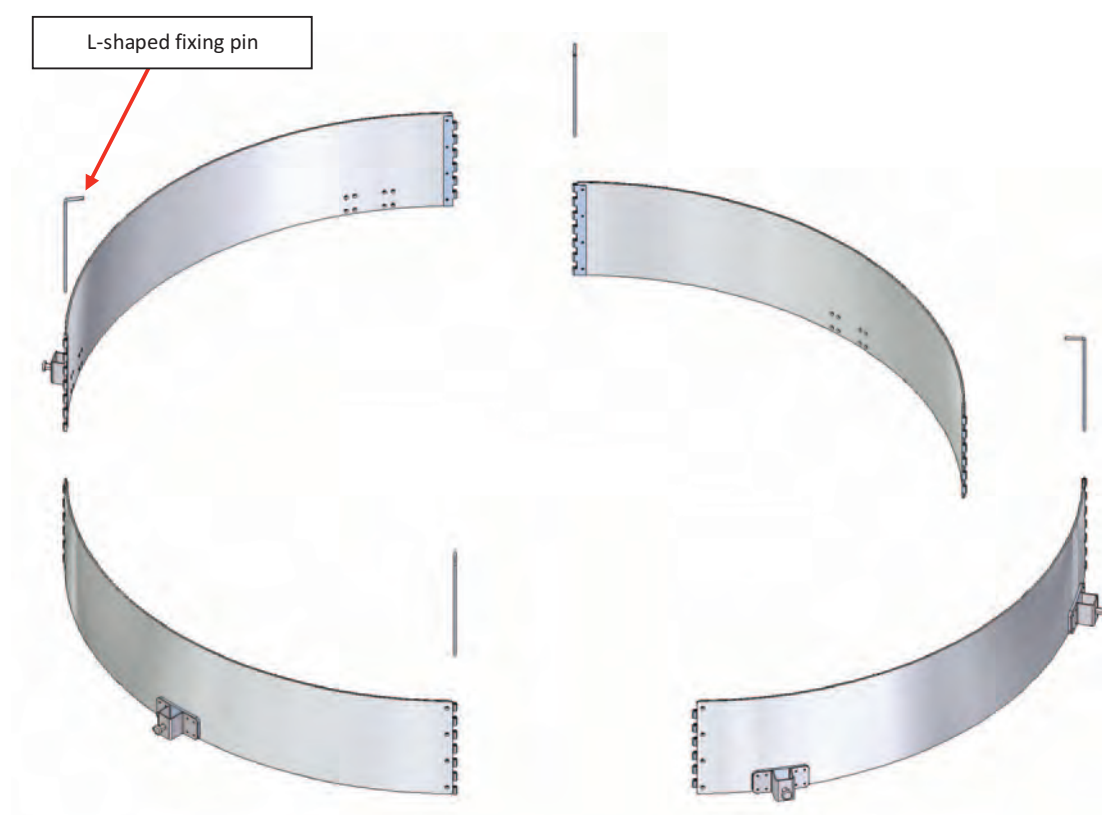


The aluminum lifting castle can be left open or in any case not fixed until the boxes are inserted. It can also be removed by unscrewing the appropriate fixing knobs

3.2 Conveying hood

To assemble the hood, it is first necessary to assemble the four parts of the aluminum cylinder and then insert and hook the rubberised tarp.

Position the four elements to form the circle, matching the numbers indicated above, and insert the L fixing pins, turn the L leg towards the inside of the cover and then insert the cover tarp until the hooks are fixed on the edge bottom of the cylinder.



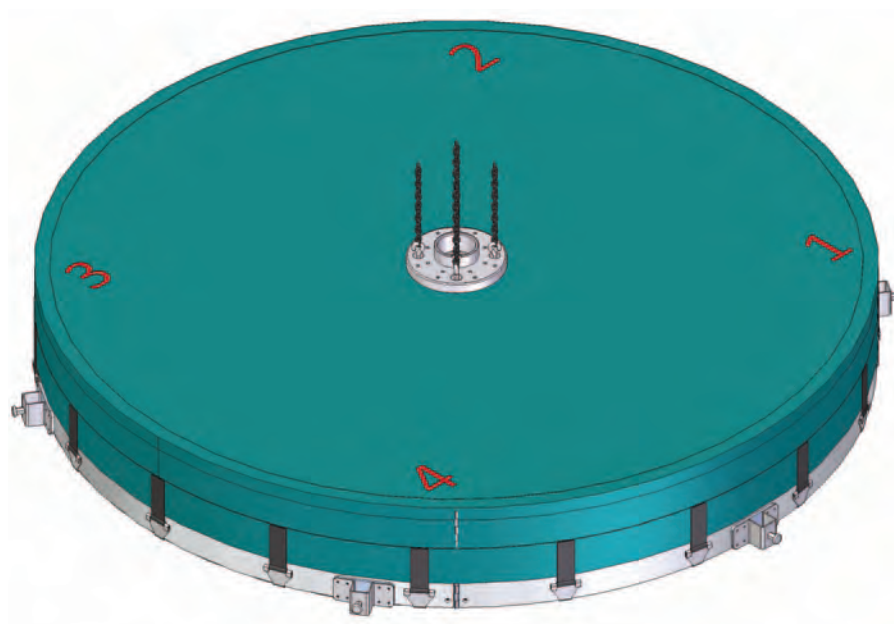
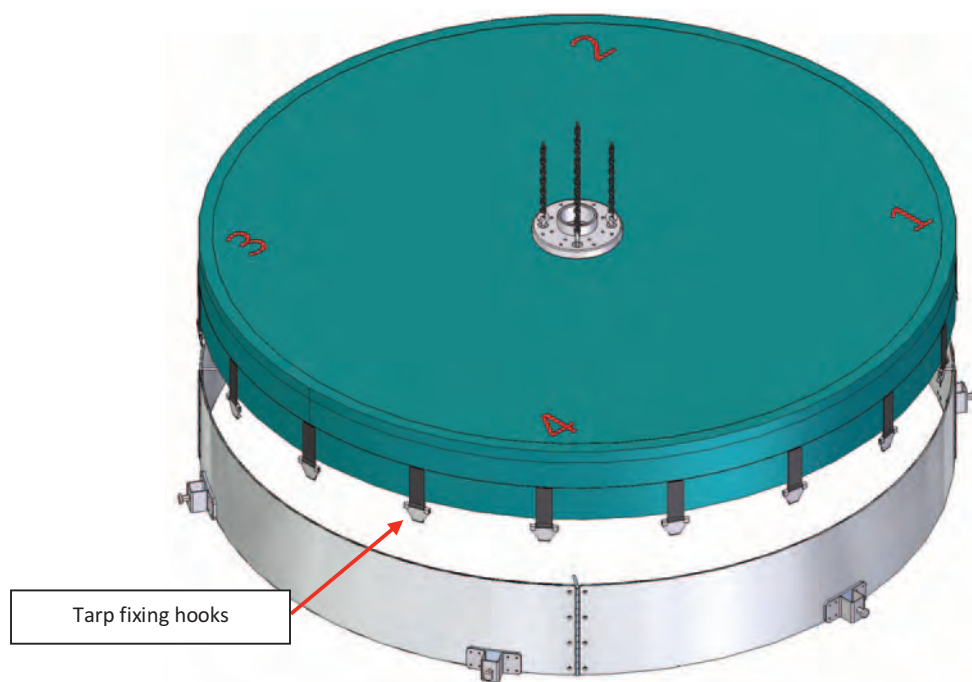


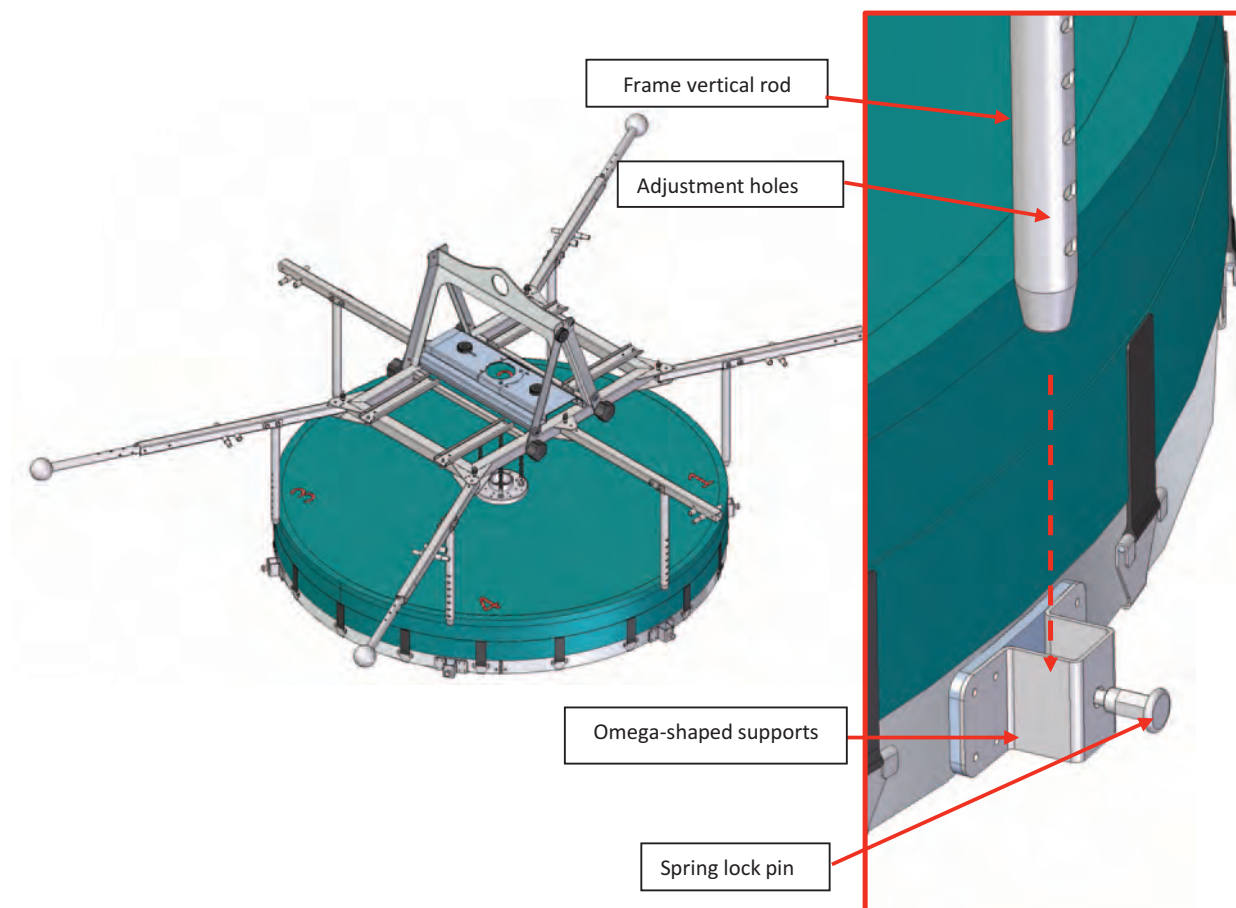
Figure 21: Assembly of the conveying hood



3.3 Assembly of the frame and conveying hood

Once the frame and the conveying hood are assembled, it is possible to proceed by joining the two parts.

The hood has 6 omega-shaped supports on which the 6 frame vertical rods are inserted. Spring-lock pins are installed on the omega supports which allow the hood to be fixed on the vertical rod.



The vertical rods presented numerous adjustment holes in order to adjust the height of the hood with respect to the waterline.

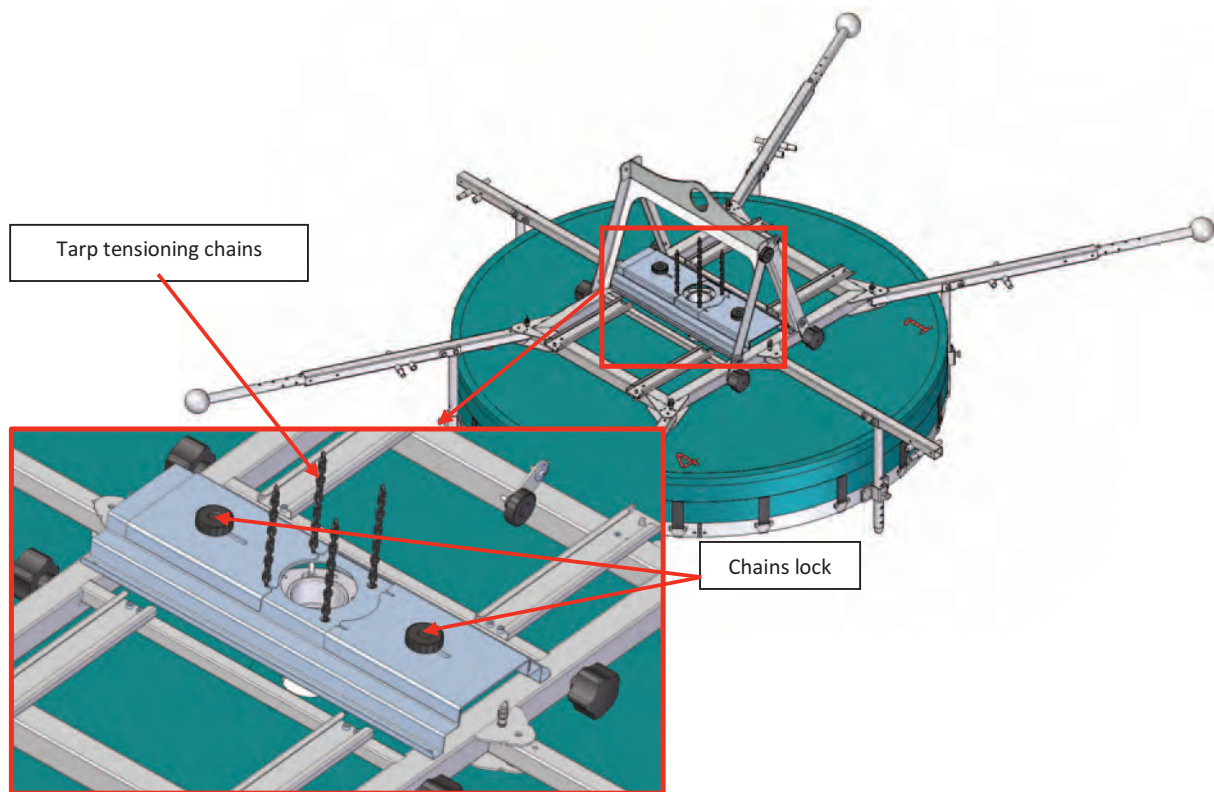
NOTE:

Make sure that all the spring lock pins reach the end of the stroke to be sure that the hood is correctly fixed to the frame.

Make sure that all the vertical rods are fixed at the same height (adjustment hole)



When the hood has been firmly fixed to the frame, it is possible to stretch the covering tarp by pulling it by means of the chains fixed on the connecting flange placed in the center of the tarp.



Loosen the knobs and slide the sheets towards the outside of the frame, thus freeing the holes on the central part of the frame. Insert the chains inside the slots provided on the frame and pull well upwards to taper the hood cover tarp.

Keeping the chains well taut, close the chains locks by sliding them towards the center of the frame in order to block the sliding of the chains. Tighten the knobs tightly.

NOTE:

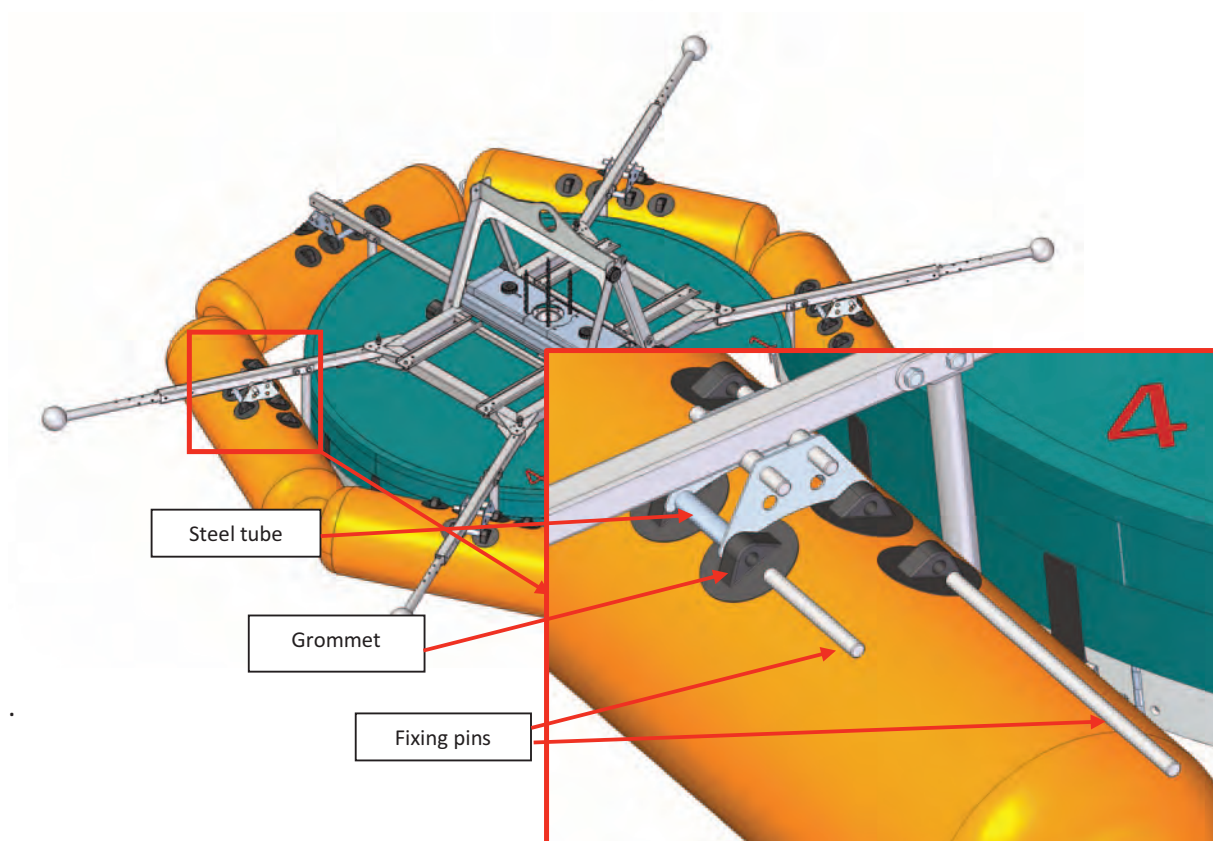
Make sure that the knobs are tightened once the chains locks are closed.

3.4 Assembly of the inflatable floats

To assemble the inflatables to the frame, it is necessary to slightly pre-inflate the cylinders with the specific inflation device provided, use the L-shaped fixing pin and bring the cylinders close to the arm in correspondence with the 2 tubes welded on the arm.

The steel tube must remain in the center of the grommets welded on the cylindrical inflatables. Once the tube and grommet are aligned, insert the two L-shaped pins.





The floating cylinders are fixed, it is possible to complete the inflation of the cylinders at the working pressure (0.24 bar).

NOTE:

To facilitate the insertion of the L-shaped pins, the cylinders must be inflated to a much lower pressure than the working pressure.

3.5 Assembly of the collection tube

To install the collector pipe on the hood, it is necessary to open the lifting castle and insert the pipe in the hole of the fitting flange. The flange is equipped with an o-ring which allows the connection to be sealed with the pipe.



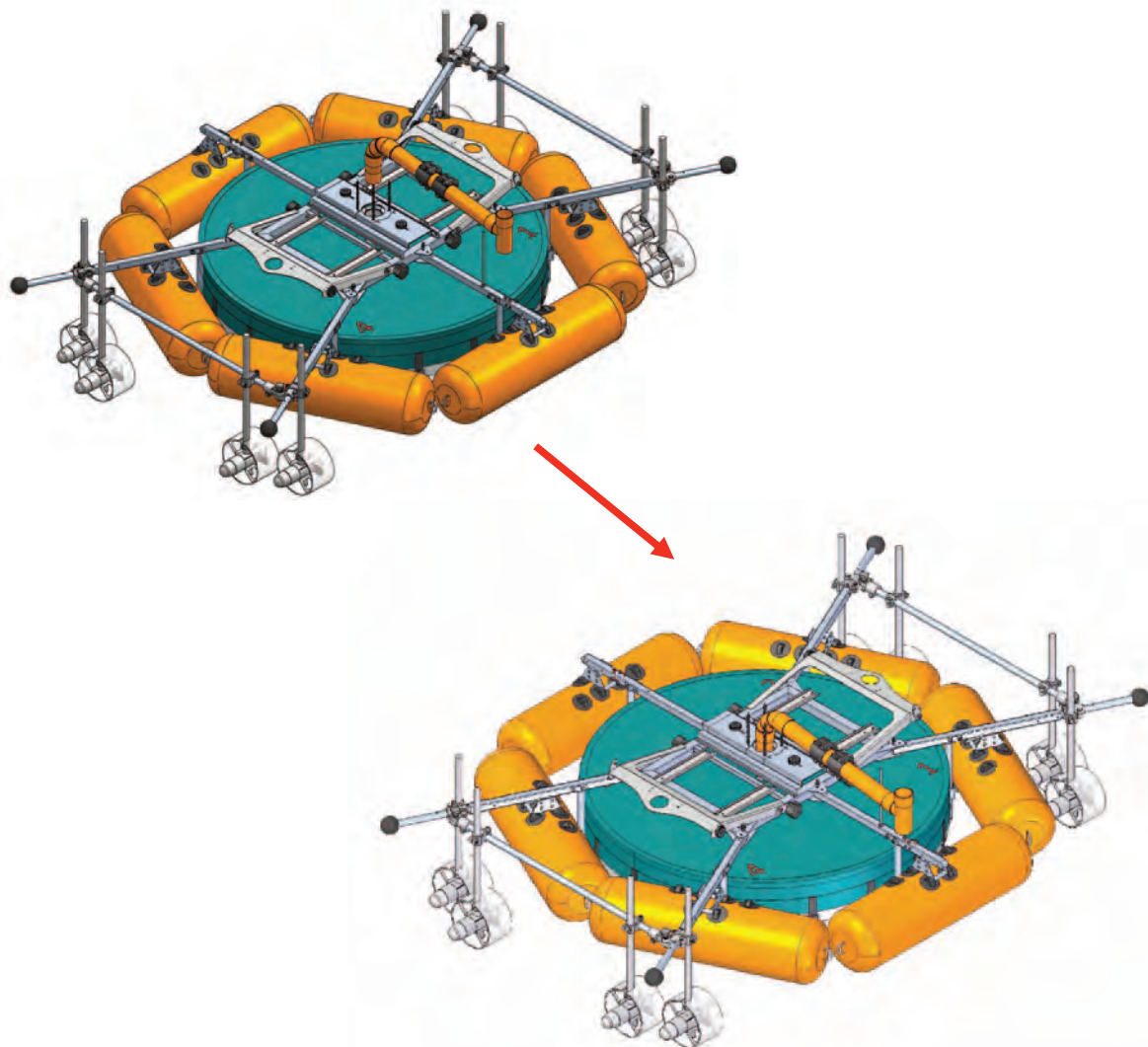


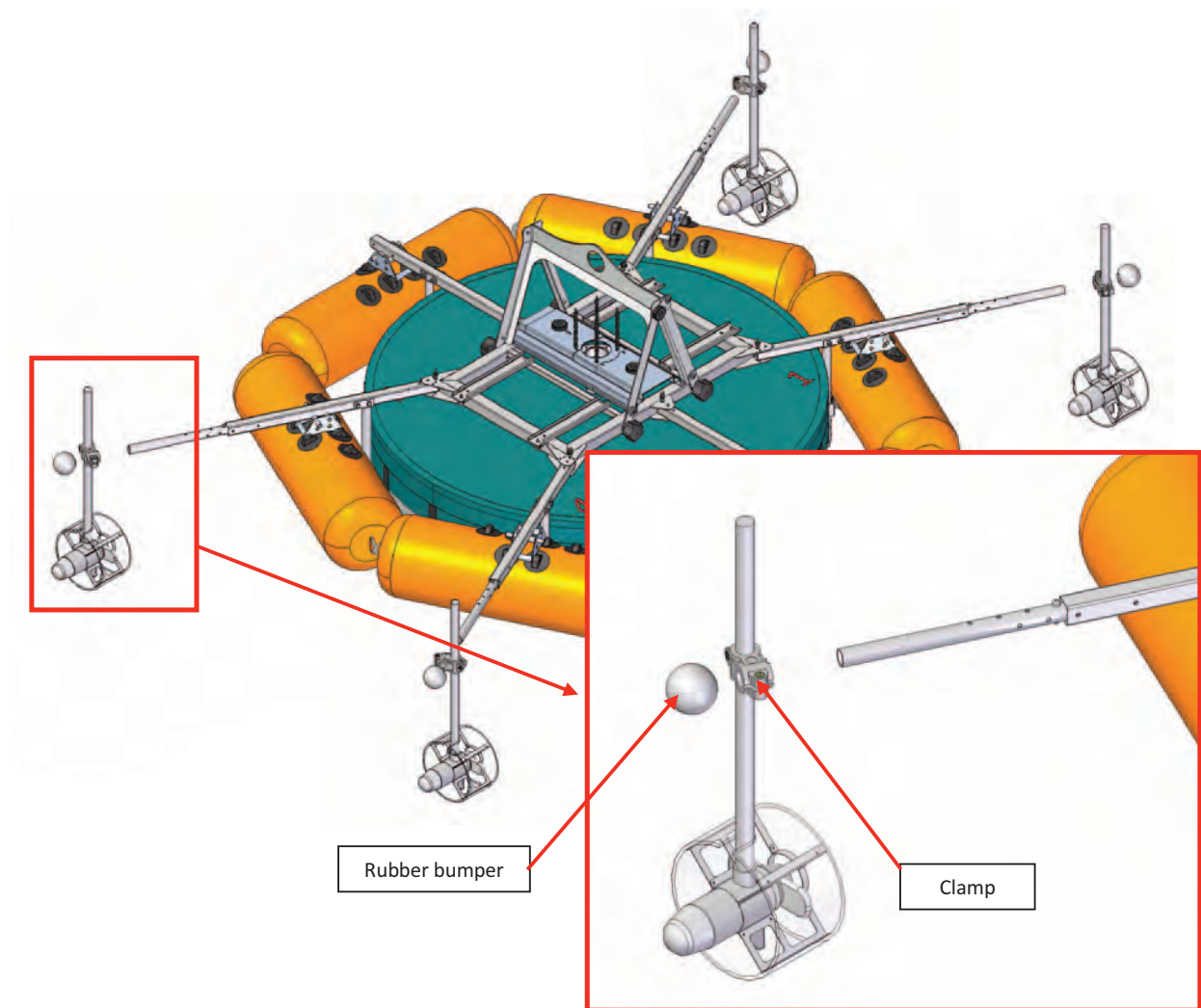
Figure 22: Assembly of the collection pipe

Close the lifting castle once the tube is assembled.

3.6 Propellers assembly

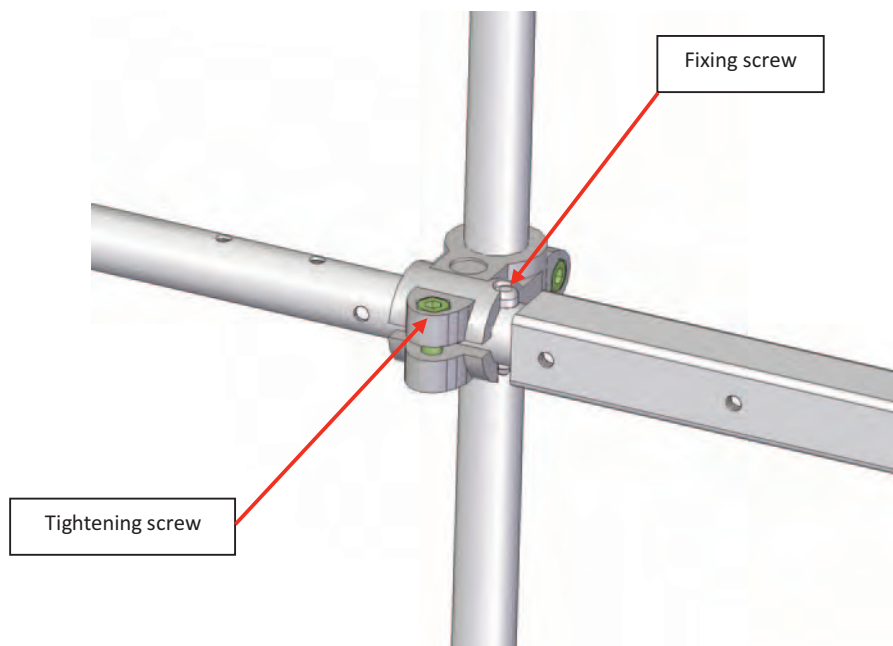
In order to assemble the propellers on the frame, it is necessary to remove the rubber bumpers, which are positioned on a protection of the longer arms, and to insert the clamp on the propellers' support vertical rod by sliding it up to the set screw on the arm.





Match the groove on the clamps with the set screw and tighten the screws on the clamps





It is possible to slide the propellers up and down and rotate them before tightening the clamp screws definitively.

At this point it is necessary to mount the remaining four propellers on the relative tubulars. Each tubular will act as a support for two propellers and will be connected, through special double-clamps, to the longer arms.

Insert the clamp on the propeller support vertical rod into the tubular and tighten the screw on the clamp. Repeat for each propeller. Fasten the tubulars on which the propellers have been mounted to the long arms using the appropriate double-clamps.

Now it is possible to mount back the rubber bumpers on the long arms.

NOTE:

When assembling the propellers, be careful to keep the same alignment for all eight propellers.



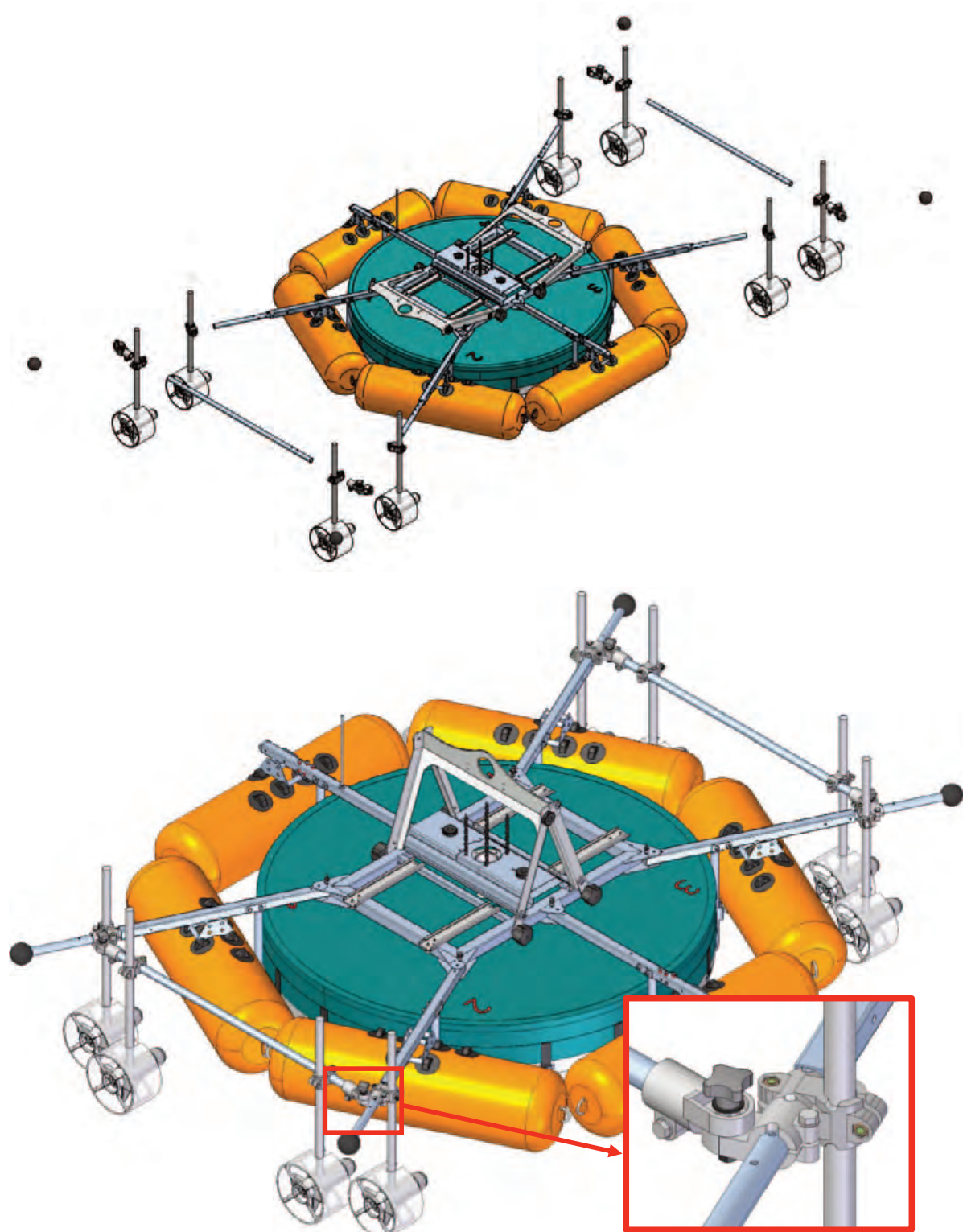


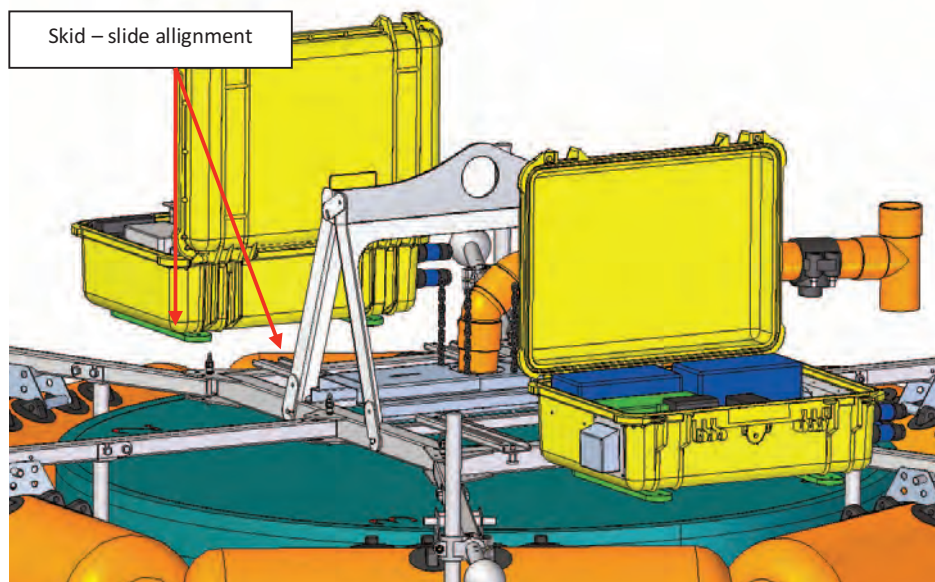
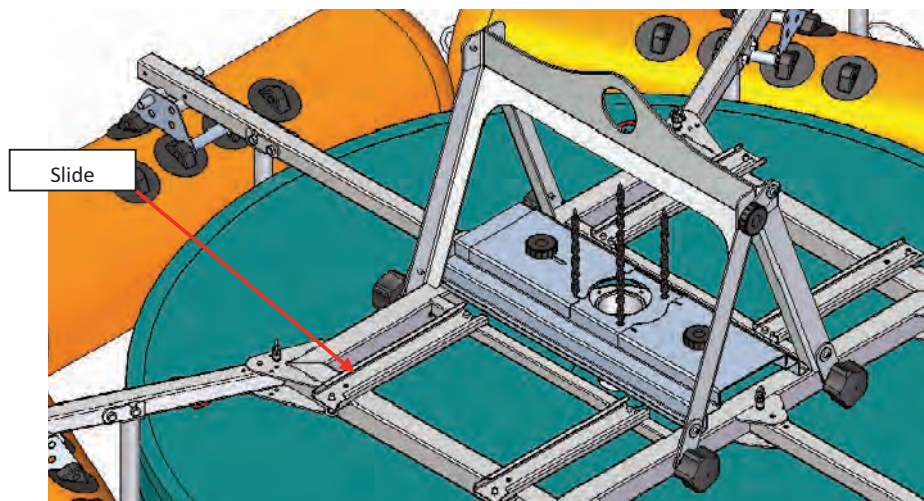
Figure 23: View of the frame with assembled propellers



Once the propellers are assembled, connect their connectors to the Control Box in the positions indicated on the connecting flange.

3.7 Control box and sampling box assembly

On the frame's upper part there are two slides for each box in which the skids under the two boxes must be inserted. Each slide is equipped with a spring pin that allows you to lock the box in an adjustable position.



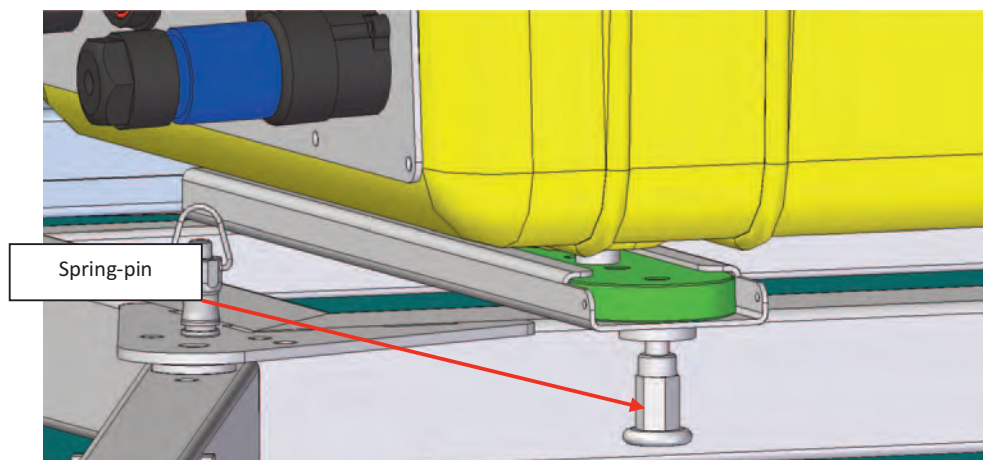


Figure 24: Control box and sampling box assembly

NOTE:

Although they are interchangeable in position, the boxes must be assembled on the frame with the connecting flange facing the collection pipe.

3.8 Probes

Dissolved oxygen probe

The dissolved oxygen probe must be connected to the orange marked connector on the connecting flange of the sampling box. The probe is equipped with a 20 mt of cable, which allows you to regulate the depth of measurement by adapting it to the depth of the tank.

Regulate the measurement depth and fix the cable on the frame.

Anemometer (airspeed)

The anemometer probe must be inserted in the collection tube inside the prepared cable gland by adjusting its depth and orientation. Then tighten the cable gland appropriately so as not allowing probe's movements.

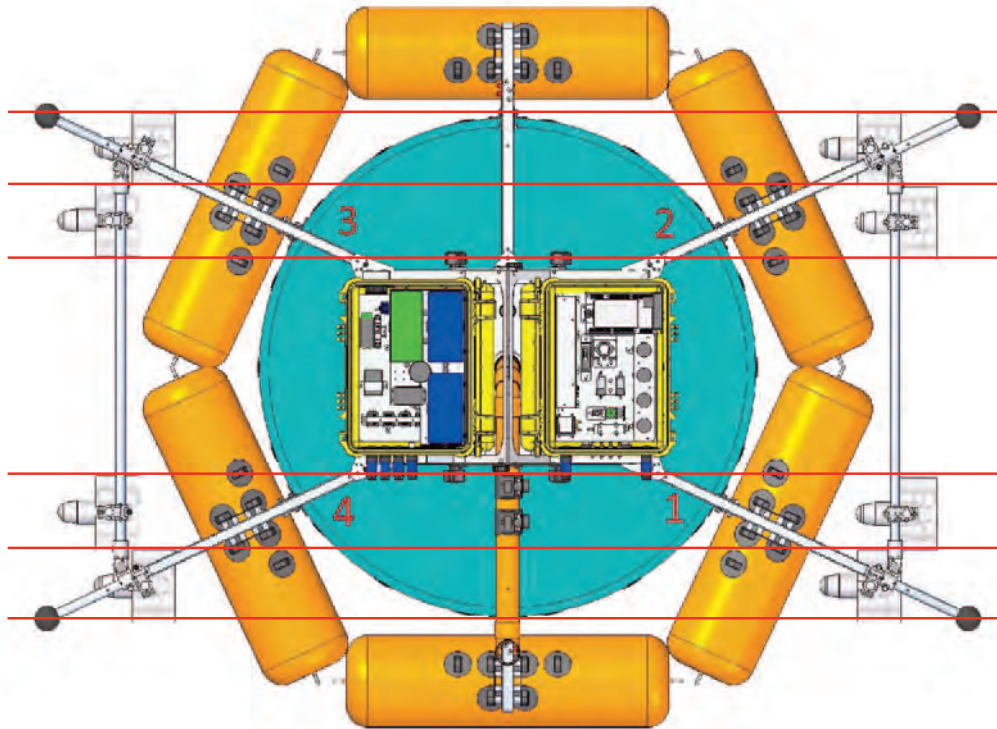
Connect the probe connector to the marked connector on the connecting flange of the Sampling Box.



3.9 Propellers alignment

Once the drone assembly operations are complete, it is necessary to check the alignment of the propellers in the direction indicated in the figure.

To check the alignment of the propellers, you can use a rope or a strip that allows you to check if the right (and left) motors are aligned in the same direction.



In case misalignments are detected, it is necessary to loosen the fixing clamp of the propellers and proceed with the alignment.



4. Starting procedure and use of the drone

Once the drone assembly is complete, it is possible to proceed with the start-up procedure to be able to use it in the oxidation tank.

4.1 Preliminary operation

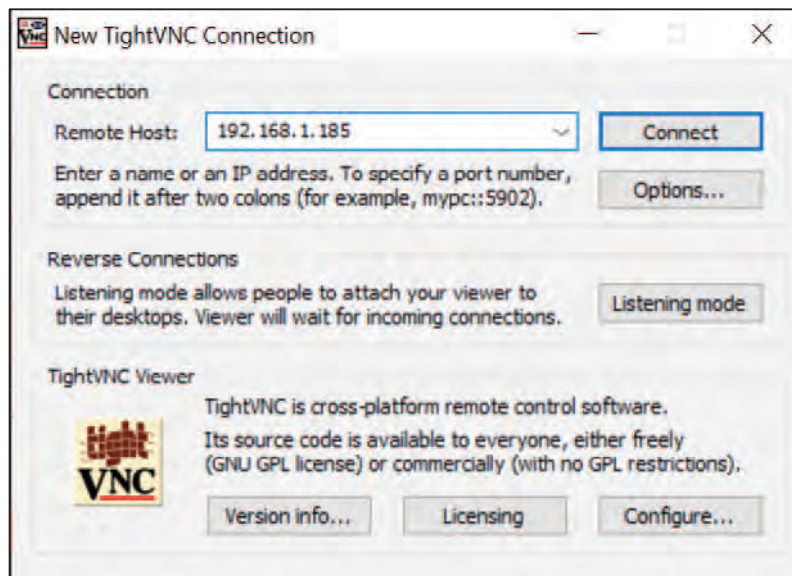
Once the propellers and the sampling box are connected to the control box, proceed as follows before putting into the water.

Place the drone in the most horizontal position possible, connect the instrumentation battery and PC to the corresponding connector and turn on the main start switch inside the control box (do not connect the propeller batteries at this time). The external green light of the control box will then turn on and after a few seconds you will hear acoustic signals from the PC. At the same time, the control unit light will first flash yellow to indicate that it has been turned on, consecutively it will flash red/blue to indicate the horizon calibration. Finally, the light will become steady, blue if the GPS is searching for the position, green if the GPS fix has been carried out.

As a first test, make sure that the engines have been assembled correctly and that the propellers rotate in a manner consistent with the bow of the vessel. Then connect the motor batteries to the corresponding connectors. The bow is indicated by a label with an arrow inside the control box door. Then turn on the remote control and, in the event that some commands are not reset during power-up, follow the instructions on the display (it is a safety check to prevent some servomechanisms from operating in an unwanted way). At this point, on the remote control, move the lever at the top left to the central position to enable manual driving and, using the main right control, operate the motors for small periods so as to check that the propellers rotate in a direction consistent with the desired direction.

Once the motors have been checked, a PC must be connected to the access point integrated in the control box. Among the available WLAN networks, search for the network with SSID "Lesswatt" and enter the password "Lesswatt2018". Once the WLAN is connected, open the TightVNC program, which must have been previously installed on your PC, and connect to the address 192.168.1.185 as in the image below. When asked for the password, type "Lesswatt2018".





Once you access the on-board PC desktop, you can view the programs that the PC automatically loads on startup: "Mission Planner" and "WS Scada". The first is necessary to control movement and positioning of the vessel, the second to view the progress of the mission from a sampling point of view. To access the control of movement, restore the Mission Planner window, and connect the control unit present on one of the COM ports (baudrate 115200 baud) by pressing the button in the upper right corner, as in the image below. If you do not know the COM port assigned to the control unit, right-click on the Windows "Start" button, select "Device Management", expand the "Ports (COM and LPT)" item, and write down the corresponding port number.





Wait for the parameters inside the control unit to be transferred to the Mission Planner. In this screen, on the top left there is the Virtual HUD with inclinometer and some navigation conditions, including the orientation of the bow with respect to the north (check that it is correctly aligned with the arrow in the control box), the GPS status and the status of the Kalman filter (EKF). On the bottom left there are the various tabs of parameters and navigation controls, including the "Quick" tab where navigation conditions are displayed, and the "Actions" tab where there are controls for starting the mission. On the right you can see the map of the place where the boat is present, whose position is determined by GPS.

NOTE:

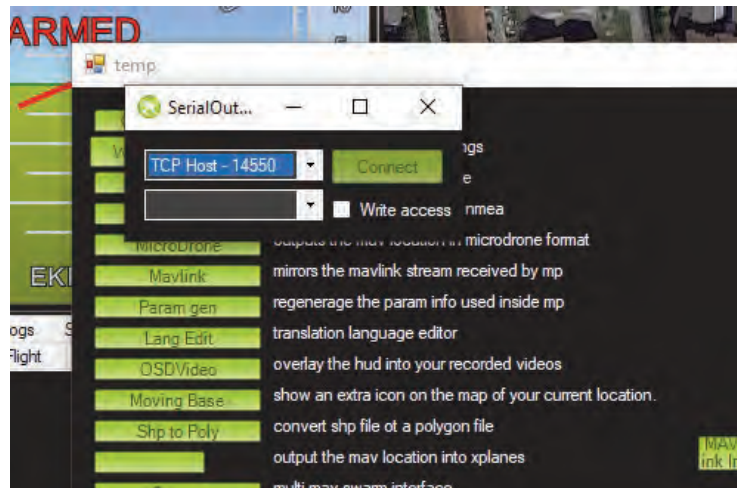
The map display is only possible if the router is equipped with a data SIM with internet connection.

At this point, press the "Ctrl + F" keys on the keyboard, to bring up the additional commands window, as in the image below.





Press the "Mavlink" button to open the data stream mirroring control window between the control unit and the Mission Planner. Within the small window that opens, select "TCP Host - 14550" in the drop-down menu at the top, and leave the drop-down menu below free, then press the "Connect" button, as in the following image.



In this way WS Scada will be able to receive the instant mission condition and automatically regulate the sampling when necessary.



4.2 GPS connection

To connect and configure the differential GPS in order to improve positioning accuracy, press the "Initial Setup" button at the top left of the Mission Planner window. Once the new screen is displayed, select the differential GPS configuration via the "Optional Hardware/RTK/GPS Inject" path on the left column, as in the image below.



To connect the differential GPS base, select the COM on the drop-down menu at the top left (baudrate 115200 baud) and press the "Connect" button, as in the following image. If you do not know the COM port assigned to the differential GPS base, right click on the Windows "Start" button, select "Device Management", expand the "Ports (COM and LPT)" item, and write down the corresponding port number.



To ensure that GPS reception is optimal, look at the "Base", "GPS" and "GLONASS" lights in the RTCM box and check that they are green. At the bottom you can observe the signal strength of each satellite received. If the intensity of many satellites is close to or below the red line, it means that reception is not optimal and the following georeferencing operation will be inaccurate.

To carry out the georeferencing operation of the differential GPS base, enter the final accuracy of the measurement in the "SurveyIn Acc (m)" box (in the image below 0.5 m) and the duration of the measurement in the "Time (s)" box (In the image below 600 s), finally press the "Restart" button. An average measurement of the geographical points received from the differential GPS base will begin, the accuracy of the measurement is proportional to the survey time. In the right part of the window it will be possible to view the progress of the measurement and the accuracy achieved. Once the measurement is finished, it is necessary to save it by pressing the "Save Current Position" button, a window will then open where you can enter the name. Once saved, the position will appear in the list below, then press the corresponding "Use" button to use the saved position in order to enable differential GPS. For subsequent missions, if the base of the differential GPS is placed exactly in the same point, you can choose this position from the list, and avoid doing the survey again.

The screenshot shows the 'M8P autoconfig' window with the 'RTCM Base' tab selected. It includes checkboxes for 'M8P/Here+' and 'M8P fw 130+', and a 'Moving Base' checkbox. Below these are input fields for 'SurveyIn Acc(m)' (0.5) and 'Time(s)' (600), along with 'Restart' and 'Save Current Position' buttons. A table lists saved positions with columns for coordinates and names.

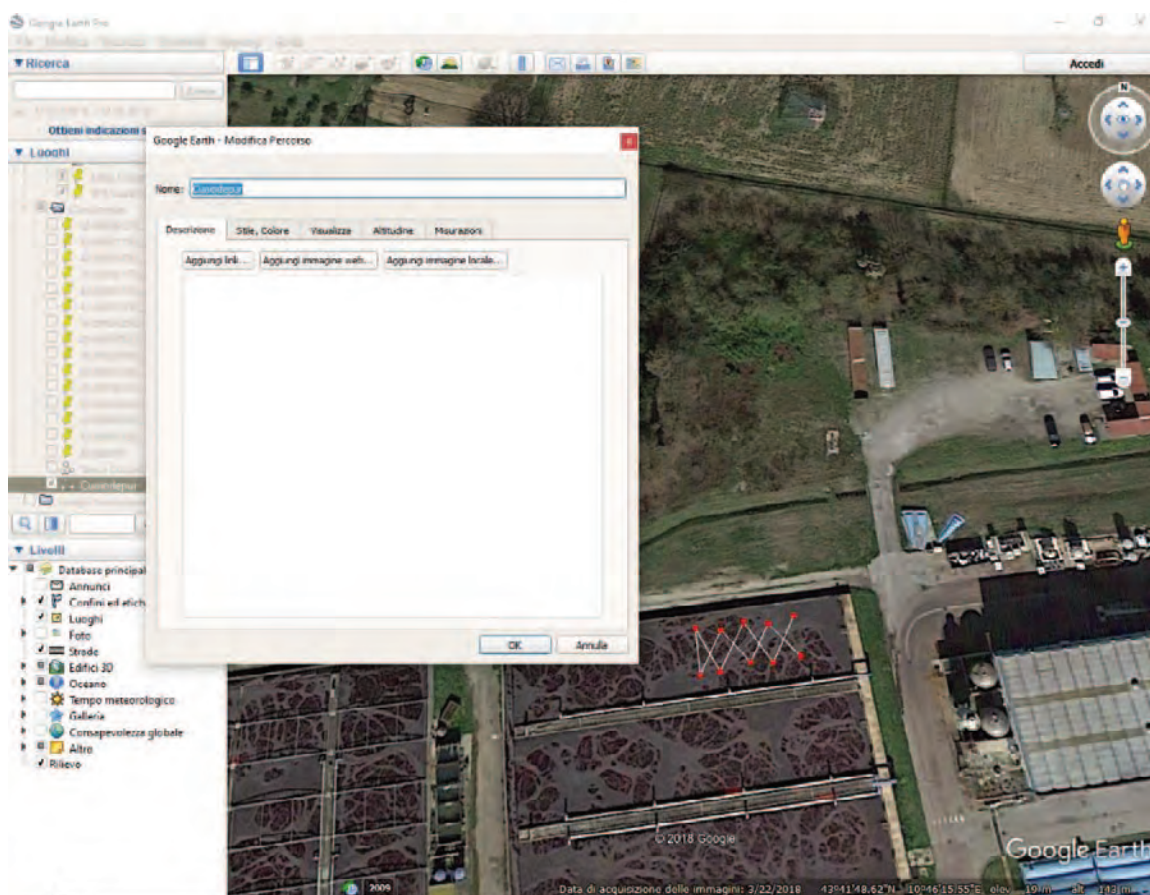
	Lat/ECEF	Long/ECEF	Alt/ECEF	Name	Use	Delete
▶	43.669802646511	10.65796237994...	77.7657966...	West	Use	Delete
	43.66982310371...	10.65767464857...	59.2536156...	West 1	Use	Delete
	43.6699131	10.6575108	62.547	West tetto divide	Use	Delete
↻						

4.3 Configuration and start of the automatic mission

From this moment it is possible to proceed with putting the boat into the water.

To configure the mission to be carried out in the tank, open the Google Earth Pro program, freely downloadable from the internet. Scroll the map and position yourself in the mission area with an appropriate zoom. Press the "Add route" button at the top. A window will appear where you can enter the path name (in the image "Cuoiodedpur"). At this point, compose the path in the tank of interest using the cursor and finally press the "OK" button. The route will be saved in the left column. Click on the name of the route with the right mouse button and select "Save place as...". Choose the format of the KML file, enter the name and press the "Save" button.



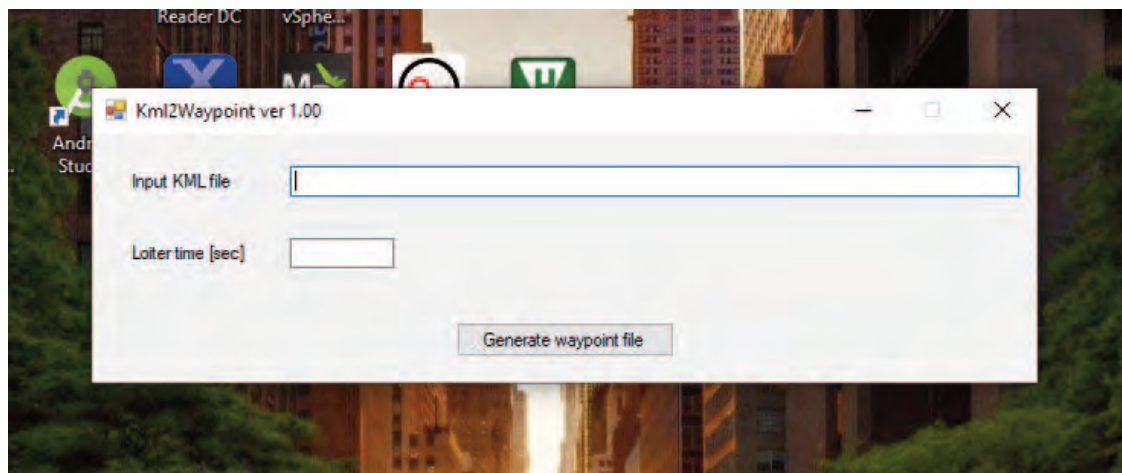


At this point, to load the coordinates of the route in the Mission Planner program and then in the drone control unit, it is necessary to convert these coordinates from KML format to WAYPOINTS. To do this, open the "**LesswattKml2Waypoint**" program and a window will appear as in the figure below. Double click in the "Input KML file" box and select the file previously saved with Google Earth Pro. In the "Loiter time [sec]" box, enter the time spent on each individual parking point. In addition to the sampling time, the parking time must also include the times necessary for its initialisation.

Therefore, the parking time is equal to the sum of the times relating to the operations to be performed on the point itself.

Finally, press the button "Generate waypoint file" and the usual save window will open. Choose the folder, enter the file name and press the "Save" button.





To enter the mission data in the drone control unit, restore the Mission Planner program window and press the "Flight Plan" button, at the top right. The screen below will appear where you can upload the mission data contained in the previously produced WAYPOINTS file.



Then press the "Load WP File" button on the right and open the WAYPOINTS format file. The table below the satellite photo will be populated with the route and parking points previously selected in Google Earth Pro. To set the starting point, move the drone to the desired position using the remote



control, and click on the link on the right "Home position". Finally, press the "Write WPs" button to load the mission into the drone control unit.

Click on the "Flight Data" button to return to the main Mission Planner screen. In the lower right part of the Virtual HUD, the best GPS mode, which the system can lock, will appear. In particular, the following methods may be used:

- "No GPS" when no GPS fix is available.
- "3D Fix" when a non-differential fix is present (only the GPS device inside the drone is used) with an accuracy of 5÷10 meters.
- "3dgps" when a non-RTK (Real Time Kinematic) traditional differential GPS fix is available with an accuracy of 3÷5 meters.
- "RTK Float" when an RTK differential GPS fix is available but the system has not been able to pinpoint the phase of the signals received from the various satellites (accuracy of about 1 meter);
- "RTK Fixed" when a differential GPS fix of the RTK type is available and the system has successfully identified the phase of the signals received from the various satellites (accuracy of about 0.1 meters).

Differential GPS modes (3dgps, RTK Float, RTK Fixed) can be used only if the differential GPS base is connected and its correct position has been indicated. Otherwise it will be possible to use only the non-differential 3D Fix mode.

To start the mission, click on the "Actions" tab located on the left of the satellite image, as in the figure below. Place the remote control in manual mode by placing the front left lever in the central position. Then press the "Auto" button to start the mission.

NOTE:

For the mission to run correctly, the remote control must remain on for safety reasons. Any disconnection of the remote control, due to low battery or shutdown, leads to the immediate interruption of the mission.

Once the mission has started, the drone will go to the points of interest and, standing on them, will start the measurement automatically, interrupting it during the journey from one parking point to another.





The mission will end when all points on the route have been analyzed. You can stop the mission at any time by pushing the front left lever of the remote control forward.

4.4 Manual mission

It is also possible to take advantage of an additional mode that does not include mission planning but is based only on the commands sent by remote control. To do this, set the front left lever of the remote control to the central position to enable manual control. Pilot the drone to the desired parking point and push the front left lever of the remote control towards yourself, in order to enable the parking function. To stop this mode and resume manual control, move the lever back to the central position. At the end of the mission push the lever forward to bring the drone to a safe position (propellers blocked).



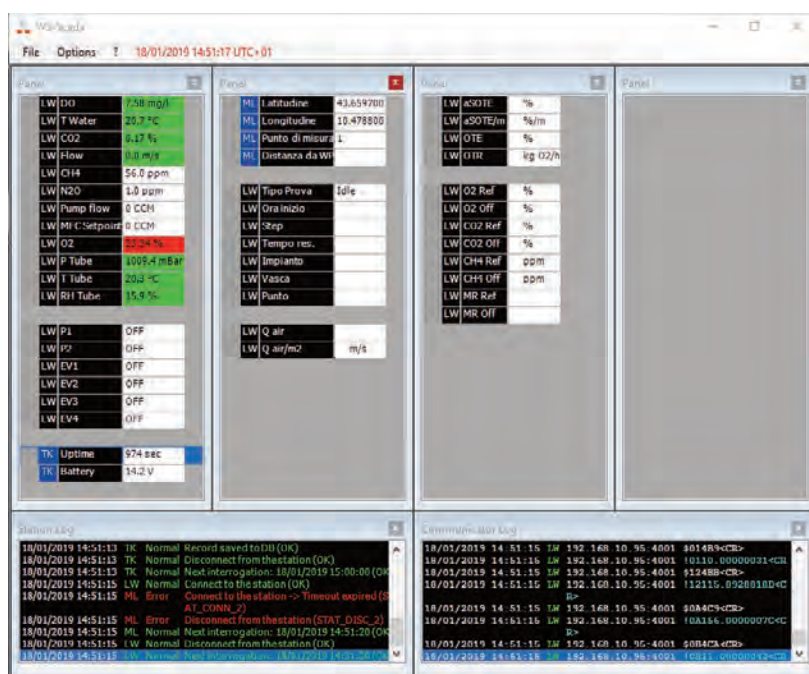


Figure 25: Remote control for drone piloting

5. WS-SCADA software

The WS-SCADA software manages the sampling phases and records the data from the various sensors. The software interfaces directly with the control card inside the sampling box.

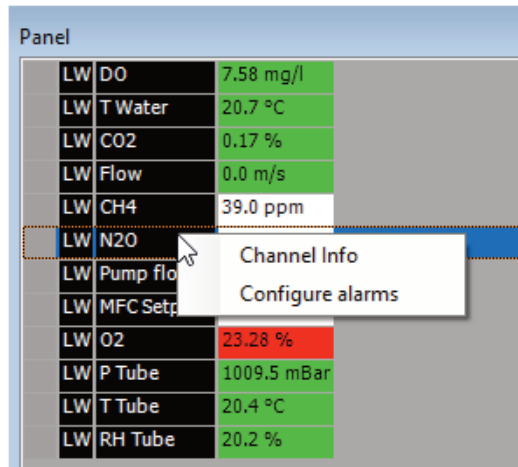
When the instrument is started it is in the "Idle" state, that is, awaiting instructions.



LW	DO	7.60 mg/l
LW	T Water	20.7 °C
LW	CO2	0.17 %
LW	Flow	0.0 m/s
LW	CH4	48.0 ppm
LW	N2O	1.0 ppm
LW	Pump flow	0 CCM
LW	MFC Setpoint	0 CCM
LW	O2	23.37 %
LW	P Tube	1009.5 mBar
LW	T Tube	20.2 °C
LW	RH Tube	11.7 %

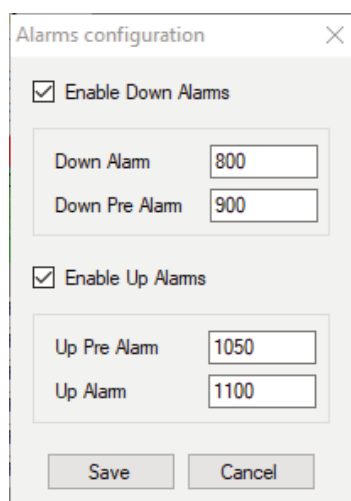
The sensor panel shows the following parameters:

- Dissolved oxygen concentration
- Water temperature
- Carbon dioxide concentration
- Airspeed
- Methane concentration
- Nitrous oxide concentration
- Pumping flow
- Set-point of the flow regulator
- Oxygen concentration
- Pressure, temperature and relative humidity in the sampling circuit



By pressing the right button on a parameter name, the Channel Menu appears. By pressing “Configure alarms” it is possible to set thresholds for displaying the parameter.





Alarms configuration

☒ Enable Down Alarms

Down Alarm: 800

Down Pre Alarm: 900

☒ Enable Up Alarms

Up Pre Alarm: 1050

Up Alarm: 1100

Save Cancel

The parameter value can take on the following colors:

- White: no threshold has been set
- Green: the value is within the threshold
- Yellow: the value is between the pre-alarm and alarm threshold
- Red: the value is beyond the alarm threshold

NOTE:

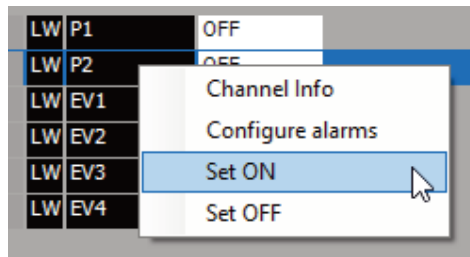
The alarms configured here are for display purposes only.

The I/O panel allows consultation of the current status of the digital outputs and their control. See the pneumatic diagram of the system for the meaning of the outputs.

LW	P1	OFF
LW	P2	OFF
LW	EV1	OFF
LW	EV2	OFF
LW	EV3	OFF
LW	EV4	OFF

The outputs are automatically driven by the software according to the different measurement phases. They can however be overwritten by pressing the right button on the name of the output (example P2) and selecting "Set ON" to activate the output or "Set OFF" to deactivate it.





A typical case is the manual activation of the EV4 output to redirect the sample output to a sampling bag.

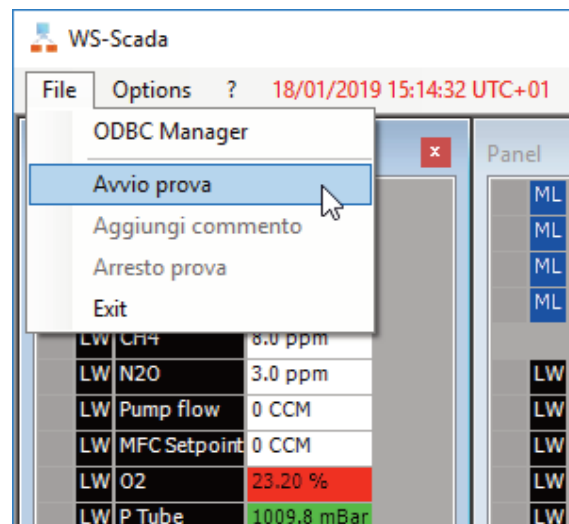
The navigation panel shows information from the MavLink telemetry of the Pixhawk control unit.

ML	Latitudine	43.659700 °
ML	Longitudine	10.478800 °
ML	Punto di misura	1
ML	Distanza da WP	15 m

The current latitude and longitude, the current measuring point and the distance in meters from the waypoint are shown.

5.1 Starting a sampling session

To start a test, press File – Avvio prova



The test start window will appear:



Avvio prova

Nome impianto: Numero Vasca: Punto campionamento:

Commento:

Profondità diffusori [m]:
 Pressione atmosferica [mBar]:
 Elevazione [m]:

Tempi

Durata prova discreta [min]:
 Durata prova rif [min]:
 Logging time [s]:

Tempo svuotamento condensa [s]:
 Durata massima svuotamento [s]:

Dimensioni

Diametro tubo scarico [mm]:
 Area cappa [m2]:
 Volume cappa [m3]:

Diametro tubo camp. [mm]:
 Livello immersione cappa [mm]:
 Lunghezza tubo camp [mm]:

Coeff. beta:
 CF:
 Coeff. teta:
 P limite:

Temperatura default [°C]:
 DO default [mg/l]:
 Flusso pompaggio [CCM]:

Fill in the fields Plant name, tank number and sampling point.

In the case of the automatic point test, the sampling point is automatically acquired by the mission information; the name of the entered point will then be ignored.

Optionally you can write a comment that will be reported in the output file.

In addition to the duration of the test, it is also possible to enter the frequency with which the system acquires data from the sensors, in this specific case every 5 seconds.

Four types of tests are available:

- 1) Reference test. The instrument acquires background values in the air.
- 2) Manual point test. The instrument is manually moved inside the tank. A single test will include a single point sampling.
- 3) Automatic point test. The instrument is moved by the automatic positioning system of the drone inside the tank. A single test will include as many sampling points as they are foreseen by the mission.
- 4) Stationary test. The test involves sampling on a single point indefinitely, without time limits.



5.2 Measurement phases

The reference test involves the following phases:



1/PUMP	Switching on the pump and activating the solenoid valves. Waiting for the flow stabilization time.
2/SAMP	Sampling from the "Reference" input. The sampling time is established in the start-up phase ("test duration ref.").
3/SAVE	Saving the report file.

The manual point test involves the following phases:

1/PUMP	Switching on the pump and activating the solenoid valves. Waiting for the flow stabilization time.
2/TESTQ	Preliminary sampling of the air speed for the determination of the time required to empty the hood volume. In no case can emptying exceed the preset value ("Maximum emptying duration")
3/SVUOT	Waiting for the hood emptying time.
4/SAMP	Sampling from the "Sample In" input. The sampling time is established in the start-up phase ("discrete test duration").
5/REMOV	Removal of any condensate from the sampling line. Removal is invoked upon the occurrence of a drop in pressure within the line during sampling. The peristaltic pump used to empty the condensate is activated for a pre-set time ("condensate emptying time"). At the end of the operation, the instrument returns to sampling.
6/SAVE	Saving the report file.



The automatic point test involves the following phases:

	WAIT FOR POSITION	The instrument is navigation phase. Waiting for the sampling point to be reached.
	1/PUMP	Switching on the pump and activating the solenoid valves. Waiting for the flow stabilization time.
	2/TESTQ	Preliminary sampling of the air speed for the determination of the time required to empty the hood volume. In no case can emptying exceed the preset value ("Maximum emptying duration")
	3/SVUOT	Waiting for the hood emptying time.
	4/SAMP	Sampling from the "Sample In" input. The sampling time is established in the start-up phase ("discrete test duration").
	5/REMOV	Removal of any condensate from the sampling line. Removal is invoked upon the occurrence of a drop in pressure within the line during sampling. The peristaltic pump used to empty the condensate is activated for a pre-set time ("condensate emptying time"). At the end of the operation, the instrument returns to sampling.
	6/SAVE	Saving the report file.
	WAIT FOR LOITER END ↓	Waiting for stationing time.. At the end, check the mission status: <ul style="list-style-type: none"> - If further measuring points are foreseen, the instrument passes waiting for the new positioning. - If no further points are foreseen, move on to the end of mission management. 
	END OF MISSION	The test is concluded.

5.3 Output files

The output files are stored in the folder C:\offgas_data\<NOME_IMPIANTO>

Where <NOME_IMPIANTO> is the name entered when starting the test.

Inside each folder will be four subfolders:

- Point tests
- Reference tests
- Stationary tests
- Raw data



Inside the folders prove_a_punti, prove_riferimento and prove_stationarie a text file will be stored for each test carried out. The file contains a summary report of the test result.

The file name contains the test start date, in the *yyyymmdd_hhmmss.txt* format.

Point test file

The file is produced at the end of each point test and contains the following information:

- Sampling point number
- Geographical coordinates of the point:
 - Latitude
 - Longitude
- Average, maximum, minimum and standard deviation of the sampled parameters:
 - α SOTE
 - α SOTE/m
 - OTE
 - Q air
 - Q air/m²
 - O₂ Off
 - CO₂ Off
 - OTR
- Any comments entered during the test start-up phase

In the case of the automatic point test, the block is repeated for each of the mission points. Vice versa, in the case of the manual point test

Reference test file

The file is produced at the end of each reference test and contains the following information:

- Average, maximum, minimum and standard deviation of the parameters:
 - CO₂
 - O₂

Raw data file

The file is produced at the end of each test, simultaneously with the report file. However, the *raw data file* contains more information:

- Type of test (points/stationary/reference]
- Plant name
- Tank number
- Notes
- Start time
- Input parameters:



- Max Emptying time
- Pressure limit
- Coeff. teta
- Sampling pump flow [CCM]
- CF
- Coeff. beta
- Hood immersion level
- Sampling tube diameter
- Sampling tube lenght
- Hood area
- Exhaust pipe diameter
- Stationary test measurements frequency
- Condensation emptying time
- Logging time
- Duration of reference test
- Duration of discrete test
- Elevation
- Atmospheric pressure
- Diffuser depth
- O₂ concentration in the air
- Discarded starting points for reference test
- Discarded starting points for points test
- Wait time after the start pump command
- Wait time after the set zero command
- Saturation concentration of O₂ in standard conditions
- Min flow
- Max air temperature
- Hood volume
- Sampling point number
- Geographical coordinates of the point:
 - Latitude
 - Longitude
- Average, standard deviation, minimum and maximum of the air flow (preliminary measure)
- The sampling table of the following parameters, acquired once every 5 seconds:
 - α SOTE [%]
 - α SOTE/m [%/m]
 - OTE [%]
 - OTR [kg O₂/h/m²]
 - DO [%]
 - Tw [°C]
 - N₂O [ppm]



- Pt [mBar]
- Tt [°C]
- RHt [%]
- Qair [Nm³/h]
- Qair/m²
- O₂ Ref [%]
- O₂ Off [%]
- N₂O raw Ref [ppm]
- N₂O raw Off [ppm]
- N₂O corretto Ref [ppm]
- N₂O corretto Off [ppm]
- CO₂ Ref [%]
- CO₂ Off [%]
- CH₄ Off [ppm]
- CH₄ Ref [ppm]
- Vanem [m/s]
- PumpFlow [ccm]
- h [m]
- Patm [mBar]

6. Prolonged stationary test

To carry out the prolonged duration stationary test, it is necessary to connect the external power supply that allows you to use the instrumentation and the acquisition system continuously.

To do this, it is necessary to disconnect the batteries and connect the external power supply which is equipped with a 50-meter-long cable that allows you to reach the instrument from the edge of the tank.

ATTENTION

It is necessary to remove the propellers from the drone before carrying out prolonged tests with the help of the external power supply.

7. End of Sampling

At the end of each measurement campaign it is necessary to wash and clean the drone before storing it given the possible presence of aggressive substances.

Place the DO probe and the anemometer inside the respective cases.



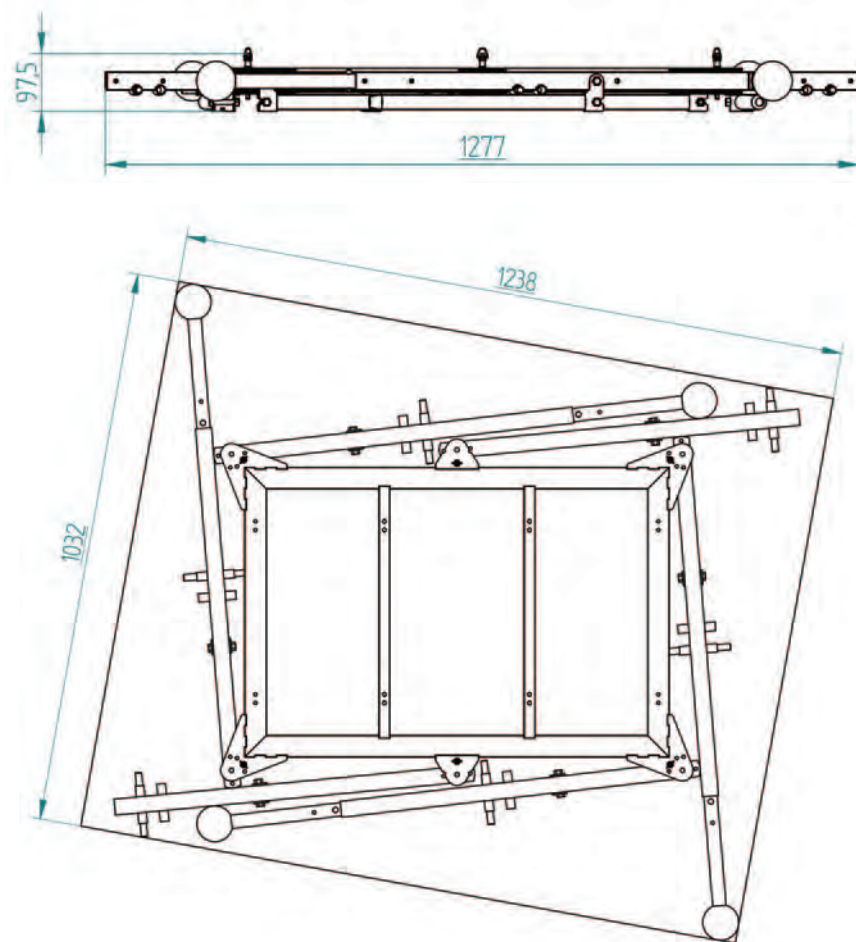
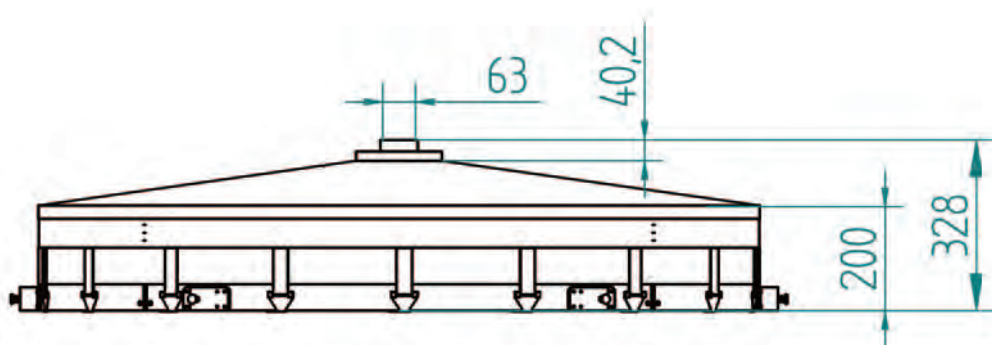


Figure 27: Dimensional drawing of the frame in closed position



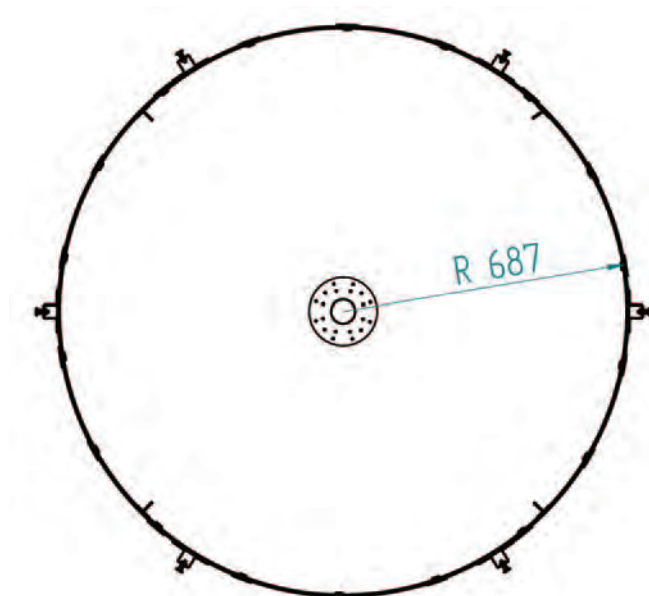


Figure 28: Dimensional drawing of the conveying hood

9. Types of measurements

It is possible to carry out two types of measurement with the LESSDRONE:

- **Point test:** measurements on several points in the oxidation tank with constant airflow. On each point the OTE and the GHGs (CO₂, N₂O and CH₄) were detected. Spatial distribution of the parameters was measured in the tank;
- **Stationary test:** measurement in a single point of the tank for an extended period of time (up to one week) under ordinary management conditions. The parameters were measured in order to assess their temporal distribution in different operating conditions (working day/public holidays, night/day, high/low load, etc.).

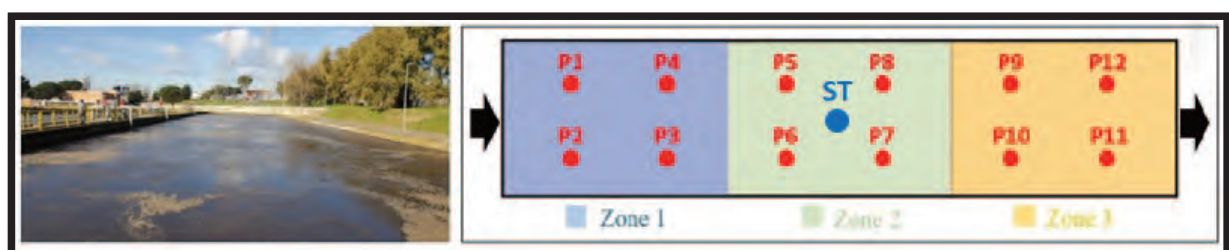


Figure 29: Example of schematic diagram of the measurement points





Figure 30: Example of carrying out a measurement with the LESSDRONE

During these tests, the gas after passing through an anemometer to evaluate the air flow, flows to the sensors for the measurements of O₂, CO₂, CH₄, N₂O. There is also a probe for measuring the DO and the temperature in the aerated mixture. The LESSDRONE evaluates the oxygen transfer efficiency under standard conditions and in the process water (α SOTE) with the off-gas method, which is based on a gas phase mass balance between the oxygen content of the reference gas (atmospheric air) and off-gas, and measures greenhouse gas concentrations.

Another type of measurement is linked to the sampling of off-gas bags for the measurement of Volatile Organic Compounds (VOCs) and odours emitted by the oxidation tanks. The WRRFs are also major sources of VOCs and odourants. VOCs include all the odourous compounds generated by degradation of organic matter in wastewater. The complaints about malodourous emissions from communities living near WRRFs have constantly increased. Thus, in recent years, the monitoring of odourous emissions has also become important in the management of WRRFs. An



off-gas aliquot can also be conveyed by the Lessdrone outside the tank via a silicone tube to inflate nalophan (or tedlar) bags (1-5 liters). These off-gas samples are subsequently analyzed in the laboratory for Volatile Organic Compounds (VOCs, by gas chromatography-mass spectrometry), hydrogen sulphide (H₂S, by gas chromatography and pulsed flame photometric detector) and odour units (via portable automatic olfactometer SM100i).



10. Introduction to the protocol for energy/GHGs minimization

The focus on carbon footprint (CF) reduction in large water resource recovery facilities (WRRFs) has gained a huge amount of attention in recent years. CF reduction in WRRFs is often mainly focused on electricity consumption, for which aeration is the largest contributor. However, direct N₂O emission from suboptimal nitrification/denitrification processes are often still a blind spot with utilities, despite the fact that it is a GHG with a 300-fold impact compared to CO₂.

Mathematical modelling, with an appropriate level of complexity, can be a huge asset for such an optimization task. Historically, mathematical modelling has been used in many cases for optimization of WRRFs operations and some protocols have been developed in that regard. However, very few studies have addressed CF minimization targets. The existing protocols usually focuses on biokinetic parameters or influent characterization.

Within the context of the LESSWATT project, a protocol is being developed with specific targets for CF reduction with respect to N₂O emissions. It takes advantage of advanced modeling paradigms and extensive data collection focusing on optimization of energy expenditure and GHG emissions. On this way, it extends the existing protocols with more emphasize on using an N₂O risk assessment modeling framework, computational fluid dynamics (CFD), and extensive high-frequency data collected by LESSDRONE, which is an innovative, automated, wireless device developed within the project for monitoring oxygen transfer efficiency (OTE) and direct greenhouse gas (GHG) in real-time during process conditions. This guide book presents the final version of the LESSWATT protocol as well as its application to four selected WRRFs representing its transferability to different process configurations and operating conditions as one of its strong advantages. It starts with demonstration of each case study which at the end will lead to the definition of the protocol itself.

11. Case studies

11.1 Case study 1: Cuoiodepur WRRF

The first case to which the LESSWATT protocol has been applied is the Cuoiodepur WRRF located in the community of San Miniato (PI) in Italy. The plant has a capacity of 850,000 PE treating combined industrial and municipal wastewater. The industrial tannery wastewater entering the plant goes through a pre-treatment and primary sedimentation stage after which it is introduced to the denitrification tank. The municipal wastewater is added to the industrial wastewater right after the denitrification and before nitrification/oxidation tank. There is an internal recycle from the end of nitrification to the beginning of denitrification. DO is controlled at 2 mg/l inside the aeration zone.



A DO probe is located at the end of the nitrification tank. After secondary sedimentation the treated wastewater goes to the tertiary treatment stage for further purification. A mass balance over the biological section of the treatment plant has been built and the flow rates plus wastewater compositions of the influent to the bioreactor as well as those of the internal and external recycles have been obtained. The historical data of the plant has been used to calibrate and validate a TIS flow sheet model of the biological treatment line that shows a good fit to the experimental data.

The N₂O risk assessment modeling framework has been applied to the data collected with LESSDRONE during a measurement campaign in May 2019. The test has been carried out under normal operating conditions of the plant. The next figure shows the results of risk assessment model. In the top graph, high DO and low DO risk scores calculated by the model as well as DO concentration are presented. It can be seen that in almost the entire period of measurement campaign the high DO risk is predominant. During this period, the DO concentration is consistently higher than 2 mg/L. The bottom graph in the figure represents a zoomed-in version of the top graph for a period of almost two days (May 17 - 19). In this graph the actual N₂O emission data measured by LESSDRONE are depicted in green. In many instances, an increase/decrease in the predicted risk score correspond to increase/decrease in the N₂O ted. At this point, reducing aeration as a potential mitigation strategy might already come to mind.

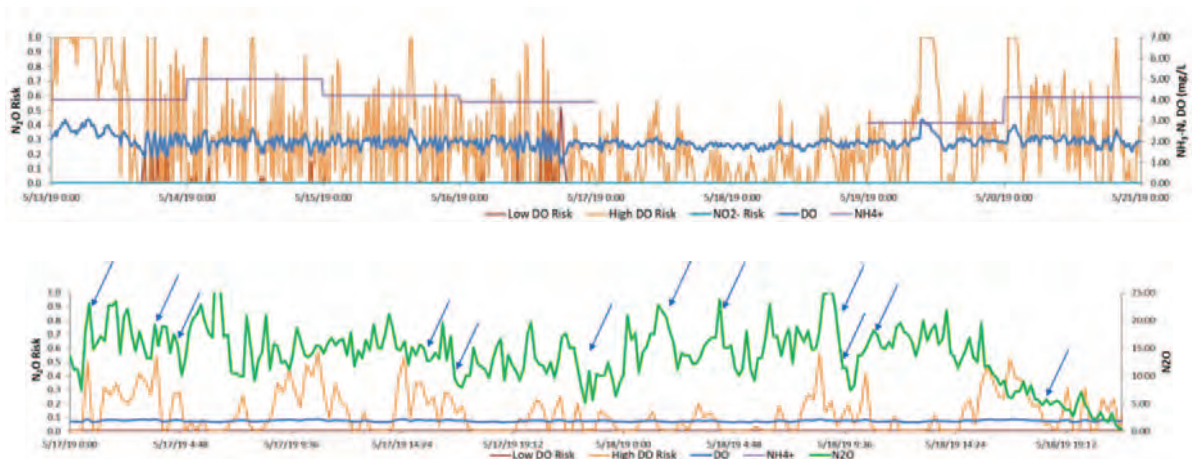


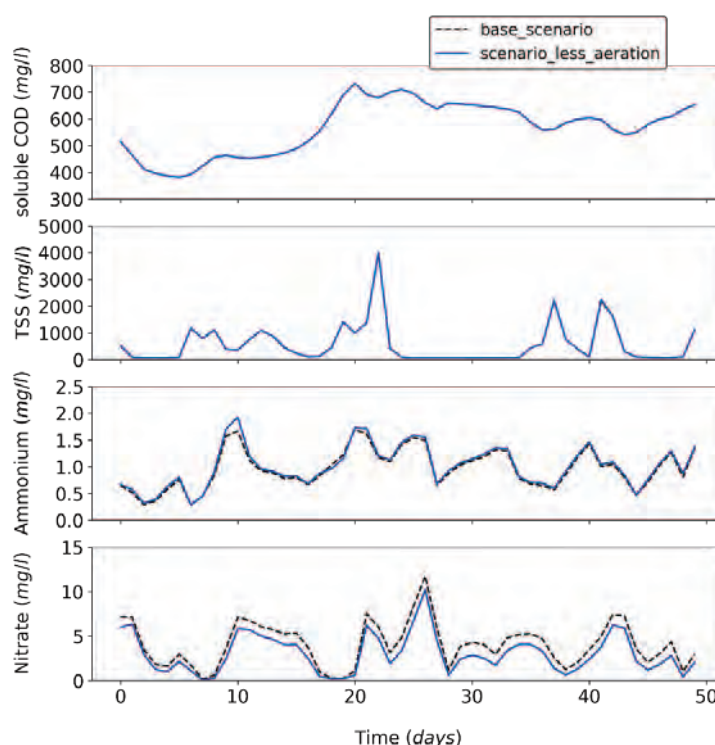
Figure 31: Top: N₂O risk score calculated by the risk assessment model and DO concentration. Bottom: Zoomed-in version of the top graph for May 17-19 with added N₂O emission data collected by LESSDRONE.

The aeration tank is also modeled using a CFD-biokinetic integrated modeling approach to study the hydrodynamics of the bioreactor and the impact of mixing patterns. The data of the tank's geometry, influent and air flow rates coming into the bioreactor as well as composition of the wastewater in the influent and recycle flows are used to build the model. Three scenarios are selected to run the CFD-biokinetic model. These scenarios are chosen based on the combined frequency distribution for air and influent flow rate coming into the bioreactor. Representing the



most frequent scenarios, three influent flow rates (high, medium and low) are defined all with the same level of air flow rates. The results of the model show almost complete mixing inside the bioreactor and the fact that hydrodynamics does not change significantly with the increase of influent flow rate. Air is present in almost everywhere with more than sufficient DO concentrations. Although the DO concentration is higher near the end, it never drops below 2 mg/l.

A new scenario has been defined representing the mitigation strategy with reduced aeration by 40%. This strategy has been evaluated with both the flow sheet and CFD-biokinetic models to see the impact of aeration reduction on the performance of the treatment. The next figure (top) shows the effluent quality predicted by the flow sheet model comparing the reference scenario (under normal operating conditions) with the new scenario in which the aeration is reduced. The outputs suggest that the aeration can be reduced with no significant compromise on the treatment performance. The results of the CFD-biokinetic model (next figure bottom) confirm this assumption by presenting insignificant impact on the hydrodynamics and treatment efficiency in the scenario with lower aeration. Interestingly, the nitrate concentration is reduced in the output of both models for the new scenario. This, taking N₂O risk assessment also into account, suggests that the new reduced DO setpoint will decrease the risk of N₂O emission since it improves the denitrification.



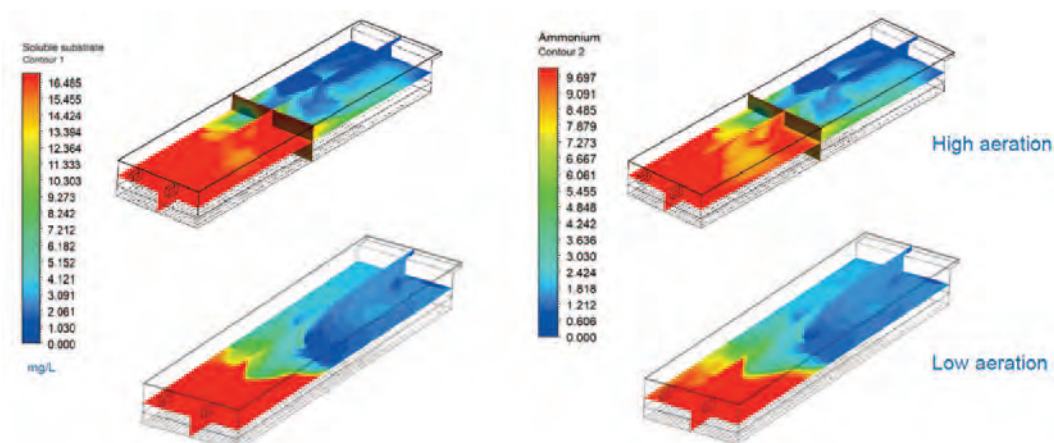


Figure 32: Comparison of the performance of treatment efficiency for the proposed mitigation strategy. Top: results of flow sheet model, Bottom: results of CFD-biokinetic model.

A new measurement campaign was carried out in June 2019 to assess the impact of the proposed mitigation strategy. During the test the DO setpoint was reduced to 1.8 mg/L. The data collected by LESSDRONE was used as the input for the N₂O risk assessment model. The next figure shows the results of the N₂O risk model before (top graph) and after (bottom graph) applying the mitigation strategy. In the first case, like the previous measurement campaign data high DO risk is predominant due to consistently high DO concentrations. The actual N₂O emission is also consistently high. Reduction of DO setpoint as the proposed mitigation strategy decreased the high DO risk significantly and consequently the N₂O emission is also reduced considerably. While the emissions were constantly higher than 8 ppmv and maximum up to around 18-20 ppmv in the first scenario, the mitigation strategy in the second scenario was able to keep the emission as low as zero most of the time with some small peaks around 2-4 ppmv.

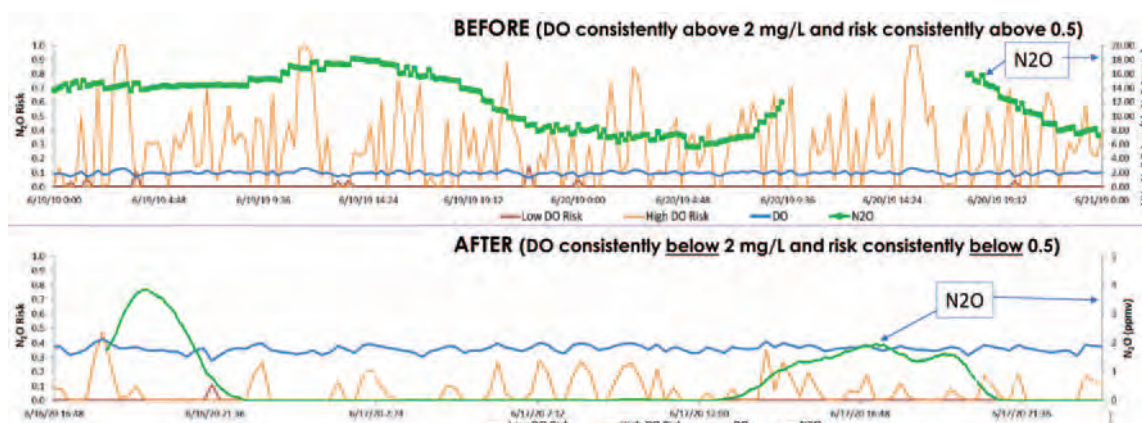


Figure 33: Results of N₂O risk assessment model for the new measurement campaign with application of mitigation strategy.



In an additional test, some sharp increases in DO concentrations have been applied (figure below). In these tests, as DO was increased to the higher risk conditions, more peaks were visible in the actual N₂O emission data.

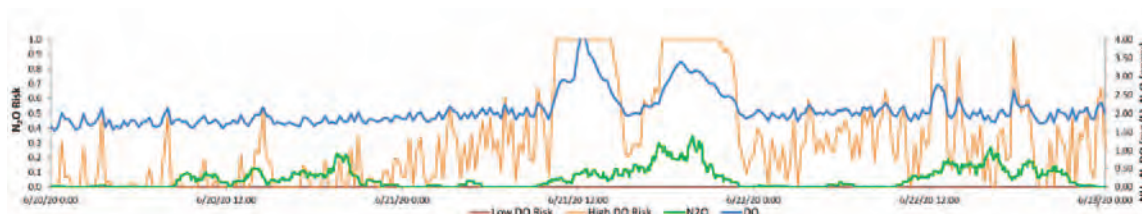


Figure 34: Testing sharp and sudden increase in the DO concentration to check the impact on both N₂O risk and emission.

The application of the proposed mitigation strategy could reduce energy expenditure of the plant by reducing the aeration which usually accounts for the biggest electricity consumption in WRRFs. The modeling studies suggest that this mitigation strategy does not compromise the performance of the treatment process as high ammonia and COD removal efficiency are achievable that suggest the over-aeration condition of the bioreactor. Moreover, under the new operating condition the risk of N₂O emission is significantly lower and this shows a direct impact on the actual N₂O emission data. Therefore, keeping DO below 2 mg/L but close to 2 mg/L yielded the lowest N₂O emissions and could be considered as a valid mitigation strategy to apply.

11.2 Case study 2: San Colombano WRRF

The San Colombano WRRF is located in Lastra a Signa, Tuscany, Italy. It treats municipal wastewater from the surrounding municipalities with the capacity of 600,000 PE. After a preliminary treatment followed by primary settling, the wastewater goes through a denitrification-nitrification biological process. The air flow is regulated by an ammonia-DO cascade controller. The wastewater goes through a secondary settling tank before being introduced to the chemical disinfection at the end. The plant consists of three parallel treatment lines each dividing further into four bioreactors. There are 6 anoxic and one aerobic zone inside each bioreactor with the DO probe located at the end of the aerobic section. There is an internal recycle flowing from the end of the aerobic section to the first three anoxic compartments. The external recycle comes from the secondary settling tank to the beginning of the bioreactor and is mixed with the influent before entering the anoxic zone.

After performing the mass balance of the biological line, all flows and compositions are obtained for the influent to the bioreactor and for all recycle flows. Also in this case, a TIS approach has been considered sufficient for the flow sheet model and the model has been calibrated and validated based on the historical data of the plant. A modified ASM3 model has been used based on the



previous modeling studies on the plant. The next figure shows the fit of the model output to the experimental data which shows a good overall performance.

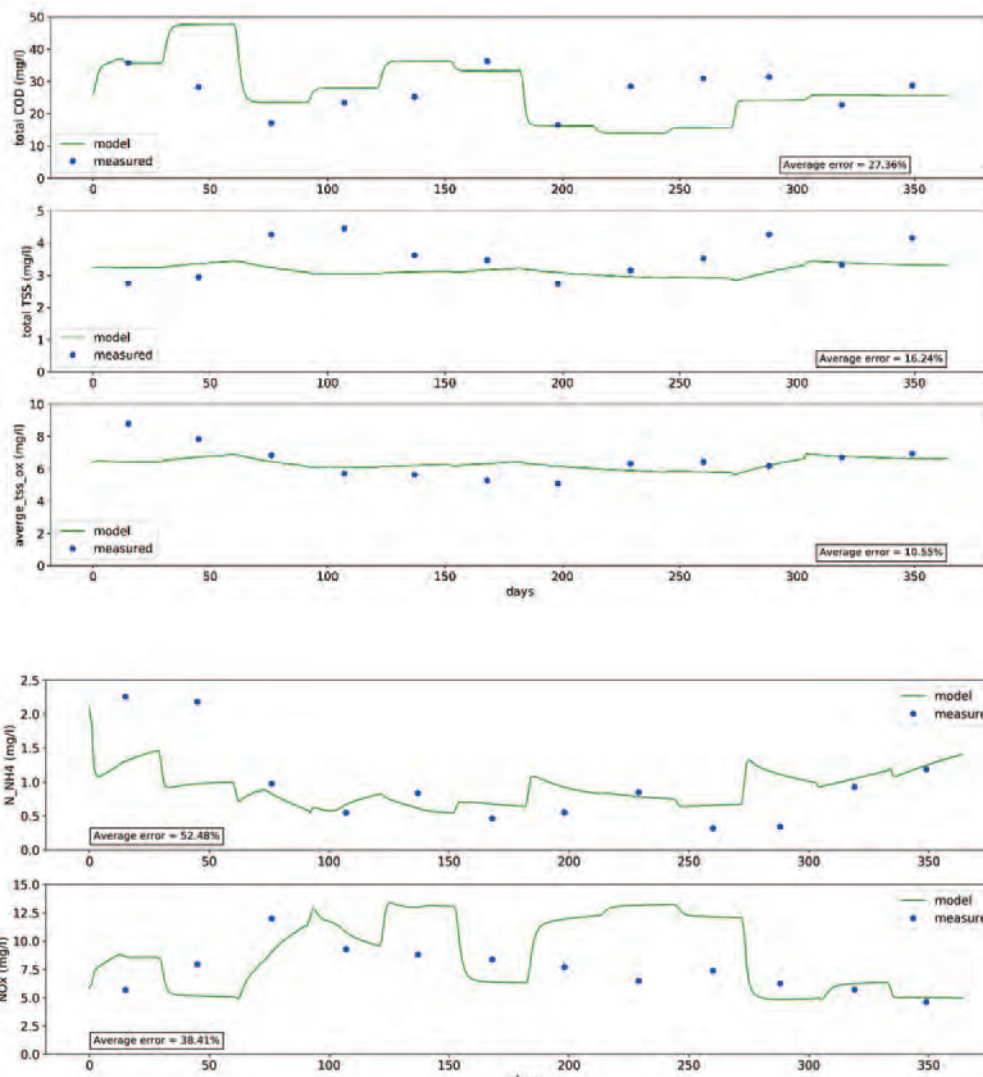


Figure 35: Results of calibrated and validated flow sheet model of San Colombano WRRF.

The N_2O risk assessment modeling has been performed on the data collected with LESSDRONE in a measurement campaign carried out in July 2020. As it can be seen in Figure 36, the low DO risk is predominant for the entire period of testing. The DO concentration is consistently lower than 1 mg/L with occasional peaks reaching up to 1.6-1.8 mg/L. The actual N_2O emissions data (Figure 37) shows only a few peaks for the emission during this time period. Figure 8 shows zoomed-in version of the previous figure for timespans that indicate peaks of N_2O emission. It can be seen in the top graph that the N_2O peaks correspond with the low DO risk. They decrease/increase as the risk decreases/increases. In two other instances (Figure 38 bottom) the increase in the N_2O emission



corresponds to also an increase of nitrate concentration in anoxic zone. This could suggest the N_2O production in the anoxic zone (Figure 39).

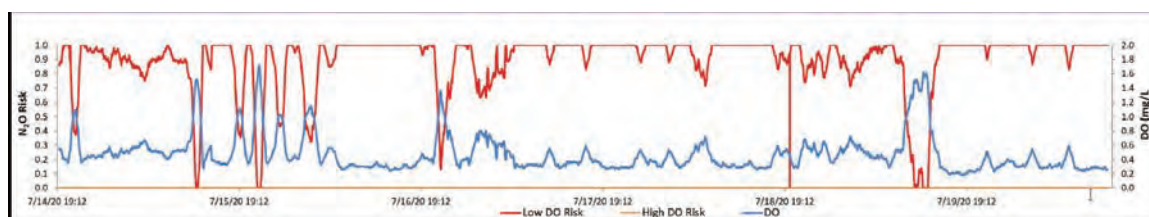


Figure 36: N_2O risk assessment model results for San Colombano WRRF.

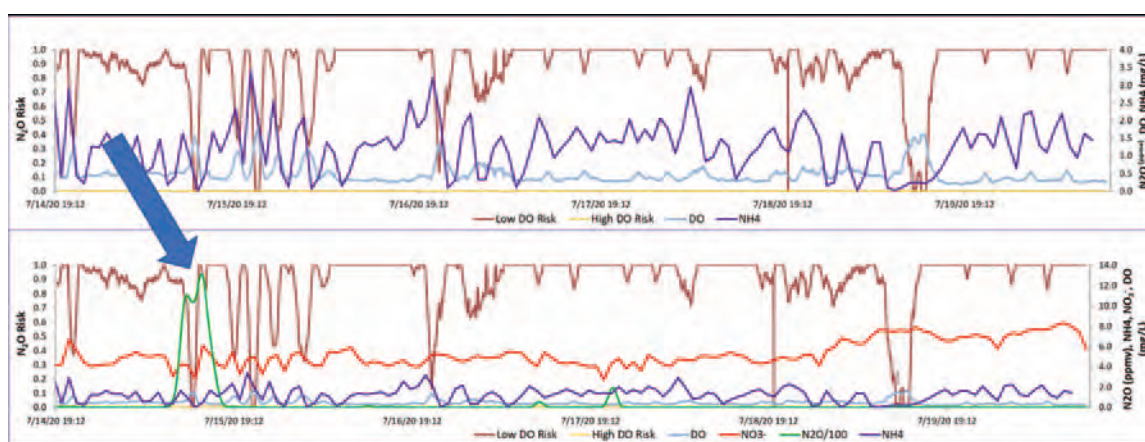
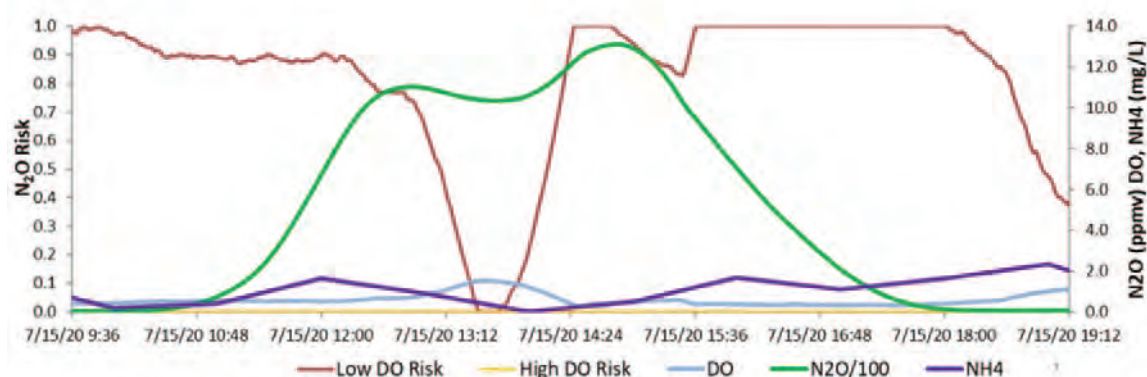


Figure 37: N_2O risk score results with the added ammonia (in top graph) and ammonia/nitrate/ N_2O emission data (in bottom graph).



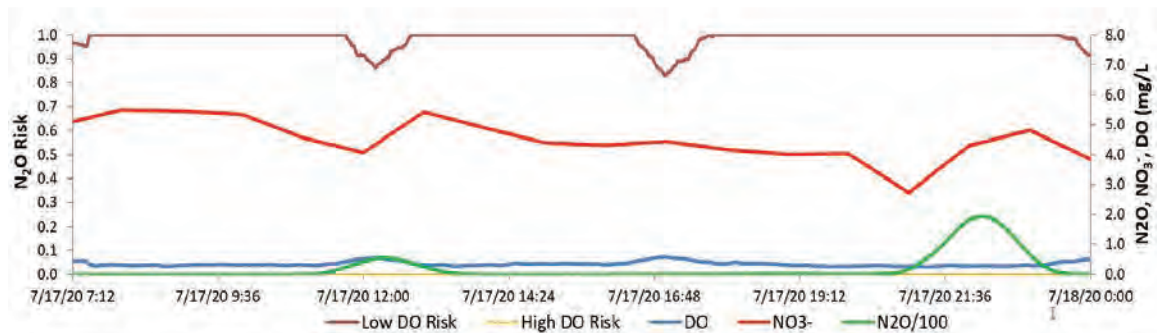


Figure 38: Zoomed-in versions of the risk score results for periods with N_2O emission peaks.

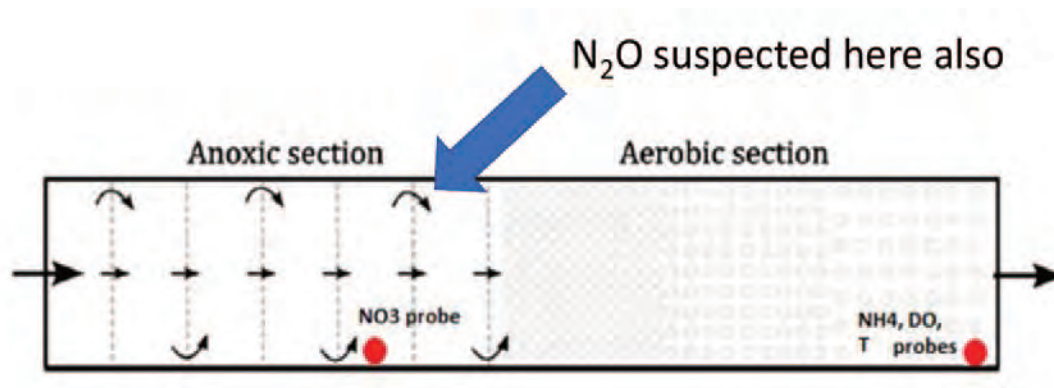


Figure 39: Potential location of the N_2O production in the anoxic zone.

The whole bioreactor including the anoxic and aeration zones is selected for building the CFD-biokinetic model. This will help understanding the mixing patterns, concentrations profiles and possible back flows that might be present at the entrance of aeration zone from the last anoxic section. The geometry data of the bioreactor (Figure 40) as well as data of the flow rates and recycle flows are used for the model.



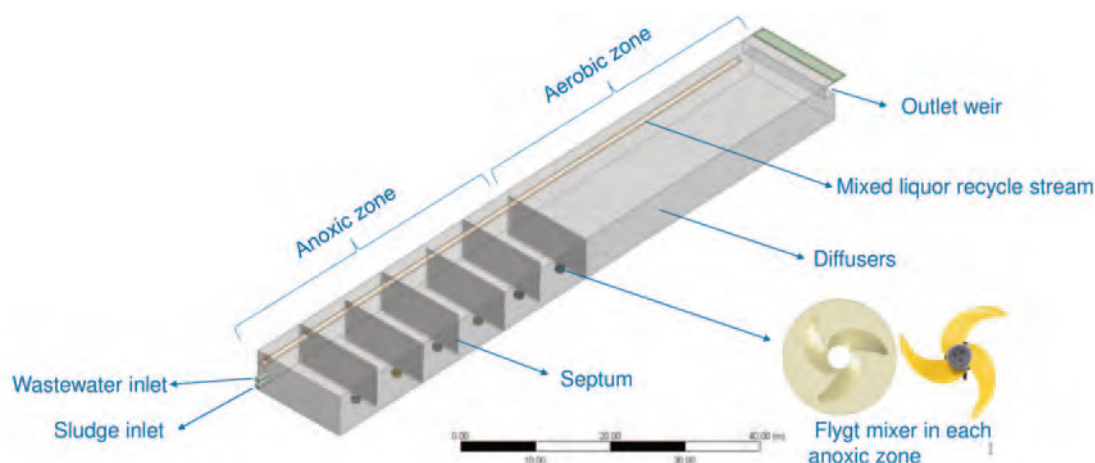


Figure 40: Geometry of the San Colombano denitrification/nitrification bioreactor.

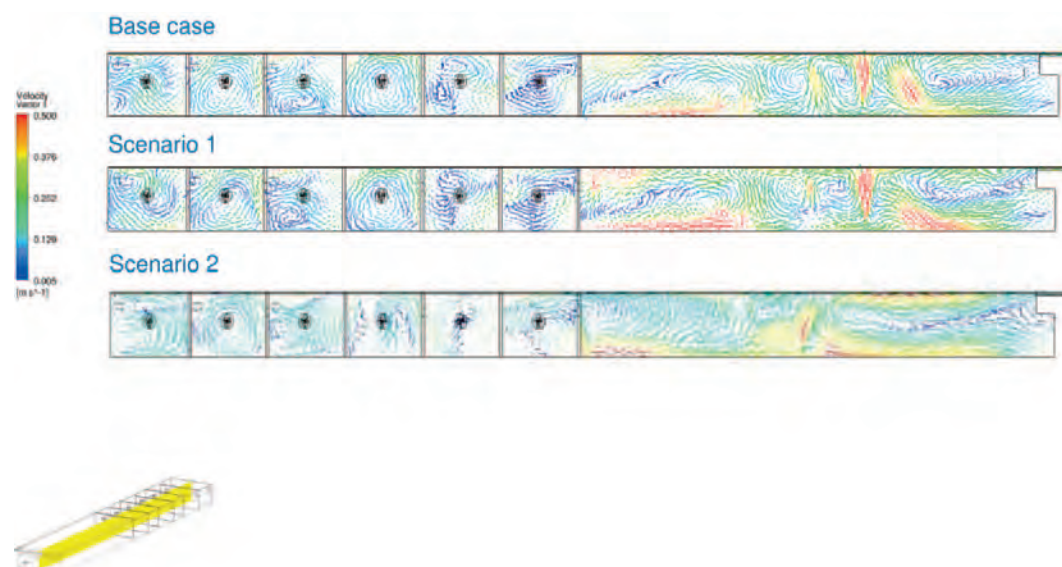
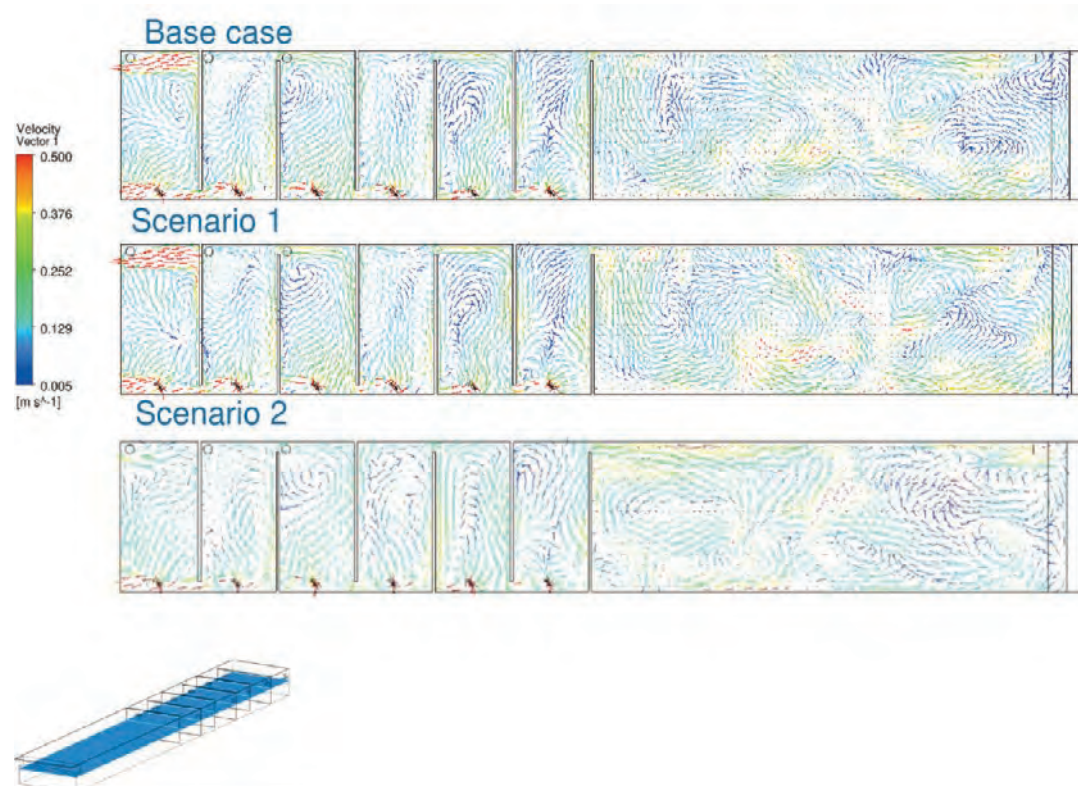
Flowrates	Base case	Scenario 1	Scenario 2
Total influent to [m ³ /h]	2500	3500	2900
Bioreactor Inlet flowrate [m ³ /h]	675	805	667
Air flow fate [m ³ /h]	900	1500	900
Internal recycle flow rate [m ³ /h]	1225	1295	1073
External recycle flow rate [m ³ /h]	700	1400	1160
Mixer rotation speed [RPM]	108	108	108

Combined frequency distribution of influent and air flow rate data as well as the influent load coming to the plant have been used to select three scenarios representing low influent low aeration, high influent high aeration and high load operating conditions.

Figure 41 shows the velocity vectors and volume fraction of air inside the bioreactor for three scenarios. The hydrodynamics do not change significantly with the change of the flow rates. Although, air is present everywhere in the aerobic zone of the bioreactor, gas holdup distributions show that air is relatively less near the anoxic zone and near the outlet, especially close to the bottom. Higher air flowrate in scenario 1 leads to higher gas concentration. In all scenarios the



highest concentration of gas occurs in the central part of aerobic zone and near the top of the reactor. Some fraction of gas enters the anoxic zone with reversed flow in all cases.



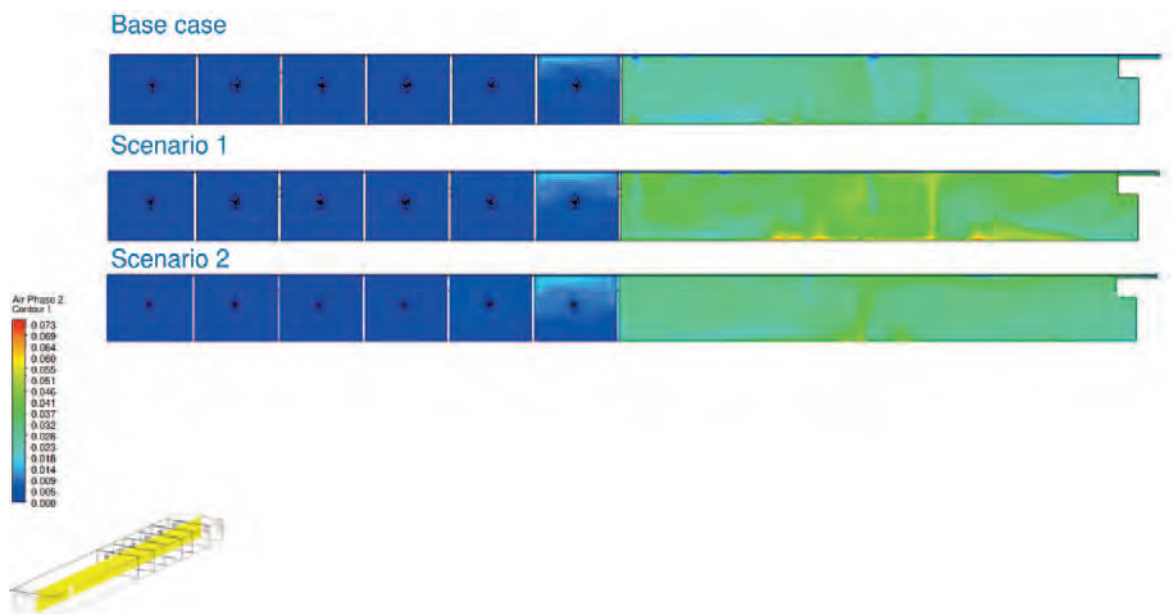


Figure 41: Results of CFD model in terms of velocity vectors (top and middle graphs) and gas holdup (bottom graph).

The influent composition data from the ASM3 model has been used for the CFD-biokinetic model. Figure 42 shows the DO concentration profile in the bioreactor for three horizontal slices. The DO shows high concentrations in almost all the aeration zone and in the last two compartments of the anoxic zone, specially near the bottom of the bioreactor. This is due to the back flow from aeration zone to anoxic zone. At the top end of the bioreactor, a small area with very low concentration of DO is also visible. This is where the DO probe is located and could explain why the measured DO data are much lower than the predicted values of CFD-biokinetic model.



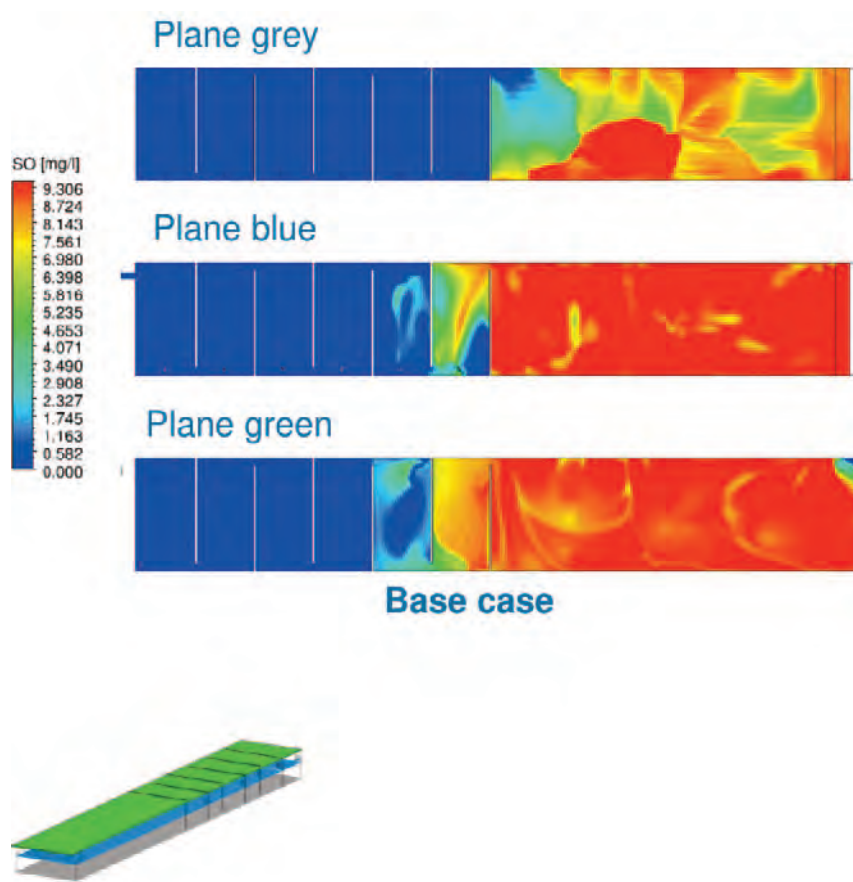


Figure 42: DO concentration profile for base case scenario.

The results for comparison of three scenarios are presented in Figure 43-Figure 45. Oxygen reaches the two last compartments of anoxic zone with a backflow from aerobic zone in all scenarios. Oxygen concentration is just slightly higher in scenario 1, even though the air flowrate is nearly twice higher than base scenario. As previously proved with gas holdup plots, oxygen is well distributed along the aerobic zone of the reactor. However, there is a little dead zone near to the bottom, at the beginning of the aerobic zone. COD is consumed very quickly in anoxic region due to its low concentration at the inlet. There is a fraction of low concentrated COD at the beginning of aerobic zone – the region of low oxygen concentration, but eventually it gets consumed in further part of the reactor. The pattern of SS concentration along the reactor is nearly the same in case of all scenarios. SS concentration is very low due to good COD removal. Concentration of nitrates is relatively higher in scenario 1 due to higher oxygen concentration. In scenario 2, overall, less nitrates are coming from inlet and external recycle and relatively high COD and hence lower nitrates in anoxic region. In all scenarios nitrates initially are consumed in anoxic zone. However, higher concentration of nitrates can be observed in last part of anoxic zone in all scenarios (due to



backflow). There are relatively more nitrates in central part of aerobic zone and relatively less in second part closer to the outlet that matches with the DO concentrations in these regions. Ammonia concentration starts decreasing in last two compartments of the anoxic zone (due to reversed flow from aerobic zone) to eventually be almost completely consumed in aerobic zone. The same pattern can be noticed in all scenarios, however, in base case concentration of ammonia is slightly higher close to the inlet due to lower flowrates.

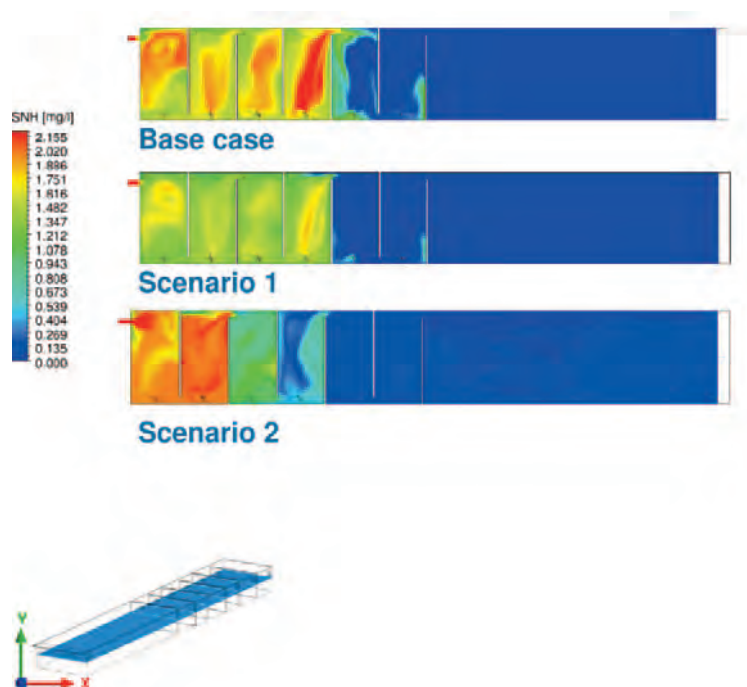


Figure 43: Results of CFD-biokinetic model for ammonia.



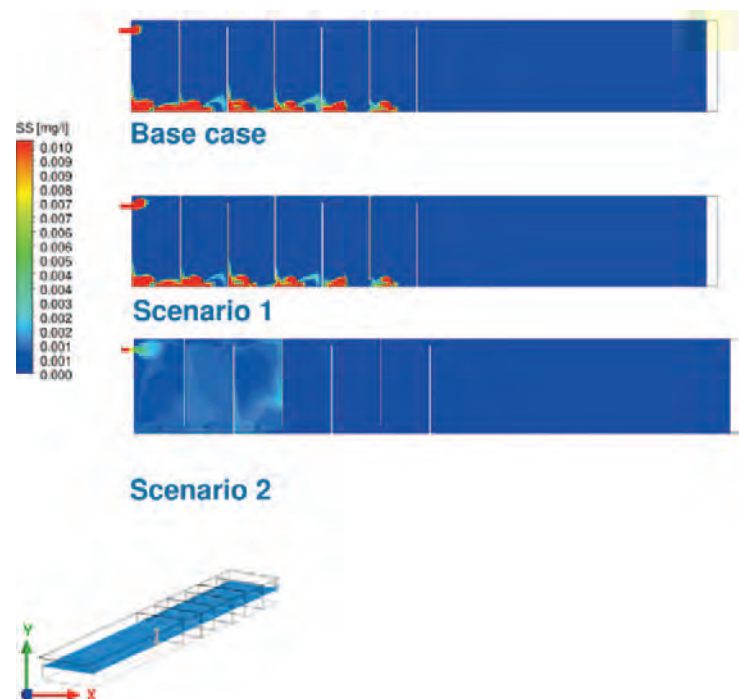


Figure 14: Results of CFD-biokinetic model for soluble substrate.

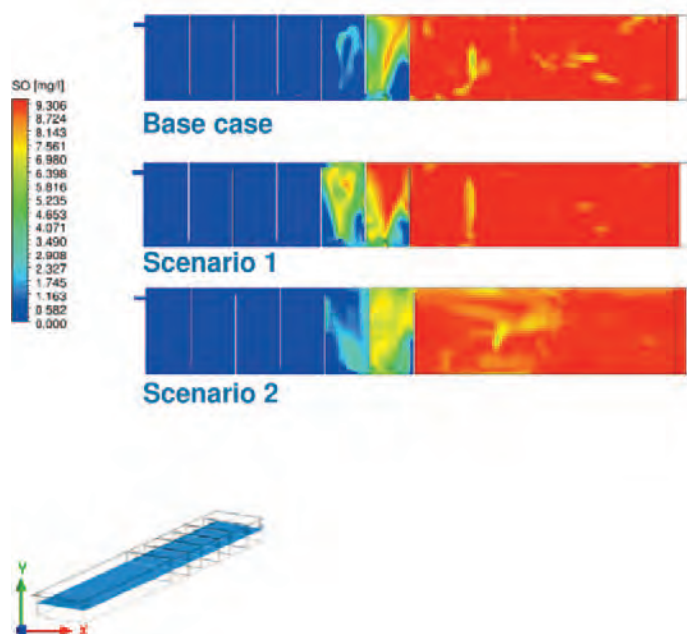


Figure 44: Results of CFD-biokinetic model for DO.



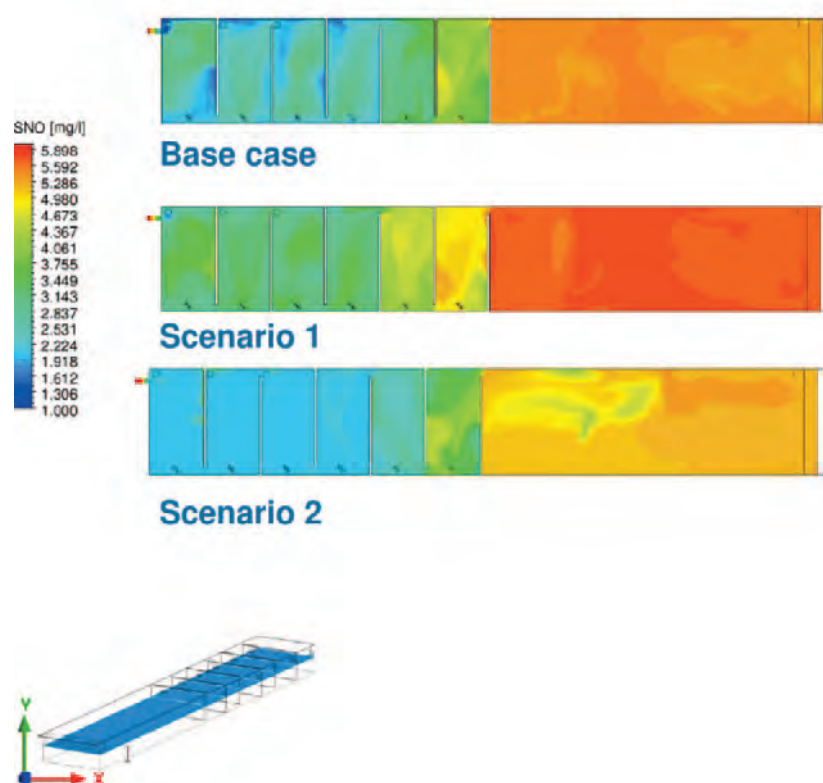


Figure 45: Results of CFD-biokinetic model for nitrate.

Figure 46 shows the Rehman-Nopens curves for soluble substrate, ammonia, nitrate and dissolved oxygen concentrations. Steepness of these curves provides overall mixing of water in the system. Steeper the curve, more uniform the mixing is. Soluble substrates are almost zero in all scenarios in almost all the bioreactors. For the other three parameters the curves show less uniformity.

The overall performance in all the scenarios is very similar even though the flow rates and influent composition has changed. This can be explained by looking at the total load to the bioreactor that doesn't change much across all the scenarios.



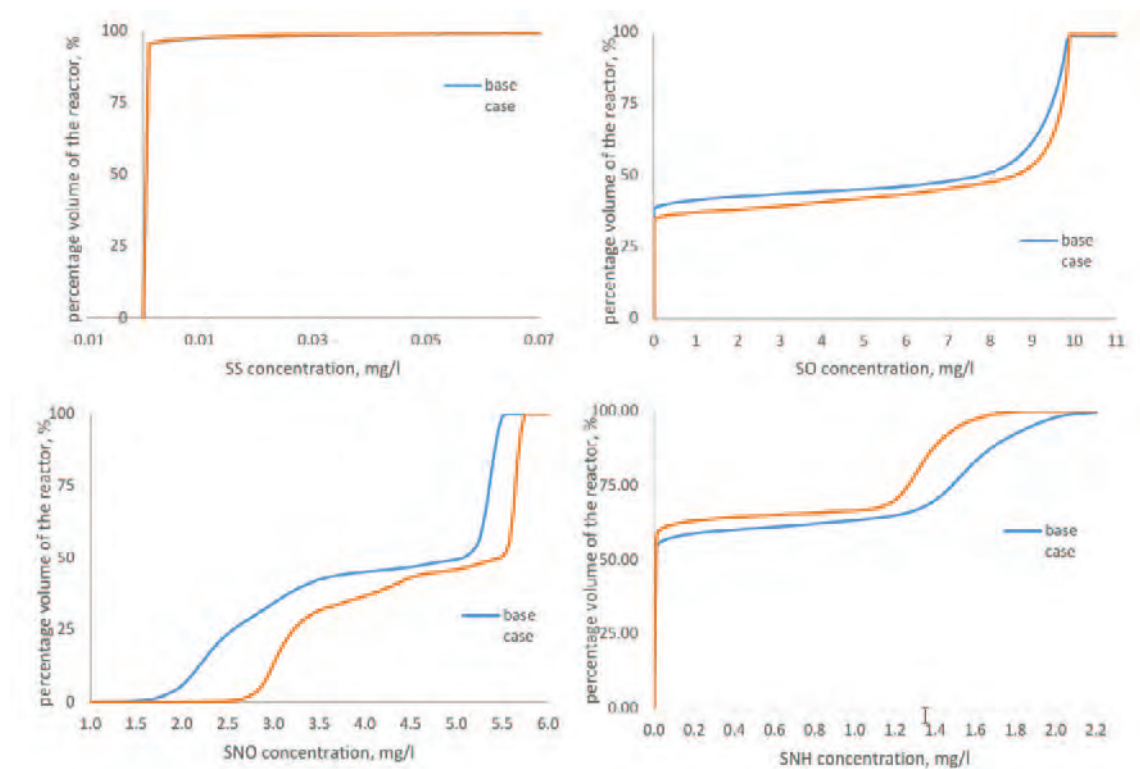


Figure 46: Rehman-Nopens curves for soluble substrate, DO, nitrate and ammonia.

A new measurement campaign has been carried out in San Colombano WRRF in April 2021 for which different operating conditions were observed. Contrary to the first campaign in which DO was consistently below 1 mg/L, in the new period of measurements the DO shows more variations and goes up to more than 2 mg/L in some instances (Figure 47). As expected, in this case high N_2O risk is observed for both high DO and low DO conditions. The N_2O emission data correspond with the risk and sharp peaks can be seen in many instances that the risk increases.

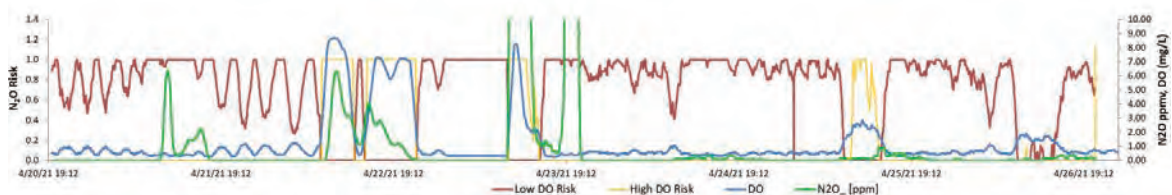


Figure 47: N_2O risk assessment model results for data collected during measurement campaign in April 2021.



Figure 48 shows the zoomed-in version of the previous figure for two time periods (top: 21-23 April, bottom 24-26 April). The top graph shows how N₂O starts to increase with Low DO risk, when DO goes below 1 mg/L and it increases with High DO risk when DO starts to go above 3 mg/L. In the bottom graph, lower peaks of N₂O are visible however, they are also corresponding to peaks of both Low DO risk and High DO risk, again as DO drops below 1 mg/L and when DO goes above 2 mg/L. Therefore, keeping DO near 2 mg/L should eliminate peaks due to both High and Low DO risk.

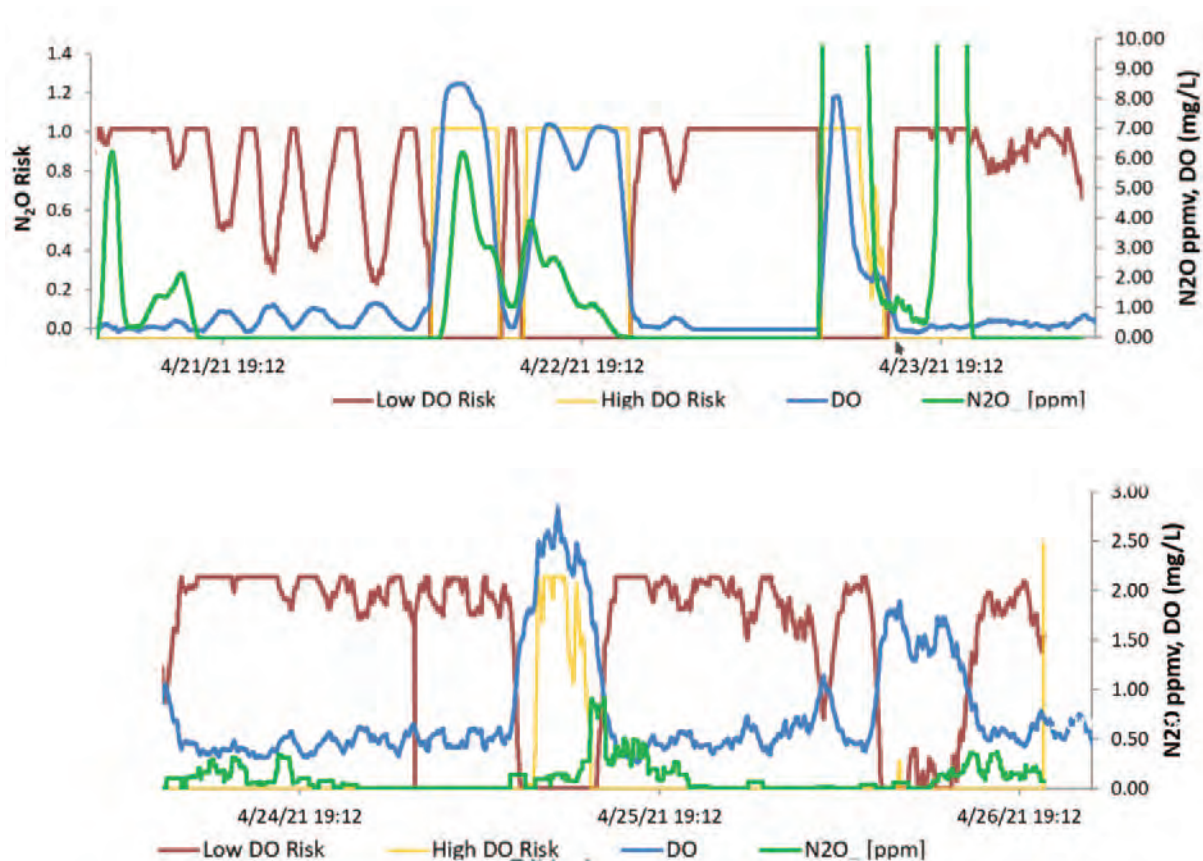


Figure 48: Zoomed-in versions of the previous figure for two time periods (21-23 April 2021 and 24-26 April 2021).

As the potential mitigation strategy, it is suggested to set the DO set point to 1.8-2 mg/L. The results of modeling studies show that this action would reduce the risk of N₂O caused by too high or too low DO concentrations and consequently the N₂O emission is expected to be mitigated.



11.3 Case study 3: Eindhoven WRRF

The Eindhoven WRRF is located in south of the Netherlands and treats municipal wastewater of the surrounding municipalities with the capacity of 750,000 PE. The treatment plant consists of three separate lines each including a primary settling tank, anaerobic/anoxic/aerobic bioreactors and four secondary settling tanks. It also includes chemical dosing in the form of ferric chloride for improving phosphorus removal. There are two internal recycles; one from anoxic to the anaerobic zone and one from the end of aerobic back to the anoxic zone. The external activated sludge recycles flows from the underflow of secondary settling tank to the beginning of the anoxic zone. The aeration is regulated by the presence of an ammonia-DO cascade controller which controls the setpoint of oxygen in the summer package. Summer package is the main aeration zone inside the aerobic bioreactor which constantly provide air flow to the system. There is also another set of diffusers called winter package which starts working based on the temperature and the incoming load to the plant. It acts as additional air flow supply. A mass balance on the whole biological treatment line leads to obtaining all required flow rates and wastewater compositions in important parts of the treatment plant like recycle ratios and influents going into the bioreactor.

A flow sheet model of the Eindhoven plant has been already developed during past modeling studies carried out. This model was first designed with the TIS approach and was calibrated and validated based on the historical data of the plant providing relatively good fit to the experimental data. However, the model needed improvements and since 2016, extensive CFD-biokinetic modeling studies have been carried out for the EH plant with the aim of understanding mixing patterns inside the aerobic bioreactor. The outcome of the CFD-biokinetic studies (Figure 49) showed that the bioreactor is not completely mixed and there are quite a lot of variations in local DO concentrations inside the bioreactor. This led to an important update of the flow sheet model by upgrading it to a compartmental model (CM). The whole aerobic bioreactor that was previously modeled as 4 tanks in series is now modeled having various compartments each representing a fraction volume of the bioreactors. These volumes are connected to each other through exchange flow rates. The CM model showed improvements on the prediction power of the model by modeling the aerobic section in more realistic way compared to conventional TIS. Figure 50 shows the results of the CM compared to the TIS model. Overall, introducing the CM improved the prediction power of the model especially for nitrate prediction which was a weak point of the TIS model. Prediction of DO concentration in aerobic tank is also improved.



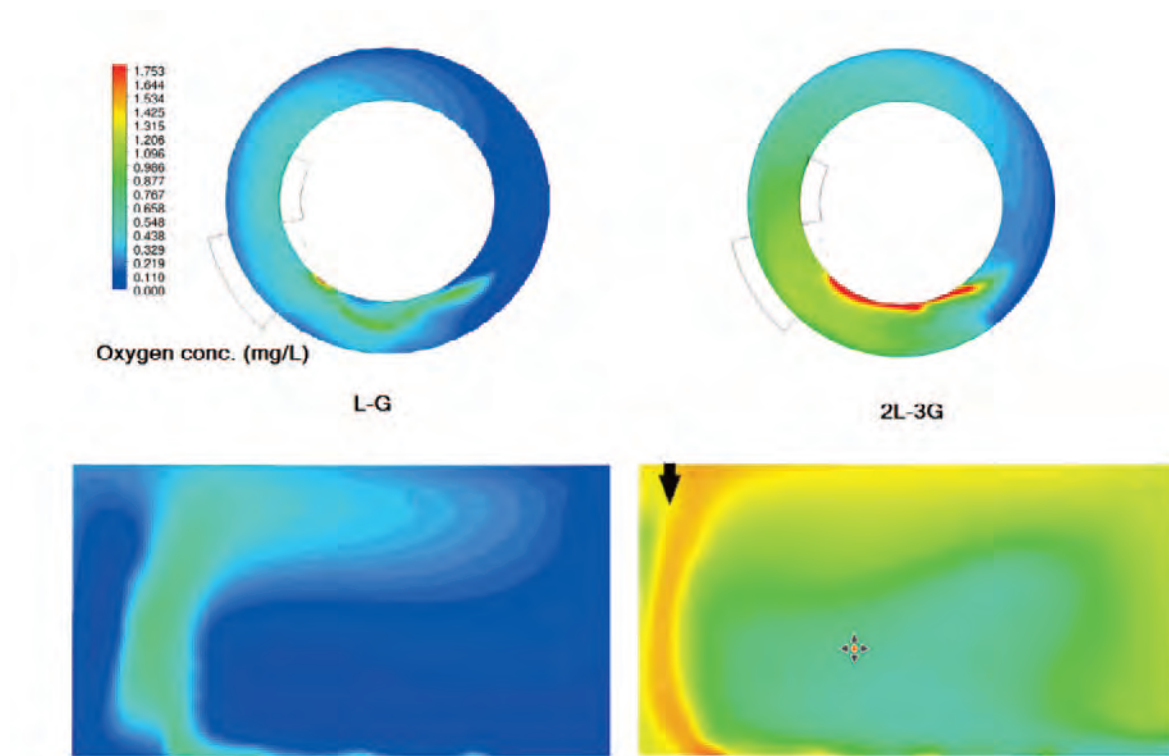


Figure 49: Results of CFD-biokinetic model for the aeration tank of Eindhoven WRRF. Left: scenario with low influent and low air flow rates, right: scenario with high influent and high air flow rates.



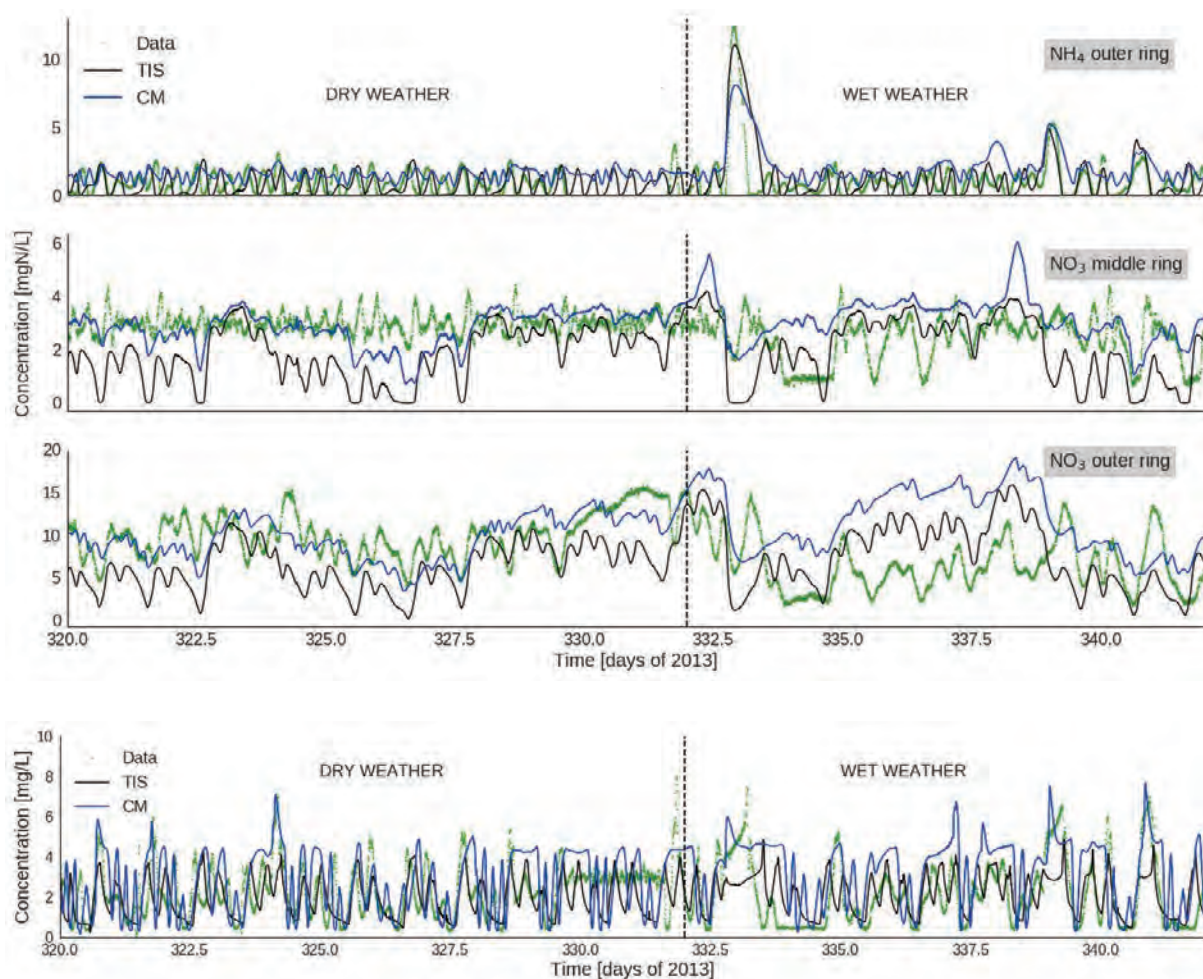


Figure 50: Comparison between the performance of compartmental model (CM) and tank-in-series (TIS) model for Eindhoven WRRF.

The results of the application of N₂O risk assessment modeling framework on the collected data from Eindhoven are presented in Figure 51. Both high DO risk and low DO risk are present without one being the predominant one for the entire period of testing. As mentioned before, the CFD-biokinetic model of the EH aerobic bioreactor showed quite a lot of variations in the local concentrations of the oxygen. This could explain the predicted risk values. Most of the time the DO concentration is either too high or too low so that the risk of N₂O emission remains high in a lot of instances. However, N₂O emission is generally low and only periodic peaks are visible in the data. Nonetheless, the peaks of N₂O emission correspond to the high-risk data predicted by the model.



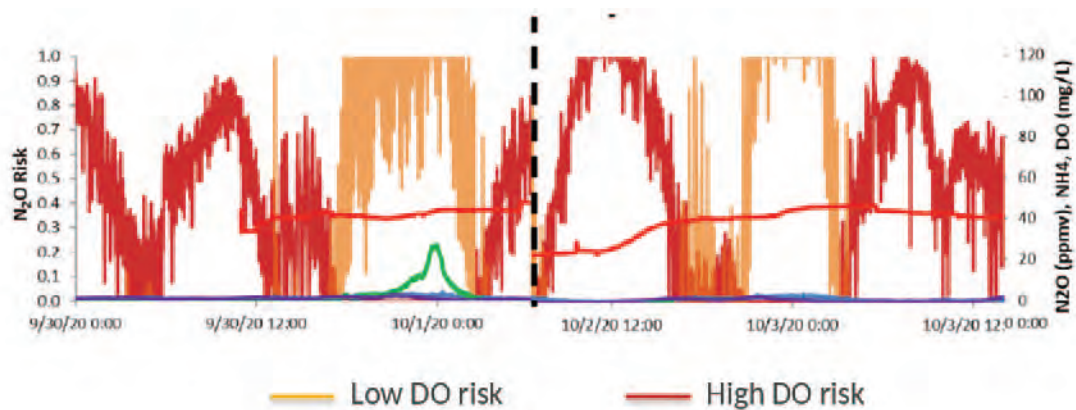


Figure 51: N_2O risk assessment model results for data collected under normal operating condition of the plant.

The risk of producing N_2O is also assessed based on hydrodynamics of the aeration zone. In this case, the DO parcels obtained as the output of the CFD-biokinetic model are fed to the N_2O risk assessment model. This leads to obtaining risk parcels spatially distributed across the bioreactor. Figure 52 shows the results of this modeling approach in terms of low DO risk and high DO risk under both low load and high load conditions. For the low DO risk under low load/flow condition the summer package mostly shows high risk due to low DO, and the risk decreases in the direction of flow with the lowest risk near the end of the summer package. This supports data from previous N_2O measurement campaigns, when N_2O was measured at the beginning and end of the summer package and higher emissions at the beginning of the summer package was seen. For the high load/flow condition, we see less low DO risk in general, obviously because we are aerating more. So, this tells us that for both conditions, we can have N_2O produced from Low DO (nitrifier denitrification).



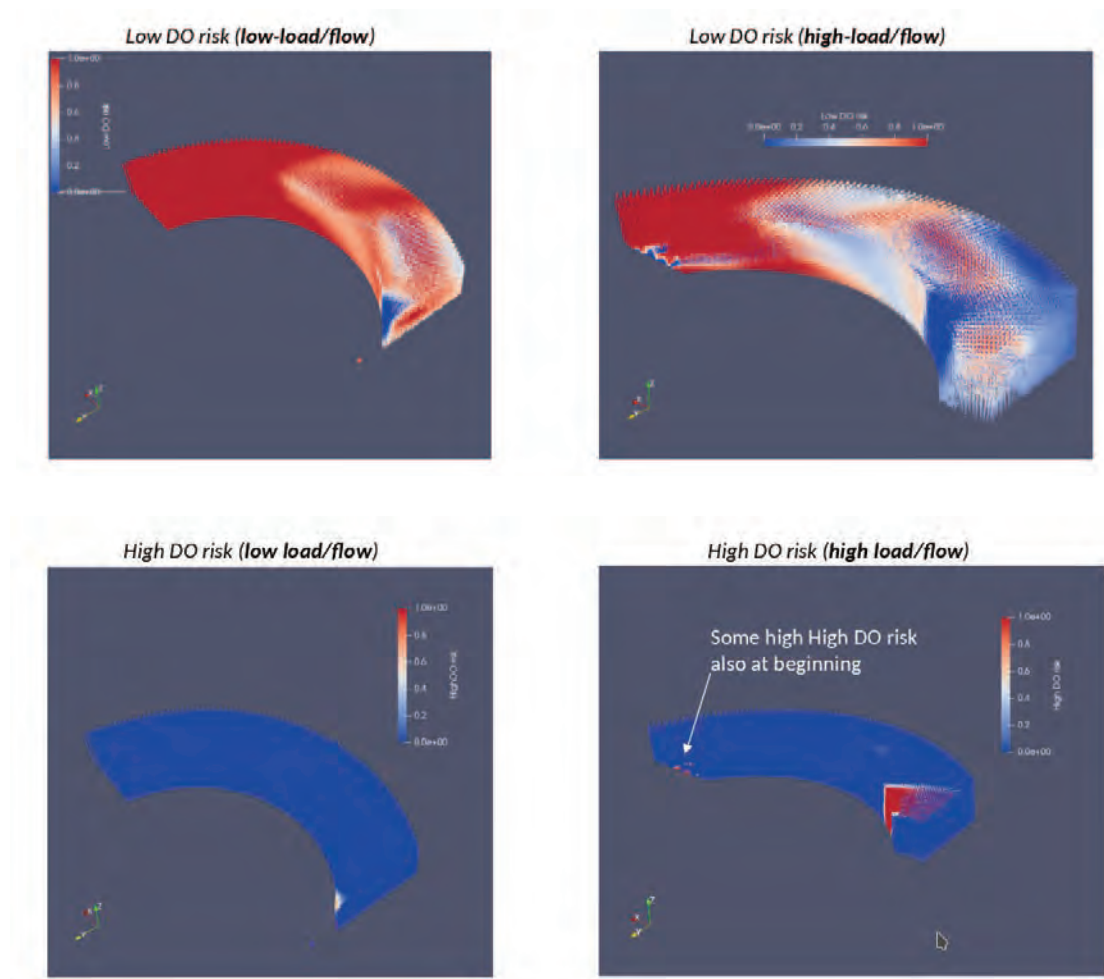


Figure 52: Results of CFD- N_2O risk integrated model. Top left: Low DO risk for a scenario with low influent load. Top right: Low DO risk for a scenario with high influent load. Bottom left: High DO risk for a scenario with low influent load, Bottom right: high DO risk for a scenario with high influent load.

For the high DO risk under low load/flow condition the summer package has very little risk due to high DO. For the high load/flow condition, one area with red high DO risk at the beginning of the summer package can be seen and one larger area at the end. Considering the low DO risk in the previous part, this confirms the possibility of N_2O being produced not only from high DO, but also from low DO conditions, so from both AOB pathways. This means that lowering DO to mitigate High DO risk can exacerbate the Low DO risk in the other part of the bioreactor.

Because reactor is not completely mixed, there is the potential for N_2O production from Low DO conditions even during conditions when DO is kept high per the DO sensor in ammonia-based DO control.



As a result, when mitigating N₂O by reducing High DO risk for Eindhoven WWTP, the new DO set point needs to be picked carefully so low DO does not dominate and then we start to increase N₂O from low DO. This advanced modelling approach led to a better understanding of how hydrodynamics can potentially impact N₂O production/mitigation and predictions of N₂O risk, as well as the importance of sensor location/placement.

As a potential mitigation strategy, reduction of the DO range was proposed. This means the maximum DO setpoint needs to be decreased and the minimum DO setpoint needs to be increased. This new scenario is first tested with the calibrated and validated CM flow sheet model of the plant to see the impact of DO setpoint change on the performance of the treatment process. Figure 53 shows the output of the model for effluent ammonia comparing the base case scenario with normal operating condition and a new scenario with the application of mitigation strategy. Although on some occasions the ammonia concentration in the effluent is higher than the base case scenario, overall the performance of the treatment is not significantly compromised which suggests that the potential mitigation strategy could be proceeded with reliably in terms of removal efficiency.

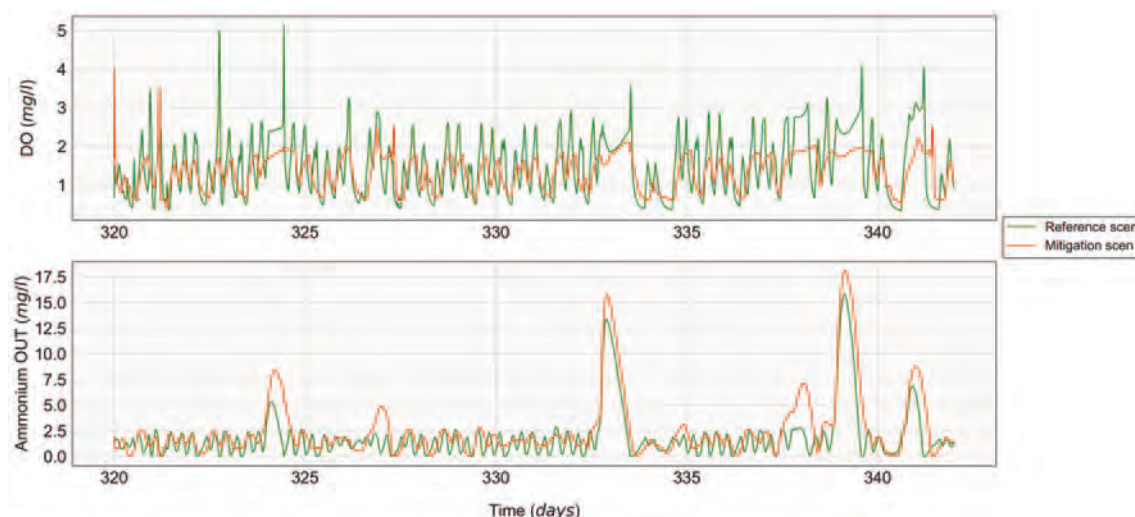


Figure 53: Comparison of the flow sheet model results for proposed mitigation strategy; scenario with reduced DO max set point and increased DO min set point.

The mitigation strategy has been then applied in practice by changing the set point of oxygen. Figure 54 shows the result of the risk model based on the data collected with LESSDRONE during this measurement campaign. The test started under normal operating condition of the plant and after one day the mitigation strategy was applied. Then the set points were set back to the normal operating conditions for another day and after that the mitigation strategy was once again tested. In both cases where the mitigation strategy is applied the risk of N₂O emission due to both high DO and low DO concentrations are significantly reduced. However, during the first period of applying the mitigation strategy, there is still a peak of N₂O emission visible. Looking at the data of the



ammonia and nitrate and comparing them to the second period in which the mitigation strategy was applied, it is a bit difficult to speculate what exactly this N_2O peak is related to. It is important to mention that this period of testing was heavily influenced by the rain events, and this is clearly visible looking at the flows in that period (Figure 55). The presence of rain event may have made seeing the impact of control actions difficult. Nonetheless, the reduction in the risk scores for both low DO and high DO risks suggest that we should expect lower N_2O emissions with the application of proposed mitigation strategy.

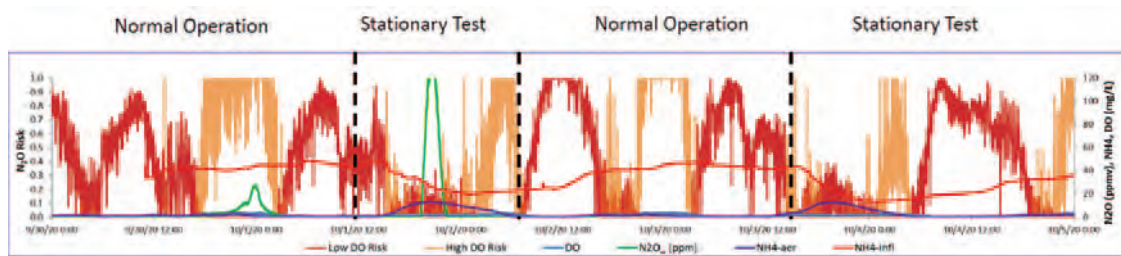


Figure 54: N_2O risk assessment model results based on a measurement campaign with application of the mitigation strategy. Stationary test periods represent the period in which the mitigation strategy is applied.

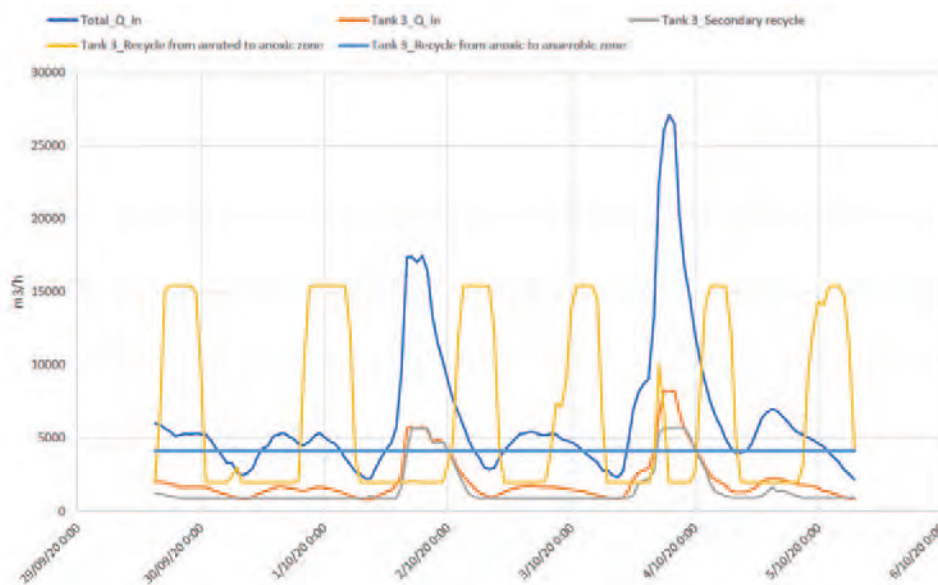


Figure 55: Flow data for the period of measurement campaign. Total_Q_in shows the impact of rain event in two instances with sharp peaks.



11.4 Case study 4: Tilburg WRRF

The last case study is the Tilburg WRRF in south of the Netherlands. This is an energy factory consisting of both water and sludge treatment lines. It has the capacity of 375,000 PE treating municipal wastewater. The water line includes primary settling tanks, nitrification/denitrification bioreactors and secondary settling tanks. The activated sludge is recycled from the secondary settling tank back to the beginning of the denitrification zone. The aeration is controlled using an ammonia-DO cascade controller.

There is not flow sheet and CFD-biokinetic model available for the Tilburg WRRF. The development of these models is not foreseen in the context of this project partly because a lot of upgrades and new constructions are under implementation or investigation at the moment. Therefore, only the N_2O risk assessment modeling was used based on a measurement campaign with LESSDRONE that was carried out during October 2020.

Figure 56 shows the results of the risk model based on the collected data. Although occasionally high DO risk conditions are visible, the low DO risk is predominant mostly. Generally, the trend of low DO risk correlates with the N_2O emission data. Looking at the ammonia data, it seems that when an ammonia peak is reached the DO starts to increase. However, this increase is not immediate, and it takes a well amount of time for the DO to reach to a high level to meet the high ammonia peak condition. This leads to the fact that in most cases the DO is quite low when the ammonia peak happens, and these low DO conditions leads to high risk of N_2O emissions. A possible mitigation strategy could be to increase the DO before the ammonia peak happens. This way the low DO condition can be avoided during the ammonia peaks and consequently the low DO risk peaks can be eliminated.

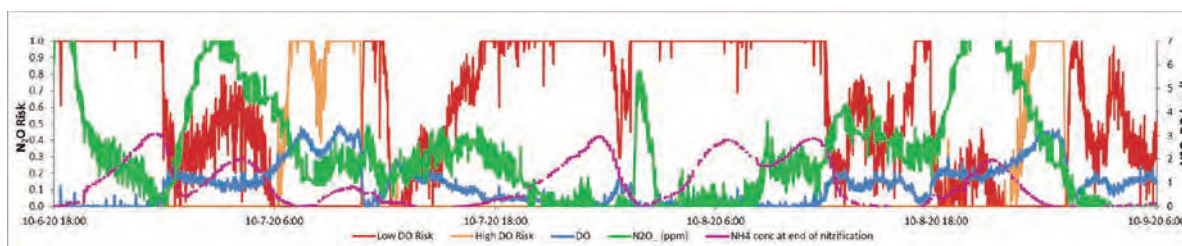


Figure 56: N_2O risk assessment model results for Tilburg WRRF. The entire measurement campaign was carried out under normal operating condition of the plant.



Unfortunately, due to the construction works present in the Tilburg WRRF at the time of the measurement campaign, the operating conditions of the plant could not be changed to test the proposed mitigation strategy. Therefore, for the purpose of this project and application of the protocol only the proposal of a potential mitigation strategy is considered to be enough.

12. LESSWATT protocol

The application of the advanced modeling paradigms to selected WRRFs has led to the definition of the LESSWATT protocol. Here a summary of the existing modeling protocols is presented followed by a through description of what LESSWATT protocol brings to the table by focusing on CF minimization targets.

The general calibration procedure follows the steps defined in the GMP Unified protocol with more focus on the sub-process model than the biokinetic parameters. The idea is to correct the deviations between model outputs and experimental measurements by sub-processes models in order to identify structural uncertainties of these models. This is because the largest uncertainties are generally associated to the influent, hydraulics, gas-liquid mass transfer and primary/secondary settling processes. The steps of the general calibration procedure include project definition, data collection and reconciliation, plant model set up, calibration and validation, simulation, and finally results interpretation. The first and crucial step is defining the objective of the modeling project. What is going to be optimized? This step is particularly important in calibration procedure as it helps to define what sub-processes or parameters are more important to calibrate. Data collection comprises the online measurement data, lab analysis, and measurement campaigns. High-frequency online data improves the accuracy of the model significantly. The raw collected online data usually has various inconsistencies to deal with, e.g., missing points, outliers, faulty duplicates. Therefore, a reliable data reconciliation and validation process should be considered.

It is only after these steps that a model of the plant can be built based on the layouts, schemes and also expert knowledge. Calibration procedure for the biokinetic model and the control systems are carried out separately. In order to calibrate the biokinetic model, the control actions are decoupled and operational data such as air flows is used as the input directly. On the other hand, for the calibration of the controllers, sensor data such as oxygen and ammonia are used as the input. The calibration and validation of the plant model is usually conducted based on both expert knowledge and mathematical methods for defining which parameters to calibrate and to what extent the parameter needs to be changed. A stepwise approach is used during the calibration process. New models are first calibrated separately based on lab tests (such as for the settling tests), then on the full-scale data of the process unit and finally integrated with the whole plant model. The calibrated model will then be validated on another data set for a different period.



Finally, the simulation results are discussed and interpreted with the experts and the output of the model is checked against the assumptions made during the modeling process.

The whole calibration process is carried out in a cyclic approach. After defining the objective of the modeling project, a first calibration cycle is performed based on the default values of the model, available data sets, assumptions and expert knowledge. After the simulations and interpretation of the results, a decision has to be made whether to go for the second iteration of the calibration procedure or not. For this aim, deep investigation needs to be done on the sources of discrepancies in the validation step. The protocol suggests to first look for issues in the structure of the sub-processes models. Mass balances and simulation of different scenarios could be helpful in this regard. In a further iteration of the calibration procedure, focus can be changed towards parameter estimation of adding more detailed sub-process models. After each iteration the results are discussed and interpreted again to assess the quality of the model outcome. It is important to note also the uncertainty of the model outcome. This is particularly important to assess whether the obtained quality of the model is enough for the objective of the modeling project defined in the first step. Again here, the uncertainty of the model outcome can be assessed by both the expert knowledge and mathematical methods, e.g., Monte-Carlo techniques.

The main objective of the LESSWATT project is not to develop an entire new protocol but is to fine tune the existing ones and adapt them in accordance with the CF reduction targets. The main targets for CF reduction in a WRRF are mitigation of GHGs emission and minimizing the energy expenditure of the plant. Therefore, the LESSWATT protocol focuses its attention on specific additional steps for improving these aspects. On the way of achieving this, the use of LESSDRONE for data collection is a crucial step. LESSDRONE directly measures the DO, OTE and GHG emissions (N_2O , CO_2 and CH_4) in the off-gas of the biological tanks. The collected data by LESSDRONE will be a valuable asset in validation of the modeling outcome and to propose a mitigation strategy.

Figure 57 shows the scheme of the LESSWATT protocol with the corresponding data requirements for each step. After defining the objective of the project, a mass balance of the WRRF is performed based on the layout of the plant. At this point, boundaries of the modeling study need to be selected. In many cases, only a part of the treatment line might have to be modeled. For instance, modeling only the aeration zone might be sufficient when the N_2O emission is dominant in this section. Boundary selection is thus closely related to the objective of the modeling study. Although not strictly necessary for the purpose of defining a mitigation strategy, a calibrated and validated flow sheet biokinetic model of the biological treatment line should be obtained based on the historical data following the general GMP protocol described before. The N_2O risk assessment modeling framework is then used to calculate N_2O risk scores based on measurement data under normal operating conditions of the plant. The model takes advantage of expert knowledge using artificial intelligence techniques and high frequency data collected by LESSDRONE. Based on this step, the operating conditions under which the risk of N_2O emission is higher are detected. This could be for



example high DO (or low DO) and nitrite (NO_2^-) concentrations during nitrification or high DO concentration, low pH and low COD/N ratio during denitrification.

It might be already possible at this stage to propose a mitigation strategy if the N_2O emission patterns can be explained by high-risk operating conditions detected by the model. This could happen for example where the bioreactor is completely and well mixed. So, both the DO and N_2O measurements by LESSDRONE can reliably represent the local concentration profiles inside the bioreactor. However, in many plants this is not the case. It could happen that the model detects a low-risk condition based on DO measurements but the N_2O data shows high emissions in the same operating condition. In these situations where some difficult-to-explain discrepancies are present in the data, it would be highly important to look at the hydrodynamics and mixing patterns inside the bioreactor. Using a CFD-biokinetic model could be a valuable asset here. CFD-biokinetic model uses the data from geometry of the tank, influent flow and airflow rates to the bioreactor and influent composition to calculate the velocity vectors, gas volume fractions and concentration profiles of different components with a very high detail (in scale of centimeters) along the spatial axes of the bioreactor.

The results of this step show if the bioreactor is not completely mixed and if there are some dead zones affecting the presence of air in those regions. In case of having very high local variations inside the bioreactor, two important additional steps could be followed. The flow sheet biokinetic model of the plant which is conventionally developed with a tank-in-series (TIS) approach can be updated to a compartmental model (CM) based on the results of CFD-biokinetic model. A CM considers the whole bioreactor as a set of different compartments with different volumes that are connected to each other through some exchange flow rates. This is in contrast with the TIS model in which the bioreactor is modeled using a number of continuously stirred tank reactors (CSTRs) connected in series. A CM can greatly improve the prediction power of the model by accounting for the effect of mixing patterns. In addition, this step is valuable for optimizing energy expenditure of the plant which is significantly affected by the mixing and aeration. The second additional step is to use the DO concentration profile calculated by the CFD-biokinetic model as the input for the N_2O risk model. This integrated CFD-biokinetic- N_2O risk model calculates the risk scores for N_2O emission spatially along the axes of the bioreactor. As a result, the effect of mixing patterns on the risk of emission could be identified which will be highly valuable for proposing an appropriate mitigation strategy.

Combining the results of all previous modeling studies with the expert knowledge, one or more potential mitigation strategies are defined for reducing the N_2O emissions and energy expenditure of the plant. Before putting the proposed mitigation strategies in test under real operating conditions, they will be evaluated through virtual testing using calibrated/validated flow sheet model (or other modeling paradigms if necessary) to investigate the impact of those actions on the performance of the treatment process. This ensures the ability to implement some mitigation strategies without compromising the treatment efficiency and still being able to meet the effluent



quality regulations. Finally, the chosen strategy will be applied in practice using LESSDRONE for data collection.

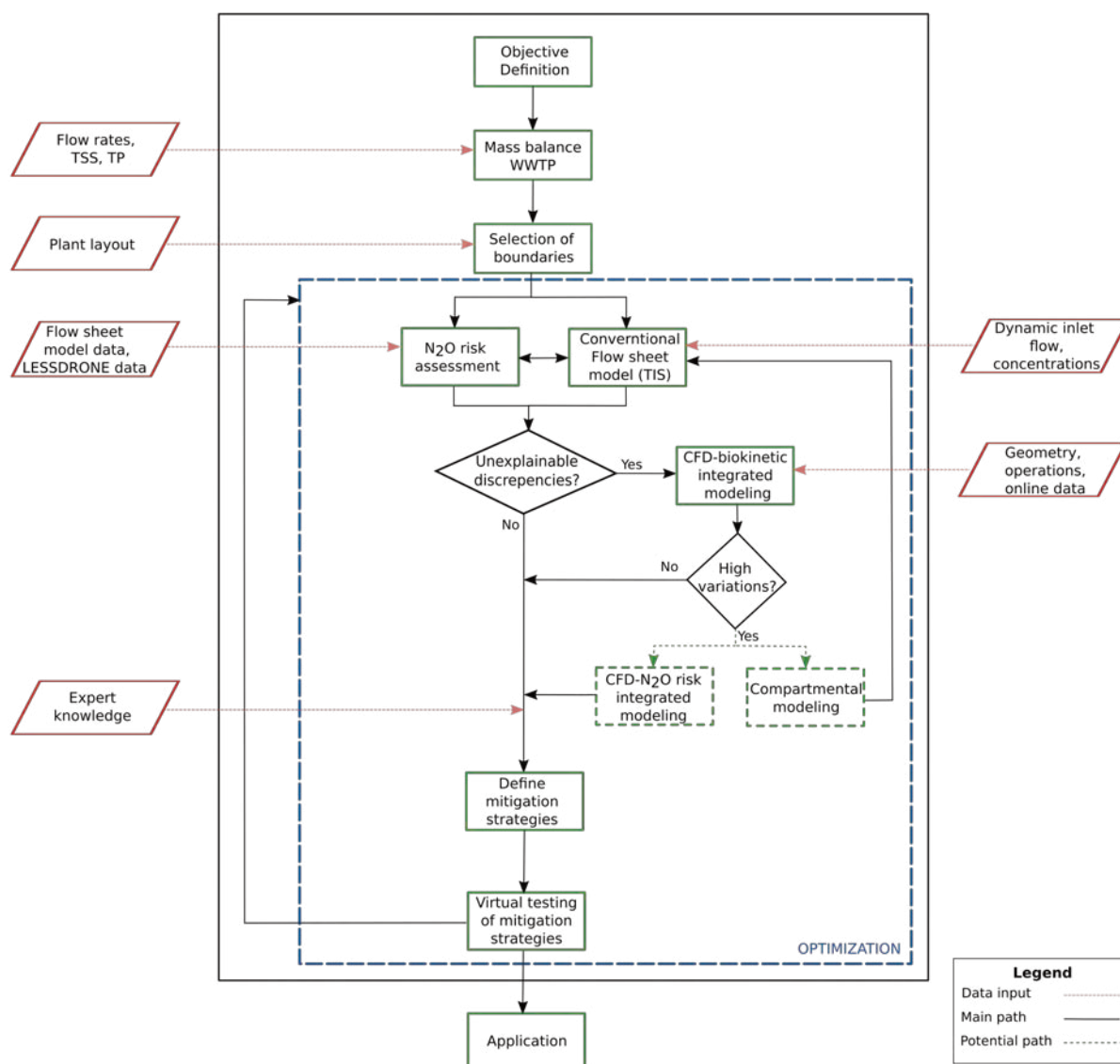


Figure 57: Scheme of the LESSWATT protocol.



A more simplified form of a protocol application is aimed at optimizing the aeration system (for example maintenance/cleaning/substitution of the air diffusers), which does not require changes in operating conditions and uses only experimental results.

Through a single measurement campaign with the LESSDRONE, it is possible to evaluate the current state of the oxidation biological compartment. The "point" tests allow to define the spatial distribution in the oxidation tank of the parameters of interest (DO, air flow, α SOTE, OTR, CO₂, CH₄, N₂O) and the "stationary" tests allow to define the temporal trend in the oxidation tank of the parameters of interest. Evaluations are made on specific energy consumption, direct and indirect emissions, correlations with influencing loads, aeration control system and sampling and analysis of liquids (quality parameters, GHGs) and gases (GHGs, VOCs, odorous compounds, olfactory units).

The repetition of several measurement campaigns (e.g. another 2 campaigns in 12 months) allows the optimization of the diffusers management (cleaning / replacement), through the determination of the α SOTE trend over time before and after cleaning if required, the evaluation of energy expenditure as the age of the speakers increases, the assessment of environmental and economic impacts and the identification of management scenarios aimed at improving oxygen transfer efficiency and minimizing energy consumption (and indirect emissions).

Finally, the biokinetic and/or fluid dynamics modeling of the oxidation compartment allows the evaluation of scenarios with different aeration control systems for the optimization of biological processes and for the minimization of energy consumption and the environmental impacts related to aeration.

For example, if the current management of the aeration does not include any control, the installation of a control with DO set-point or NH₄ set-point can be envisaged; otherwise, if the current management of the aeration already includes a control with DO set-point, the optimization of the control itself or the installation of a more advanced control with NH₄ set-point can be provided; finally, if the current management of the aeration provides for a control with NH₄ set-point, the optimization of the control itself can be envisaged.

